

A population of eruptive variable protostars in VVV

C. Contreras Peña^{1,4,2,*}, P. W. Lucas², D. Minniti^{1,7}, R. Kurtev^{3,4}, W. Stimson², C. Navarro Molina^{4,3}, J. Borissova^{3,4}, N. Kumar², M.A. Thompson², T. Gledhill², R. Terzi², D. Froebrich⁵, and A. Caratti o Garatti⁶

¹ Departamento de Ciencias Fisicas, Universidad Andres Bello, Republica 220, Santiago, Chile

² Centre for Astrophysics Research, University of Hertfordshire, Hatfield, AL10 9AB, UK

³ Instituto de Física y Astronomía, Universidad de Valparaíso, ave. Gran Bretaña, 1111, Casilla 5030, Valparaíso, Chile

⁴ Millennium Institute of Astrophysics, Av. Vicuna Mackenna 4860, 782-0436, Macul, Santiago, Chile

⁵ Centre for Astrophysics and Planetary Science, University of Kent, Canterbury CT2 7NH, UK

⁶ Dublin Institute for Advanced Studies, School of Cosmic Physics, Astronomy & Astrophysics Section, 31 Fitzwilliam Place, Dublin 2, Ireland

⁷ Vatican Observatory, V00120 Vatican City State, Italy

2 October 2018

ABSTRACT

We present the results of a search for high amplitude infrared variable stars in 119 deg² of the Galactic midplane covered by the Vista Variables in the Via Lactea (VVV) survey. We find 816 variables with $\Delta K_s > 1$ mag in the 2010-2012 data, almost all of which are new discoveries. The sample is strongly concentrated toward areas of star formation. Stars found in these areas show characteristics that support classification as young stellar objects (YSOs), these comprising about 50% of the sample. This provides further evidence that YSOs are the commonest high amplitude infrared variable stars. Analysis of the 2010-2014 time series of objects in SFRs shows that the overall amplitude of variability increases towards younger evolutionary classes (class I and flat-spectrum sources). The earlier evolutionary classes show higher r.m.s. variability on all timescales longer than 25 days but the reverse trend is seen at shorter timescales, where class II YSOs are more variable. We divide our likely YSOs into different types according to their light curve morphology. We find 106 objects with eruptive light curves, 45 dippers, 39 faders, 24 eclipsing binaries, 65 long-term periodic variables ($P > 100$ days) and 162 short-term variables. Eruptive YSOs and faders tend to have the highest amplitudes and eruptive systems have the reddest SEDs. The 2 epochs of VVV JHKs multicolour-data indicate that extinction is not the main cause of variability in these systems and follow up spectroscopy in a companion paper (Paper 2) verifies high accretion rates in the eruptive systems. These discoveries increase the number of eruptive variable YSOs by a factor of at least 5. The majority are optically obscured systems at earlier stages of evolution than the known FUor and EXor types of eruptive YSO. We find that eruptive variability is at least an order of magnitude more common in class I YSOs than class II YSOs. The typical 1 to 4 year duration of the outbursts is between those of EXors and FUors.

Key words: infrared: stars – stars: low-mass – stars: pre-main-sequence – stars: AGB and post-AGB – stars: protostars – stars: variables: T Tauri, Herbig Ae/Be.

1 INTRODUCTION

The VISTA Variables in the Via Lactea (VVV, Minniti et al. 2010) survey has mapped a 560 deg² area containing $\sim 3 \times 10^8$ point sources with multi-epoch near-infrared photometry. The surveyed area includes the Milky Way bulge and an adjacent section of the mid plane. The survey has

already produced a deep near-infrared Atlas in 5 bandpasses (Z , Y , J , H , K_s), and the final product will include a 2nd epoch of the multi-filter data and a catalogue of more than 10^6 variable sources.

One of the main scientific goals expected to arise from the final product of VVV is the finding of rare variable sources such as Cataclysmic Variables and RS CVn stars, among others (see Catelan et al. 2013, for a discussion on classes of near-infrared variable stars that are being stud-

* E-mail:c.contreras2@herts.ac.uk (CCP)

ied by VVV). One of the most important outcomes is the possibility of finding eruptive variable Young Stellar Objects (YSOs) undergoing unstable accretion. Such objects are usually assigned to one of two sub-classes: FUors, named after FU Orionis, have long duration outbursts (from tens to hundreds of years); EXors, named for EX Lupi, have outbursts of much shorter duration (from few weeks to several months). Both categories were optically defined in the first instance and fewer than 20 are known in total (see e.g., Reipurth & Aspin 2010; Scholz et al. 2013; Audard et al. 2014), very likely because YSOs with high accretion rates tend to suffer high optical extinction by circumstellar matter. For thorough reviews of the theory and observations in this subject see Hartmann & Kenyon (1996); Reipurth & Aspin (2010); Audard et al. (2014). Given that VVV is the first near infrared time domain survey of a large portion of the Galaxy, it is reasonable to hope for a substantial yield of new eruptive variable YSOs in the dataset. In particular, we would expect the survey to probe for high amplitude variability that occurs on typical timescales of up to a few years, which corresponds more to EXors (or their younger, more obscured counterparts) than to FUors. Eruptive variable YSOs are important because it is thought that highly variable accretion may be common amongst protostars, though rarely observed owing to a duty cycle consisting of long periods of slow accretion and much shorter periods of unstable accretion at a much higher rate. If this is true, it might explain both the observed under-luminosity of low-mass, class I YSOs (the “Luminosity problem” (see e.g. Kenyon et al. 1990; Evans et al. 2009; Caratti o Garatti et al. 2012)) and the wide scatter seen in the HR diagrams of pre-main sequence clusters (Baraffe, Chabrier, & Gallardo 2009; Baraffe, Vorobyov, & Chabrier 2012).

In the search for this rare class of eruptive variable stars, Contreras Peña et al. (2014) studied near-infrared high-amplitude variability in the Galactic plane using the two epochs of UKIDSS Galactic Plane Survey (UGPS) K band data (Lawrence et al. 2007; Lucas et al. 2008). Contreras Peña et al. found that $\sim 66\%$ of high-amplitude variable stars selected from UGPS data releases DR5 and DR7 are located in star forming regions (SFRs) and have characteristics of YSOs. They concluded that YSOs likely dominate the Galactic disc population of high-amplitude variable stars in the near-infrared. Spectroscopic follow-up confirmed four new additions to the eruptive variable class. These objects showed a mixture of the characteristics of the optically-defined EXor and FUor subclasses. Two of them were deeply embedded sources with very steep 1 to 5 μm spectral energy distributions (SEDs), though showing “flat spectrum” SEDs at longer wavelengths. Such deeply embedded eruptive variables are regarded as a potentially distinct additional sub-class, though only a few had been detected previously: OO Ser, V2775 Ori, HOPS 383 and GM Cha (see Hodapp et al. 1996; Kóspál et al. 2007; Persi et al. 2007; Caratti o Garatti et al. 2011; Safron et al. 2015). With the aims of determining the incidence of eruptive variability among YSOs and characterising the phenomenon, we have undertaken a search of the multi-epoch VVV dataset. In contrast to UGPS, the ongoing VVV survey offers several dozen epochs of Ks data over a time baseline of a few years.

We have divided the results of this work in two publica-

tions. In this first study we present the method of the search and a general discussion on the photometric characteristics of the whole sample of high amplitude variables in the near-infrared. We present the follow-up and spectroscopic characteristics of a large sub-sample of candidate eruptive variable stars in a companion publication (hereinafter referred to as paper II).

In Sect. 2 of this work we describe the VVV survey, the data and the method used to select high amplitude infrared variables. Section 3 describes the make up and general properties of the sample, the evidence for clustering and the apparent association with SFRs. In this section we also classify the light curves of variables found outside SFRs and use this information to estimate the contamination of our high amplitude YSO sample by other types of variable star. We then estimate the high amplitude YSO source density from our sample and compare the average space density with those of other high amplitude infrared variables. In Sect. 4 we discuss the physical mechanisms that drive variability in YSOs and classify our YSOs via light curve morphology. This yields some ideas concerning which of the known mechanisms might be responsible for the observed variability. We test these mechanisms using two epoch JHK_s data. Then we discuss the trends in the likely YSOs as a function of evolutionary status based on their spectral energy distribution. Finally we discuss the large sample of likely eruptive variables. Section 6 presents a summary of our results.

2 VVV

The regions covered by the VVV survey comprise the Bulge region within $-10^\circ < l < +10^\circ$ and $-10^\circ < b < +5^\circ$ and the disc region in $295^\circ < l < 350^\circ$ and $-2^\circ < b < +2^\circ$ (see e.g., Minniti et al. 2010).

The data is collected by the Visible and Infrared Survey Telescope for Astronomy (VISTA). This is a 4m telescope located in Cerro Paranal Observatory in Chile and is designed to conduct large-scale surveys of the southern sky at near-infrared wavelengths, covering $0.9 < \lambda < 2.5 \mu\text{m}$. The telescope is equipped with a near-infrared camera consisting of an array of sixteen 2048×2048 pix detectors, with a typical pixel scale of $0.^{\prime\prime}339$, with each detector covering 694×694 arcsec 2 . The detectors are set in a 4×4 array and have large spacing along the X and Y axis. Therefore a single pointing, called a “pawprint”, covers 0.59° giving partial coverage of a particular field of view. A continuous coverage of a particular field is achieved by combining six single pointing with appropriate offsets. This combined image is called a tile. The instrument has five broad-band filters $ZYJHK_s$ available and two narrow filters at 0.98 and $1.18 \mu\text{m}$. VVV uses all 5 broadband filters.

The images are combined and processed at the Cambridge Astronomical Survey Unit (CASU). The tile catalogues are produced from the image resulting from combining six pawprints. The catalogues provide parameters such as positions and fluxes from different aperture sizes. A flag indicating the most probable morphological classification is also provided, with “-1” indicating stellar sources, “-2” borderline stellar, “1” non-stellar, “0” noise, “-7” indicating sources containing bad pixels and finally class=-9

related to saturation (for more details on all of the above, see Saito et al. 2012).

Quality control (QC) grades are also given by ESO according to requirements provided by the observer. These include constraints on parameters such as airmass, sky transparency, moon distance, seeing and ellipticity of the observations. According to whether observations fulfil the constraints established by the observer, these are classified as fully satisfied (QC A), almost satisfied, where for example only 10% of the constraints are violated (QC B) and finally not satisfied (QC C).

2.1 Selection Method

In order to search for variable stars we used the multi-epoch database of VVV comprising the observations of disc tiles with $|b| \leq 1^\circ$ taken between 2010 and 2012. We added the 2013 and 2014 data later to assist our analysis but they were not used in the selection. The catalogues were requested and downloaded from the CASU. We used catalogues of observations with QC grades A, B or C. Catalogues with QC grades C are still considered in order to increase the number of epochs. Some of them were still useful for our purposes. However, a small number of catalogues still presented some issues (e.g. zero point errors, bad seeing) making them useless, and as such were eliminated from the analysis. The number of catalogues in each tile varied from 14 to 23 epochs, with a median of 17 epochs per tile. When the 2013–14 data were added, the number of epochs available for the light curves rose to between 43 and 58. K_s photometry is derived from *apermag3* aperture fluxes ($2''$ diameter aperture).

For each tile, the individual catalogues are merged into a single master catalogue. The first catalogue to be used as a reference was selected as the catalogue with the highest number of sources on it. In every case this corresponded to the catalogue from the deep K_s observation (80 s on source), which was taken contemporaneously with the J and H band data (in 2010). For all other epochs the time on source was 16 s.

Figure 1 shows the typical scatter shown by stars at different magnitudes across the analysed range. In here we can see considerable scatter at bright magnitudes, due to effects of saturation, and the faint end of the distribution, which is dominated by photon noise. High amplitude variable star candidates are selected from the master catalogue from stars which fulfilled the following criteria in the 2010–12 data:

- (i) Detection with a stellar morphological classification (class = -1) in every available epoch.
- (ii) Ellipticity with $\text{ell} < 0.3$ in every epoch.
- (iii) The absolute difference (ΔK_s) between the brightest ($K_{s,\max}$) and faintest point ($K_{s,\min}$) in the light curve of the source to be larger than 1 magnitude (similar to the analysis in Contreras Peña et al. 2014).

The requirement for a detection at every available epoch in the 2010–12 interval was designed to exclude most transient objects such as novae, as well as reducing the number of false positives. This was the initial classification scheme. However, we observed that for each tile we were selecting a large number of sources as variable star candidates. Figure 2 shows the average K_s magnitude vs ΔK_s for variable stars in one of the VVV tiles. The figure shows that the majority of

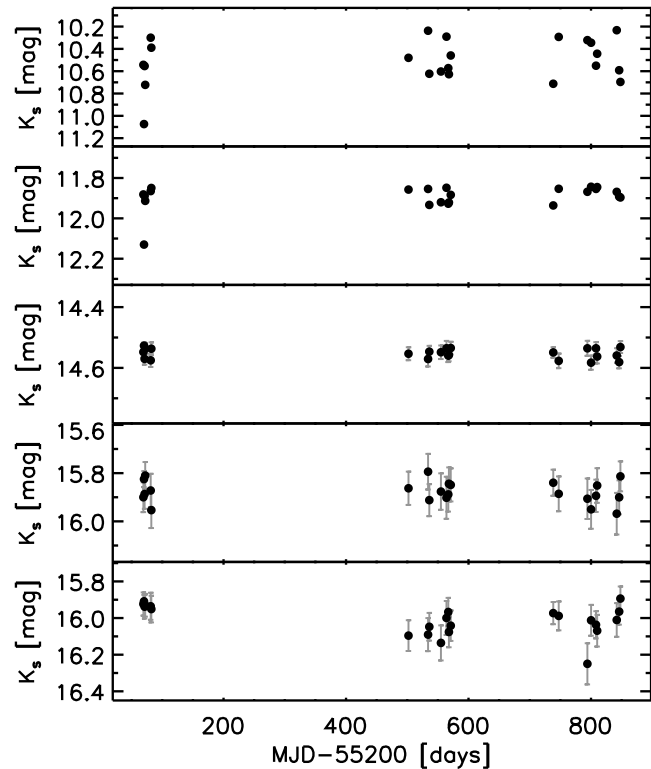


Figure 1. 2010–2012 light curves of “non-variable” VVV objects (i.e. not classified as high-amplitude variables in our analysis). These are presented to show the typical scatter in magnitude across the analysed magnitude range.

stars selected in the original classification scheme are located at the bright and faint ends of the distribution. The latter arise due to unreliable photometry at this faintest part. The VISTA detectors also become increasingly non-linear when reaching the saturation level. This non-linearity is corrected for in the creation of the catalogues, but differences between the magnitudes of the same object can still be observed, even for objects classified as stellar sources (Saito et al. 2012). Figure 10 in Saito et al. (2012) shows that when comparing the K_s magnitudes of stellar sources found in overlapping regions of adjacent disc tiles, stars found at the brighter end show an increasing difference in magnitude (an effect also observed in Cioni et al. 2011; Gonzalez et al. 2011). This effect would explain the large differences observed at the brighter end of Fig. 2. This part of the distribution also shows marked “finger-like” sequences. Each of the sequences can be explained by the fact that the VISTA detectors have different saturation levels. In order to minimize these effects we applied an additional cut.

(iv) We separated the average K_s distribution of Fig. 2 into bins of 0.5 magnitudes and derived the mean and standard deviation, σ , on ΔK_s for each bin. In order to select an object as a candidate variable star we required its ΔK_s to be 3σ above the mean ΔK_s at the corresponding magnitude level. This 3σ line is shown in red in Fig. 2 where we can see that it is able to account for the non-linearity effects at the bright end of the distribution.

This additional constraint reduced the number of variable star candidates by a large factor. The initial requirements yield 158478 stars; the additional cut reduced this to 5085

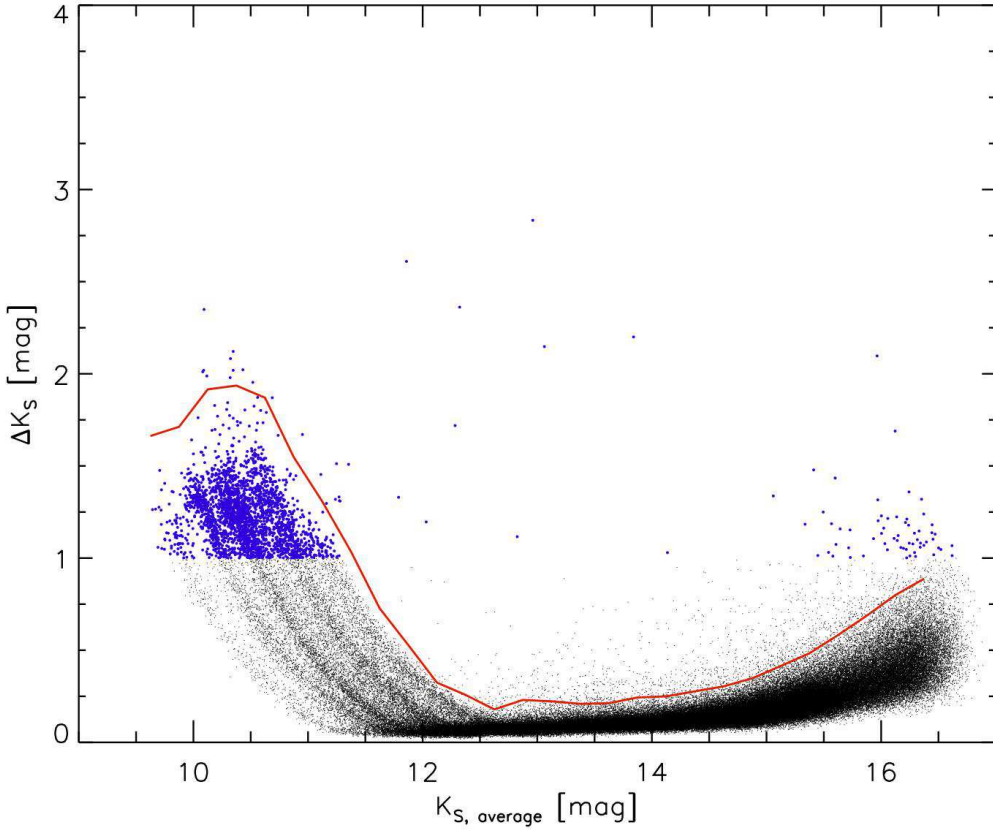


Figure 2. K_s vs ΔK_s for one of the VVV tiles studied in this work, showing stars with $\text{class} = -1$ and $\text{ellipticity} < 0.3$ in every epoch (black circles). Variable star candidates which fulfil the condition $\Delta K_s > 1$ magnitude are shown as blue circles. The red solid line marks the additional 3σ cut applied to the objects as explained in the text. Stars above this line are selected for subsequent visual inspection.

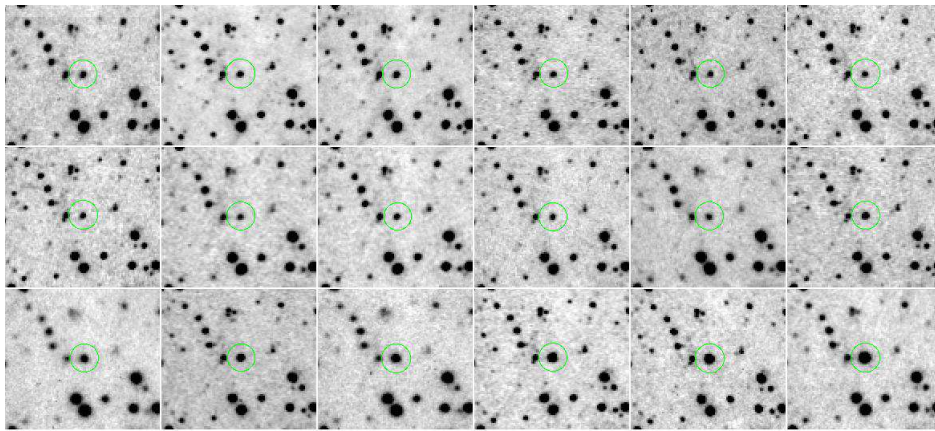


Figure 3. Example of the images used to visually inspect variable star candidates. In this case we show the images, taken between 2010 and 2012, of variable star VVVv322. Each image has a size of $30'' \times 30''$. The star gets brighter towards the end of the sequence.

stars. After the catalogue-based selection, we constructed $1' \times 1'$ cut-out images around each candidate for every available epoch. Variable stars were confirmed as real through visual inspection of the individual images (an example is shown in Fig. 3). The most common causes for the appearance of false positives were, bad pixels in the images, sat-

uration of bright sources, diffraction spikes and stars that were found on the edge of tiles.

This selection method yielded a total of 840 real variable stars. However, 25 of them are found twice as they are covered by adjacent tiles in VVV. The final list of VVV high-amplitude infrared variables consists of 816 stars. This

includes one variable star, VVVv815, that showed large variability in 2010 but did not meet all the selection criteria (see below). One other variable star in tile d046 was left out of early versions of the list but added to the end as VVVv816 shortly before this study was completed. The average magnitude for objects in the selected sample was found in the range $10.3 < K_s < 16.9$ mag.

Our requirement for a high quality detection at every epoch between 2010 and 2012 (see items (i) and (ii)) reduces the number of candidates requiring visual inspection but it is bound to cause us to miss some real variables, very likely including some the faintest or highest amplitude variables if they dropped below $K_s \sim 16$ during that time. A significant fraction of all VVV sources are blended with adjacent stars and they can fail to pass our cuts on the morphological class and ellipticity at one or more epochs in consequence. However, sources that pass these quality cuts are likely to be unblended and therefore to have reliable photometry. (Photometry from the VISTA pipeline is not always reliable for faint stars in crowded fields (see e.g. Saito et al. 2012)). In order to check the reliability of the pipeline photometry, especially for faint sources with $K_s = 15 - 16$ magnitudes, we obtained PSF photometry of all stars in tile d069 with DoPHOT (Schechter et al. 1993). The results confirmed that the variables found by our selection have reliable pipeline photometry. This is illustrated in Fig. 4 for variable star VVVv316, where the comparison of DoPHOT and VISTA pipeline photometry shows close agreement.

We investigated the incompleteness of our selection by examining two widely separated VVV disc tiles (d064 and d083), in which we removed our class and ellipticity cuts and required a minimum of only one detection in each year from 2010 to 2012 (with a stellar profile classification). This continues to select against transients and perhaps the most extreme variable YSOs but it allows us to assess incompleteness due to blending, which can cause sources to be absent or to have different profile classifications at different epochs. We found that this more relaxed selection added over 400 additional candidates in the two tiles down to (mean) $K_s = 15.5$, an increase of more than a factor of 10. Following visual inspection (see below), we found that the number of real high amplitude variables was increased by a factor of ~ 2 , up to a limit of $K_s = 15.5$. At fainter mean magnitudes the completeness of our selection with criteria (i) to (iv) falls more steeply because most high amplitude variables will not satisfy the quality cuts at every epoch as the sensitivity limit is approached.

A case of this selection effect is found in a variable star VVVv815 mentioned above. It showed a large variation ($\Delta K_s > 1$ magnitude) in the analysis of an early release of 2010 data. However, the star does not show up as a variable star candidate in the analysis described above. Inspection of the master catalogue for the respective tile shows that the star has a classification different from stellar in 3 out of 18 epochs available for tile d090 in the 2010–2012 period. This star is included in our final list of VVV high-amplitude variables because it is also part of the sample that has follow up spectroscopic observations.

The number of stars in the analysed VVV area that fulfil items 1 and 2 above is 12 789 000 stars. Considering

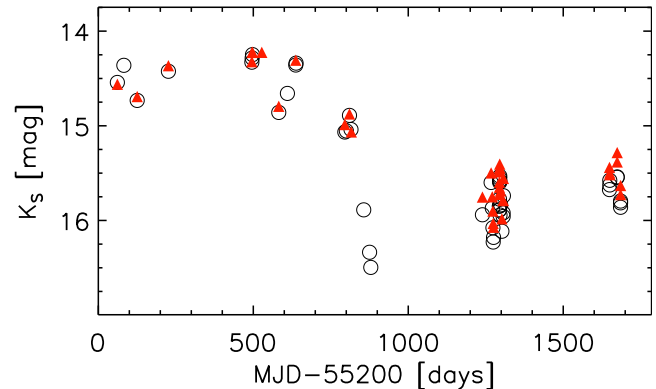


Figure 4. PSF (red triangles) vs aperture photometry (open circles) of star VVVv316. PSF photometry is shown only for data points classified as “good” or “good but faint” by DoPHOT.

the number of real variable stars we see that high-amplitude infrared variability was observed in approximately 1 out of 15000 stars in the Galactic mid-plane at $295 < l < 350^\circ$.

2.2 Issues with saturation

The aforementioned problems of saturation still affect a small number of stars in our sample. This effect can become important when individual epochs of stars in our sample are brighter than $K_s = 12$ magnitudes. Saturation will reduce the flux at the inner core of the star, thus the magnitude of the star derived by using smaller diameter for the aperture than the default $2''$ aperture, will be fainter than the magnitude obtained from the default aperture.

In order to check whether the star is saturated we first obtain the magnitudes from aperture photometry using the measure fluxed from five different diameters for the apertures. These diameters are $1''$ (Apermag1), $1.41''$ (Apermag2), $2''$ (Apermag3), $2.82''$ (Apermag4) and $4''$ (Apermag5). We find that saturated stars show relatively large differences between the magnitudes from the first three apertures, and we set a threshold for saturation as stars having both $\text{Apermag1-Apermag3} > 0.05$ mag and $\text{Apermag2-Apermag3} > 0.02$ mag. Thus any individual epoch of a star with $\text{Apermag3} < 12$ mag (in the K_s passband) and having these differences is flagged as saturated.

In order to correct for saturation, we follow Irwin (2009) and defined a ring outside the saturated core, to obtain a new flux estimate. We then determine an aperture correction for the ring from a set of bright, unsaturated stars found within $5'$ of our object of interest. In our analysis we derived new fluxes using the ring defined by Apermag2 and Apermag4. Comparison with 2MASS K_s photometry indicates that this choice of apertures extends the dynamic range by 2.5 magnitudes, relative to the pipeline photometry. We caution that comparison with 2MASS K_s photometry indicates that while this approach provides correct magnitudes, the uncertainties are large, typically 0.2 magnitudes.

**3 HIGH AMPLITUDE INFRARED
VARIABLES FROM VVV**

3.1 General characteristics

Object ID	VVV Designation	α (J2000)	δ (J2000)	l (degrees)	b (degrees)	Z (mag)	Z_{err} (mag)	Y (mag)	Y_{err} (mag)	J (mag)	J_{err} (mag)	H (mag)	H_{err} (mag)	K_s (mag)	$K_{s,err}$ (mag)	ΔK_s (mag)	α_{class}	SFR	Class
VVVv1	VVV J114135.16-622055.51	11:41:35.16	-62:20:55.51	294.92603	-0.56770140	—	—	—	—	17.99	0.06	15.95	0.02	14.44	0.01	1.34	-0.29	y	STV
VVVv2	VVV J114412.94-623449.09	11:44:12.94	-62:34:49.09	295.28005	-0.71145503	—	—	—	—	—	—	18.78	0.23	15.71	0.03	2.52	1.22	y	STV
VVVv3	VVV J115113.03-623729.29	11:51:13.03	-62:37:29.29	296.07199	-0.55784490	13.17	0.01	12.93	0.01	12.90	0.01	12.70	0.01	12.24	0.01	2.21	—	n	Known
VVVv4	VVV J115808.69-630708.60	11:58:08.69	-63:07:08.60	296.95057	-0.86785395	—	—	—	—	18.23	0.08	16.62	0.04	15.32	0.02	1.10	-0.24	y	STV
VVVv5	VVV J115959.68-622613.20	11:59:59.68	-62:26:13.20	297.02026	-0.15716131	17.69	0.02	16.62	0.01	15.87	0.01	15.25	0.01	13.53	0.01	1.30	—	n	LPV
VVVv6	VVV J115937.81-631109.77	11:59:37.81	-63:11:09.77	297.12836	-0.89953352	19.02	0.05	18.08	0.04	16.80	0.02	15.95	0.02	15.50	0.02	1.02	—	n	EB
VVVv7	VVV J120202.67-623615.60	12:02:02.67	-62:36:15.60	297.28472	-0.27538112	—	—	—	—	—	—	—	—	17.22	0.12	1.60	2.39	y	Eruptive
VVVv8	VVV J120059.11-631636.18	12:00:59.11	-63:16:36.18	297.29582	-0.95838309	—	—	—	—	—	—	—	—	16.86	0.09	1.38	0.64	y	Eruptive
VVVv9	VVV J120217.23-623647.83	12:02:17.23	-62:36:47.83	297.31381	-0.27887510	—	—	—	—	18.29	0.08	16.33	0.03	14.64	0.01	2.78	-0.39	y	Dipper
VVVv10	VVV J120250.85-622437.62	12:02:50.85	-62:24:37.62	297.33912	-0.067488967	18.57	0.04	18.23	0.05	16.97	0.03	16.35	0.03	16.07	0.04	1.19	—	n	STV
VVVv11	VVV J120436.62-625704.60	12:04:36.62	-62:57:04.60	297.63741	-0.56188470	20.20	0.19	19.01	0.13	17.87	0.07	16.79	0.05	16.08	0.08	1.10	—	n	STV
VVVv12	VVV J121033.19-630755.71	12:10:33.19	-63:07:55.71	298.33185	-0.62611408	—	—	—	—	—	—	16.30	0.03	15.04	0.03	1.74	0.28	y	Fader
VVVv13	VVV J121216.83-624838.32	12:12:16.83	-62:48:38.32	298.47603	-0.27813948	—	—	—	—	—	—	—	—	16.72	0.14	1.40	1.39	y	STV
VVVv14	VVV J121218.13-624904.48	12:12:18.13	-62:49:04.48	298.47958	-0.28494801	19.48	0.10	18.88	0.12	17.84	0.06	16.74	0.05	15.56	0.05	1.29	0.88	y	LPV-YSO
VVVv15	VVV J121226.09-624416.97	12:12:26.09	-62:44:16.97	298.48252	-0.20370785	19.00	0.07	17.72	0.04	16.57	0.02	15.60	0.02	15.04	0.03	1.09	—	y	EB
VVVv16	VVV J121329.76-624107.74	12:13:29.76	-62:41:07.74	298.59498	-0.13364186	18.01	0.03	17.13	0.02	16.06	0.01	14.72	0.01	13.66	0.01	1.29	0.92	y	Eruptive
VVVv17	VVV J121352.08-625549.90	12:13:52.08	-62:55:49.90	298.67278	-0.36986131	—	—	—	—	—	—	17.79	0.12	16.41	0.10	1.22	0.44	y	STV
VVVv18	VVV J121950.31-632142.24	12:19:50.31	-63:21:42.24	299.39868	-0.70694696	17.82	0.02	17.29	0.02	16.20	0.01	15.52	0.01	15.32	0.02	1.04	—	n	STV
VVVv19	VVV J122255.30-632352.56	12:22:55.30	-63:23:52.56	299.74594	-0.70270007	19.56	0.08	18.67	0.06	17.55	0.04	16.40	0.03	15.61	0.03	1.82	—	n	EB
VVVv20	VVV J122827.97-625713.97	12:28:27.97	-62:57:13.97	300.32402	-0.19848910	—	—	—	—	17.38	0.04	14.10	0.01	11.70	0.01	1.71	0.60	y	Eruptive
VVVv21	VVV J122902.24-625234.10	12:29:02.24	-62:52:34.10	300.38193	-0.11533229	—	—	—	—	—	—	17.12	0.05	15.80	0.03	1.79	0.86	y	LPV-YSO
VVVv22	VVV J123105.60-624457.34	12:31:05.60	-62:44:57.34	300.60547	0.030572382	—	—	—	—	18.81	0.14	16.94	0.05	15.55	0.03	1.73	-0.34	y	STV
VVVv23	VVV J123128.53-624433.10	12:31:28.53	-62:44:33.10	300.64855	0.040704993	19.44	0.07	18.37	0.05	17.14	0.03	15.57	0.02	14.40	0.01	1.51	-0.20	y	Fader
VVVv24	VVV J123235.68-634319.61	12:32:35.68	-63:43:19.61	300.84794	-0.92661506	17.17	0.01	16.13	0.01	14.05	0.01	12.95	0.01	12.23	0.01	1.20	—	n	LPV
VVVv25	VVV J123514.37-624715.63	12:35:14.37	-62:47:15.63	301.08129	0.025874751	—	—	—	—	—	—	16.01	0.02	12.34	0.01	1.68	0.22	y	Eruptive
VVVv26	VVV J123845.66-631136.03	12:38:45.66	-63:11:36.03	301.50320	-0.35674318	—	—	—	—	19.67	0.29	16.70	0.04	14.71	0.01	2.45	1.07	y	Eruptive
VVVv27	VVV J123848.33-633939.15	12:38:48.33	-63:39:39.15	301.53114	-0.82346677	—	—	—	—	—	—	—	—	12.04	0.01	2.73	—	n	LPV
VVVv28	VVV J123911.54-630524.76	12:39:11.54	-63:05:24.76	301.54688	-0.25137729	—	—	—	—	—	—	18.91	0.32	16.78	0.09	1.39	0.54	y	STV
VVVv29	VVV J123931.48-630720.38	12:39:31.48	-63:07:20.38	301.58593	-0.28169556	—	—	—	—	—	—	—	—	16.94	0.10	2.13	1.32	y	Eruptive
VVVv30	VVV J124140.56-635033.57	12:41:40.56	-63:50:33.57	301.85616	-0.99128045	17.92	0.02	17.22	0.02	16.40	0.02	15.66	0.02	15.23	0.02	1.22	—	n	EB
VVVv31	VVV J124140.15-635918.05	12:41:40.15	-63:59:18.05	301.86093	-1.1368922	13.91	0.01	13.27	0.01	12.46	0.01	12.08	0.01	11.69	0.01	1.15	—	n	LPV
VVVv32	VVV J124357.15-625445.09	12:43:57.15	-62:54:45.09	302.07991	-0.053137952	19.58	0.07	18.08	0.04	16.07	0.01	14.07	0.01	12.45	0.01	2.49	0.33	y	LPV-YSO
VVVv33	VVV J124425.05-631355.76	12:44:25.05	-63:13:55.76	302.14153	-0.37116019	—	—	—	—	—	—	18.10	0.16	16.43	0.07	1.37	—	n	STV
VVVv34	VVV J125029.87-625124.93	12:50:29.87	-62:51:24.93	302.82470	0.014648658	19.22	0.05	18.32	0.05	17.86	0.06	16.70	0.04	15.71	0.03	1.30	-0.34	y	STV
VVVv35	VVV J125206.52-635711.52	12:52:06.52	-63:57:11.52	303.00557	-1.0815235	17.62	0.01	16.85	0.01	17.13	0.03	16.21	0.03	15.97	0.04	1.24	—	n	EB
VVVv36	VVV J125917.72-633008.44	12:59:17.72	-63:30:08.44	303.80825	-0.64394398	14.38	0.01	13.84	0.01	13.27	0.01	12.56	0.01	11.81	0.01	1.03	-0.11	y	Eruptive
VVVv37	VVV J130243.05-631130.00	13:02:43.05	-63:11:30.00	304.20331	-0.34774357	18.80	0.03	17.75	0.03	16.74	0.02	15.89	0.02	15.38	0.03	1.34	—	n	STV
VVVv38	VVV J130311.38-631439.09	13:03:11.38	-63:14:39.09	304.25411	-0.40259280	—	—	—	—	—	—	17.79	0.13	16.32	0.07	1.41	1.20	y	STV
VVVv39	VVV J130440.98-635313.45	13:04:40.98	-63:53:13.45	304.38893	-1.0527733	18.67	0.03	17.89	0.03	17.57	0.05	16.38	0.04	15.49	0.03	1.51	—	n	STV
VVVv40	VVV J130600.43-630144.40	13:06:00.43	-63:01:44.40	304.58298	-0.20394282	20.71	0.20	19.49	0.14	16.52	0.02	15.42	0.02	14.69	0.01	1.24	—	n	EB

Table 1. Parameters of the high-amplitude variables from VVV. For the description of the columns see Sect. 3.1. Here we show the first 40 sources in the list. The complete list is available online.

The selection method of Sect. 2.1 yields 816 high amplitude ($\Delta K_s > 1$ mag) infrared variables. In order to study the properties of these stars, we searched for additional information in available public databases. This search can be summarized as follows:

- **SIMBAD** We query the SIMBAD database (Wenger et al. 2000) for astronomical objects within a radius of $5'$ centred on the VVV object.

- **Vizier** Additional information was provided with the use of the Vizier database (Ochsenbein et al. 2000). In here we queried whether the VVV object was found within $2''$ of objects found in astronomical catalogues that were not available in SIMBAD.

- **The NASA/IPAC Infrared Science Archive (IRSA)** In here we queried for additional information in several near- and mid-infrared public surveys, which include 2MASS (Skrutskie et al. 2006), DENIS (Epcstein et al. 1994), *Spitzer*/GLIMPSE surveys (see e.g., Benjamin et al. 2003), WISE (Wright et al. 2010), Akari (Murakami et al. 2007) and MSX6C (Price et al. 2001). The search was done automatically using the IDL scripts provided at the IRSA website. The catalogues were queried for objects found within a $10''$ radius of the VVV object. In most cases, several objects are found at these distances, then we only selected the nearest object to our star. In order to confirm whether these detections correspond to our variable star, $1' \times 1'$ VVV images around the star were visually inspected.

In addition, we used the WISE image service within IRSA to inspect multi-colour images of the areas around our variable stars, in order to establish a possible association of the VVV object with a SFR.

The general properties of the sample can be found in Table 1. Column 1 presents the original designation given to the sources. Column 2 corresponds to the full VVV designation for the source. Coordinates for the objects are given in Columns 3 and 4, with columns 5 and 6 presenting the Galactic coordinates of the sources. In columns 7, 8, 9, 10 and 11 we present the nearly contemporaneous Z , Y , J , H , K_s photometry from VVV. Column 12 gives ΔK_s , the absolute value of the peak-to-trough difference from the 2010–2014 light curves from VVV. Column 13 presents α_{class} , the 2 to $23\mu m$ spectral index parameter that relates to the evolutionary class of sources that appear to be associated with SFRs (the method and data used to estimate this parameter is explained in Sect. 4.3). In column 14 we present whether the object is likely associated with SFRs or not. Finally column 15 presents the classification of the object from its light curve. The latter is discussed throughout the text.

Most of the variable stars are unknown from searches in SIMBAD and Vizier (~ 98 per cent). Among the known variables there are 2 novae, Nova Cen 2005 and Nova Cen 2008 (Hughes et al. 2010; Saito et al. 2013), 2 eclipsing binaries (EBs), EROS2-GSA J132758-631449 and PT Cen (Derue et al. 2002; Budding et al. 2004), 1 high-mass X-ray binary, BR Cir (see e.g. Tudose et al. 2008) and 9 OH/IR stars. Among the objects not previously classified as variable stars, 159 are found in the Spitzer/GLIMPSE catalogue of intrinsically red sources from (Robitaille et al. 2008), with the majority being classified as likely YSOs from their mid-IR colours and brightness.

3.2 YSO population

At this point, the reader should note that most of the variables are listed as spatially associated with SFRs (~ 54 per cent, see Sect. 3.3 and 4) and these stars have spectral indices that indicate a Class I or flat spectrum evolutionary status, therefore they are likely in an early evolutionary stage. They are usually sufficiently red to be undetected ($i > 21$ mag) in sensitive panoramic optical surveys such as VPHAS+ (Drew et al. 2014) unlike most of the known FUor and EXors. The spectral indices of the YSOs are discussed later in Sect. 4.3 following classification of the light curves and an attempt to decontaminate chance projections of other variables in SFRs.

3.3 Association with SFRs

Figure 5 shows the distribution for the 816 VVV variables across the Galactic midplane. It can be seen that our objects appear to be highly clustered, with their distribution following that of the SFRs from the Avedisova et al. (2002) catalogue (red diamonds in the bottom plot of Fig. 5). To study the apparent clustering, we derive the two-point angular correlation function, $w(\theta)$ and the nearest neighbour distribution of the sample of high amplitude variables. To derive $w(\theta)$, we follow Bate et al. (1998) and first estimate the mean surface density of companions (MSDC). For each star, we compute the angular separation, θ , to all other stars, and bin the separation into annuli of separation θ to $\theta + \delta\theta$. The MSDC results from dividing the number of pairs found, N_p , at a given separation by the area of the annulus, and dividing by the total number of stars, N_* , or

$$MSDC = \frac{N_p}{2\pi\theta\delta\theta N_*}$$

The latter relates to $w(\theta)$ as

$$w(\theta) = MSDC \times \frac{A}{N_*} - 1$$

where A is the area covered by the survey (Bate et al. 1998, and references therein). This correlation function is valid as long as the separations θ are smaller than the angular length of the sample. We show the two-point correlation function in Fig. 6. We can see that we don't find any pairs for separations $\theta < 20''$, hence $w(\theta) = -1$. For separations between $20''$ and $100''$ $w(\theta)$ is larger than the values expected for random pairings ($w(\theta) = 0$) and it remains somewhat above zero for separations up to a few hundred arcseconds. This nearest neighbour distribution of Fig. 6, also shows an excess of close neighbours at distances $R < 200''$, compared to the expected number from a random (Poisson) distribution. Thus we are confident that we are tracing clustering in the VVV sample, on a spatial scale similar to that of distant Galactic clusters and star formation regions.

As an illustration of how variable stars in VVV are preferentially located in areas of star formation, Fig. 7 shows the K_s image of the area covered in tile d065. Twenty five highly variable stars are found in this tile, and it is clear that these are not evenly distributed along the area covered in d065, and instead are found clustered around an area of star for-

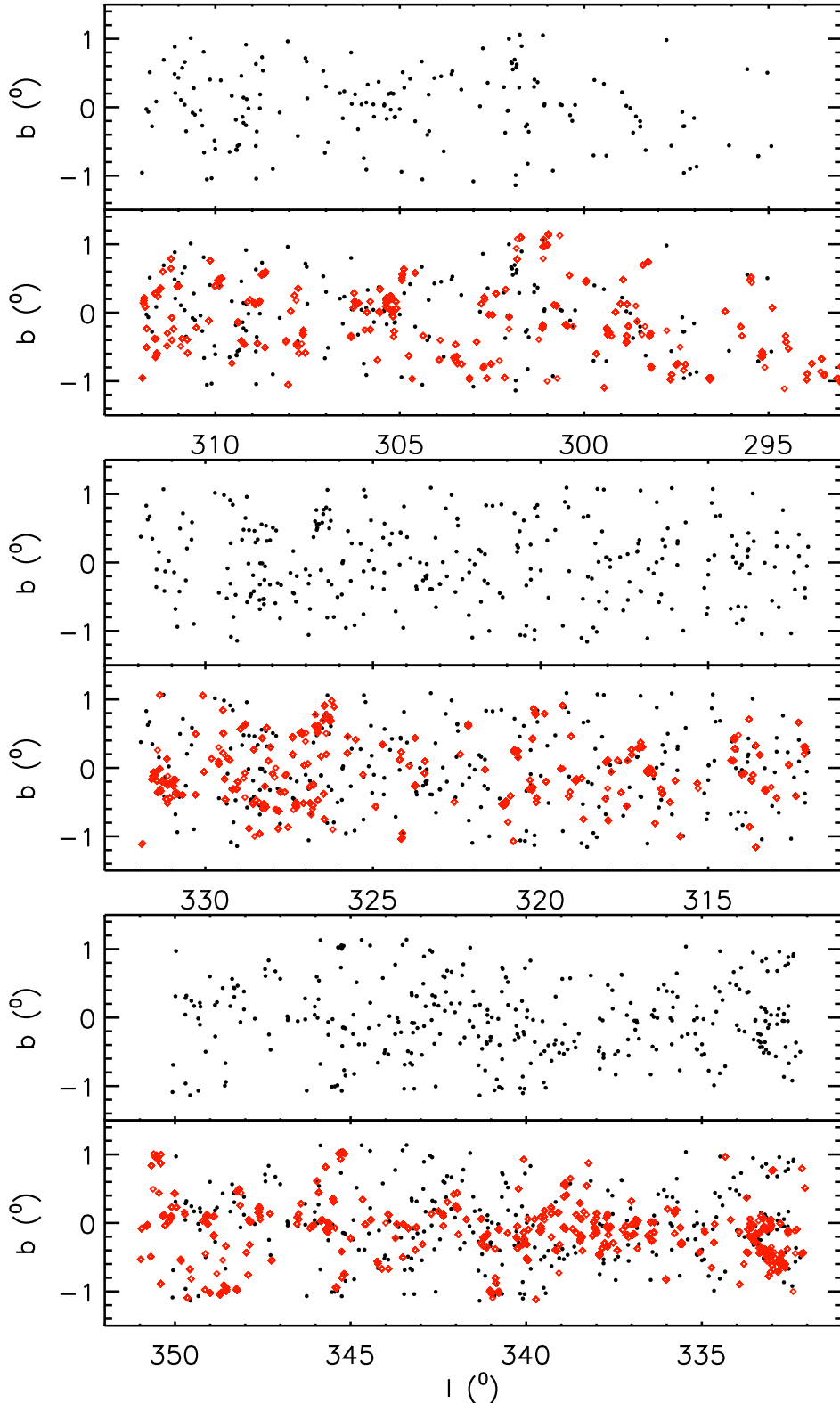


Figure 5. Galactic distribution of the 816 high amplitude variable stars (black circles) selected from VVV (top), the bottom graph shows the same distribution, but this time including the areas of star formation from the Avedisova (2002) catalogue (red diamonds).

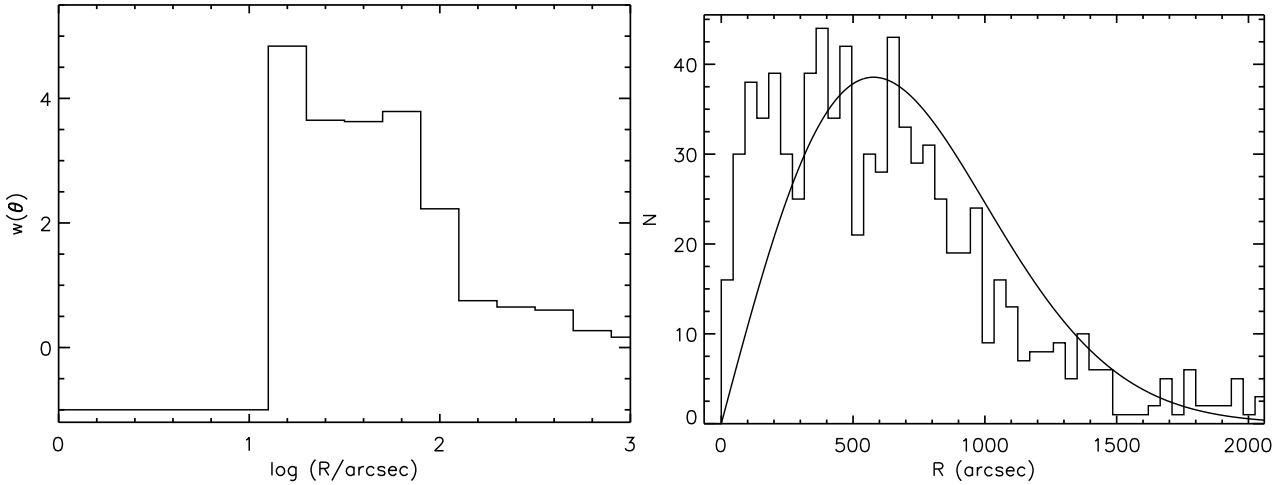


Figure 6. (left) Two-point angular correlation function of the sample of VVV high-amplitude variables. (right) Nearest neighbour distribution for the same sample. The smooth curve represents the expected distribution of a random (Poisson) distribution.

mation, which is better appreciated in the cut-out image from WISE (Wright et al. 2010).

To establish a likely association with a SFR we used the criteria established in the UGPS search (see Contreras Peña et al. 2014), which were based on entries in the SIMBAD database and the Avedisova catalogue within a 5' radius of each high amplitude variable. In addition we also check WISE images for evidence of star formation in the area of the object, e.g. evidence of bright extended 12 μm emission near the location of the objects or the finding of several stars with red W1-W2 colours (sources appearing green, yellow or red in WISE colour images) around the VVV object. We find that 530 of our variable stars are spatially associated with SFRs, which represents 65% of the sample, remarkably similar to the observed association in UGPS objects (Contreras Peña et al. 2014).

3.4 Contamination by non-YSOs

In Contreras Peña et al. (2014), we estimated that about 10% of objects are probable chance associations with SFRs. This number is likely to be larger in our current analysis given that: (i) we are sampling mid-plane sightlines across the Galactic disk; (ii) the higher extinction in the Galactic midplane and the brighter saturation limit of VVV than UGPS, allows for a larger number of bright evolved variable stars to show up in our results. To determine the percentage of objects that might be catalogued as likely associated with SFRs by chance, we used the following method:

- a) Create a master catalogue of objects in the 76 tiles that were classified as stars in each of the epochs from the 2010–2012 analysis.
- b) Select 816 stars randomly from this catalogue and query SIMBAD for objects found in a 5' radius.
- c) Count the number of objects within this radius that were classified in any of the categories that could relate to star formation. This categories included TT Tauri and Herbig Ae/Be stars, HII regions, Dark clouds, dense cores, mm and smm source, FU Orionis stars, among others.
- d) Repeat items b through c 40 times.

Figure 8 shows the number of stars found within 5' of the VVV object and that were classified in the categories shown above, N_{simbad} vs the percentage of VVV objects with this number. It is already apparent that the percentage of chance selection will be higher than the estimated from GPS. However, we note that in order for an object to be flagged as associated with an SFR in Table 1, we needed at least 4 SIMBAD objects to appear within the 5' radius, thus giving us an estimate that ~30% of the non-YSO population is spatially associated with an SFR by chance. Inspection of WISE images of 100 randomly selected sources yields a similar fraction of chance associations but most of these were also identified as SFR-associated from the SIMBAD results, so the WISE data only slightly increased the chance association fraction. The Avedisova catalogue added an even smaller fraction of chance associations not indicated by the SIMBAD and WISE data, so the final chance association probability for non-YSOs with star formation regions is 35%.

The number of non-YSOs in the SFR-associated sample is less than 35% because non-YSOs do not dominate the full high amplitude sample but constitute about half of it. We found 286/816 (35%) of variables found outside SFRs, i.e. in 65% of the area, suggesting that 54% ($35/0.65$) of the sample is composed of objects other than YSOs but this neglects the fact that some YSOs will be members of SFRs that are not known in the literature nor visible in WISE images (see Sect. 3.5). Consequently, random addition of 35% of half of the total sample of 816 variables to the SFR-associated sample would be expected to cause only 27% contamination of the SFR-associated subsample by non-YSOs. This conclusion that the SFR-associated population of variables is dominated by bona-fide YSOs is supported by the two colour diagrams (figures 10 and 22) and light curves of the population (see Sect. 3.5 and Sect. 4.1), which differ from those outside SFRs. We note that the results of spectroscopic follow-up of a subsample of VVV objects associated with SFRs (Paper II) show a figure of 25%, a consistent figure despite some additional selection effects in that subsample

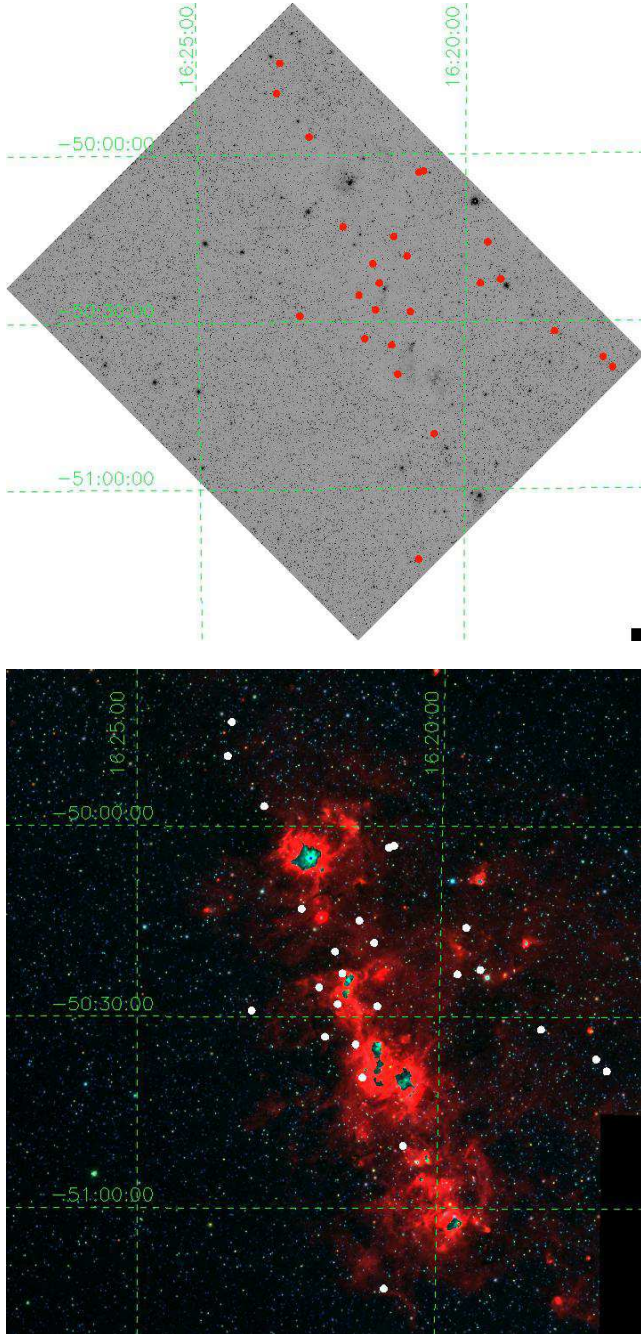


Figure 7. The top graph shows the K_s image of tile d065 along with the high amplitude variable stars found in this region. The clustering of the variable stars is already apparent in this image. The bottom graph shows the WISE false colour image of the same region (blue=3.5 μm , green=4.6 μm , red=12 μm). In here, the fact that variable stars preferentially locate around areas of star formation can be better appreciated.

3.5 Properties of Variables outside SFRs

To establish the nature of the objects that could be contaminating our sample of likely YSOs, and may also be interesting variable stars, we study the properties of objects found outside areas of star formation.. Many of these are listed in Simbad as IR sources (from the IRAS and MSX6C catalogues) and associated with OH masers, as well as be-

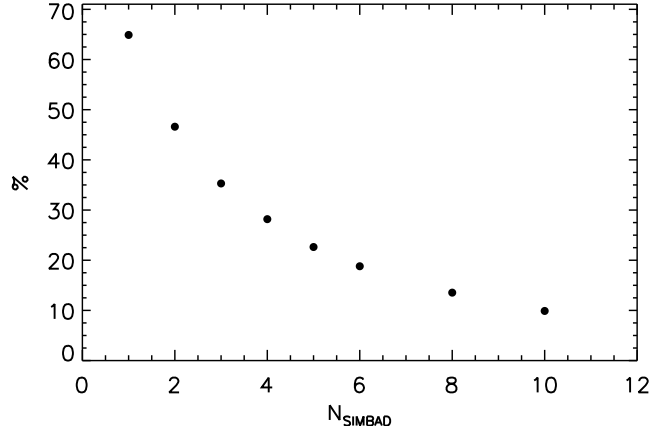


Figure 8. Percentage of objects flagged as likely associated with SFRs as a function of the number of objects classified in the categories that could relate to star formation found within a 5' radius query in SIMBAD.

ing catalogued as evolved stars in previous surveys. Visual inspection of their light curves also shows that a large percentage of objects have periodic variability, with $P > 100$ days, whilst the remainder of the sample shows variability over shorter timescales in the order of $P < 20$ days. We use the phase dispersion minimization (PDM, Stellingwerf 1978) algorithm found in the NOAO package in IRAF to search for a period in the light curve of these objects. This allows us to derive the periods or at least the approximate timescale of the variability of objects found outside areas of star formation. To provide a comparison with the PDM results we also used the GATSPY LOMBSCARGLEFAST implementation of the Lomb Scargle algorithm, which benefits from automatic optimisation of the frequency grid so that significant periods are not missed. We found that PDM was generally better for the purpose of this initial investigation. The Lomb Scargle algorithm is designed to detect sinusoidal variations whereas PDM makes no assumptions about the form of the light curve and is therefore much more sensitive to the periods of eclipsing binaries, for example. The Lomb Scargle method did help with the classification of a small number of long period variables (LPVs).

Out of the 286 stars in this subsample, 5 objects correspond to known objects from the literature (novae, EBs and a high mass X-ray binary), 45% of them are LPVs and 17% are EBs where we are able to measure a period. In addition, 30% of the sample is comprised of objects in which variability seems to occur on short timescales. The light curves of many objects in the latter group resemble those of EBs with measured periods, but with only 1 or 2 dips sampled in the dataset. We suspect that most of these could also be EBs but we are not able to establish the periods. Finally, we also find 18 objects (6%) that do not appear to belong to any of the former classes. In Fig. 9 we show two examples of objects belonging to these different subclasses where a period could be derived. The LPV VVVv215 is typical of many of the dusty Mira variables in the dataset that show long term trends caused by changes in the extinction of the circumstellar dust shell. These trends are superimposed on the pulsational, approximately sinusoidal variations, with the result

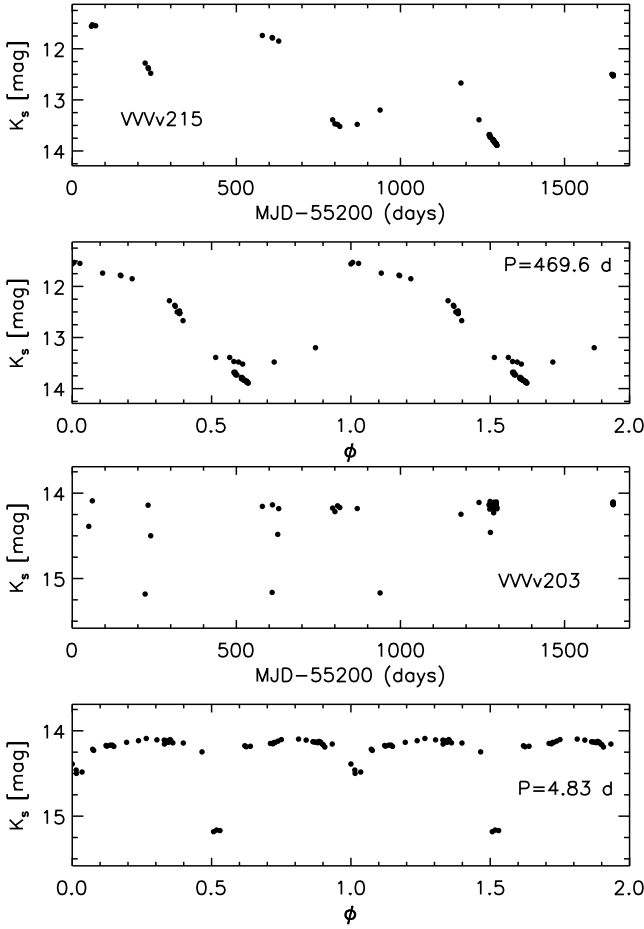


Figure 9. Examples of K_s light curves for objects not associated with SFRs. (top) the long period variable VVVv215. (bottom) the eclipsing binary VVVv203.

that the K_s magnitude at a given point in the phase curve can differ between cycles.

The objects belonging to different classes show very different properties. Figure 10 shows the K_s distribution for these objects, where it can be seen that the LPVs dominate the bright end of the distribution with a peak at $K_s \sim 11.8$ magnitudes, and showing a sharp drop at brighter magnitudes, probably due to the effects of saturation. EBs and other classes are usually found at fainter magnitudes. The near-infrared colours of the two samples (bottom plot of Fig. 10) show that LPVs tend to be highly reddened objects or have larger $(H - K_s)$ colours than EBs and other classes, which usually have the colours of lightly reddened main sequence and giant stars. We will see in Sect. 4 that this low reddening and lack of K band excess (in most cases) distinguishes the EBs and other shorter period variables from the sample spatially associated with SFRs, so contamination of the SFR sample by these shorter-period variables should not be very significant.

The colour-colour diagram of Fig. 10 also supports the idea that this sample might contain some bona fide YSOs that are not revealed by our searches of SIMBAD and the WISE images, as mentioned in our discussion of contamination. In the figure we observe objects (red circles) that show $(H - K_s)$ colour excesses and are neither known vari-

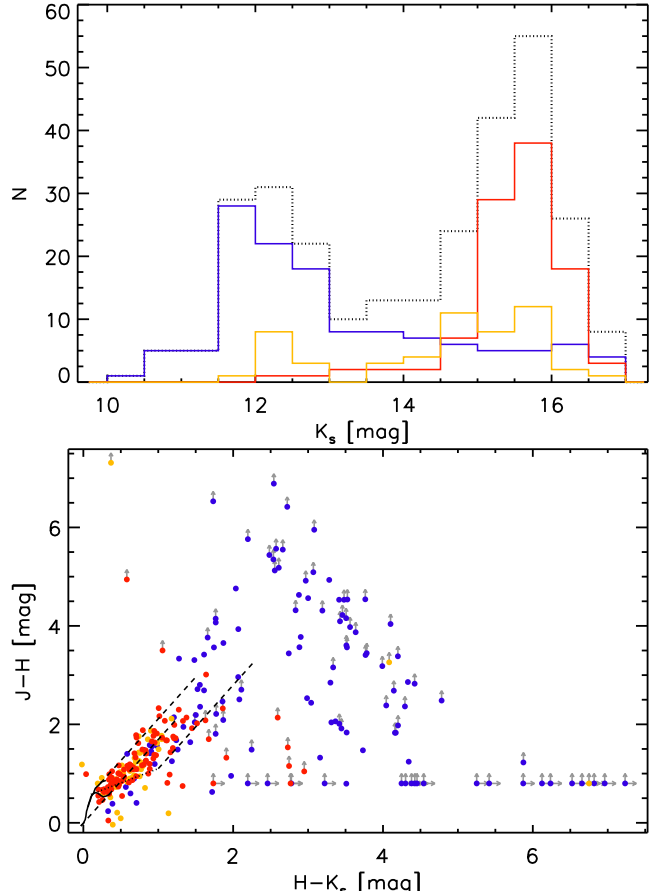


Figure 10. (top) Overall K_s distribution (from 2010 data) of objects not associated with SFRs (dotted line), and the same distribution separated for LPVs (solid blue line), EBs and known objects (solid orange line), and other classes of variable stars (solid red line). (bottom) $(J - H)$, $(H - K_s)$ colour-colour diagram for LPVs (blue circles), EBs and known objects (orange circles), and other classes of variable stars (red circles). In the diagram, arrows mark upper limits. The solid curve at the lower left indicates the colours of main sequence stars. The short-dashed line is the CTTS locus of Meyer et al. (1997) and the long-dashed lines are reddening vectors.

ables nor classified as LPVs or EBs. By simply selecting red circles located to the right of the reddening vector passing through the reddest main sequence stars we estimate that 44 objects have colours consistent with a YSO nature. This would represent 15% of objects outside SFRs and 5% of the full sample of 816 variables. A more detailed study would of course be needed to confirm their nature as YSOs. We also note that the lower left part of the CTTS locus plotted in the figure extends into the region occupied by lightly reddened main sequence stars, so in principle some of these individual red circles can potentially be YSOs.

The bright LPVs are very likely pulsating Asymptotic Giant Branch (AGB) stars. These type of stars are usually divided into Mira variables, which are characterized by displaying variability of $\Delta K > 0.4$ magnitudes and with periods in the range $100 < P < 400$ d, and dust-enshrouded AGB stars (usually named variable OH/IR stars), which are heavily obscured in the optical due to the thick circumstellar envelopes (CSE) developed by heavy mass loss

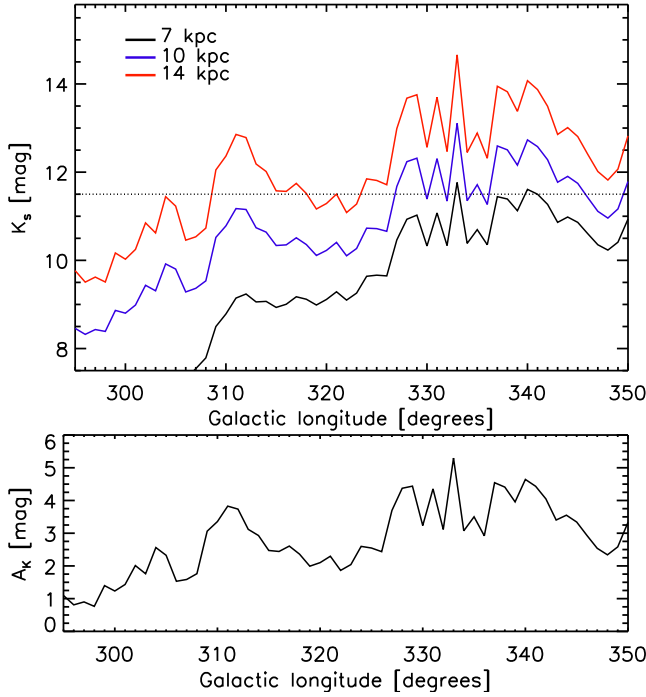


Figure 11. (top) Apparent K_s magnitude, derived as explained in the text, for a Mira variable located at the Galactic disc edge (solid red line). The same value is shown for a Mira located at lower Galactic radii $R_{GC} = 10$ kpc (blue line) and $R_{GC} = 7$ kpc (black line). The magnitude where the number of detections for LPVs drops ($K_s = 11.5$ magnitudes) is marked by a dotted line. (bottom) K-band extinction as a function of Galactic longitude.

($\sim 10^{-4} M_\odot \text{ yr}^{-1}$). The latter objects display larger amplitudes in the K-band (up to 4 magnitudes) and have periods between $400 < P < 2000$ d (for the above, see e.g. Jiménez-Esteban et al. 2006a; Whitelock et al. 2008).

AGB stars are bright objects and should be saturated at the magnitudes covered in VVV. However, due to the large extinctions towards the Galactic mid-plane we are more likely to observe these type of objects in VVV compared to our previous UKIDSS study. We can estimate the apparent magnitude of Mira variables at the different Galactic longitudes covered in VVV, and by assuming that these objects are located at the Galactic disc edge ($R_{GC} = 14$ kpc Minniti et al. 2011) and then considering other Galactocentric radii. At a given longitude, l , we derive A_V as the mean value of the interstellar extinction found at latitudes b between -1° and 1° . The interstellar extinction is taken from the Schlegel et al. (1998) reddening maps, and corrected following Schlafly & Finkbeiner (2011), i.e. $E(B-V) = 0.86E(B-V)_{\text{Schlegel}}$. We then assume that extinction increases linearly with distance, at a rate A_V/D_{edge} (mag kpc $^{-1}$), with D_{edge} the distance to the Galactic disc edge at the corresponding l . We finally take the absolute magnitude as $M_K = -7.25$ (Whitelock et al. 2008).

Figure 11 shows the estimated apparent magnitudes of Mira variables at different l and at varying R_{GC} . In the figure we also show the magnitude, $K_s = 11.5$, that marks the drop in the number of the detection of these objects, as observed in the histograms of the K_s distribution (Fig. 10). We can see as we move away from the Galactic center, a Mira

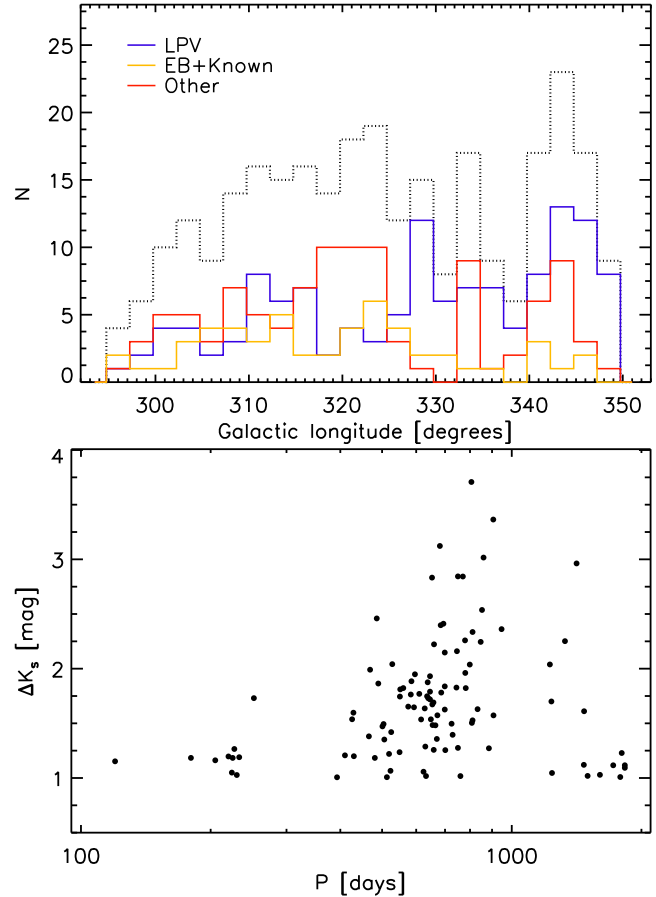


Figure 12. (top) Overall Galactic longitude distribution of objects outside SFRs (black line). We also show the same distribution divided into LPVs (blue line), EBs and known objects (orange line), and other classes of variable stars (red line). (bottom) Period vs K_s amplitude for LPVs with a measured period.

variable would most likely saturate in VVV, especially at $l < 310^\circ$. This occurs due to the effects of having relatively larger extinctions towards the Galactic center (see bottom plot of Fig. 11) and that a star at $R_{GC} = 14$ kpc is located farther away from the observer as l approaches $l = 0^\circ$. We note that Ishihara et al. (2011) finds that most AGB stars are found at $R_{GC} < 10$ kpc so if we place a Mira variable at smaller Galactic radii ($R_{GC} = 7, 10$ kpc), we see that is less likely for such a star to show up in our sample. However, variable OH/IR stars which undergo heavy mass loss, are heavily extinguished due to their thick circumstellar envelope, and thus are fainter than Mira variables (AGB stars with optically thick envelopes are found to be ~ 5 K_s magnitudes fainter than objects with optically thin envelopes in the work of Jiménez-Esteban et al. 2006b) and thus less likely to saturate in VVV, even at large distances. Then most AGB stars in our sample are probably dust-enshrouded objects.

The observations confirm the expected from the analysis above. Figure 12 shows that the number of LPVs increases as we come closer to the Galactic center. In addition, when taking into account AGB stars with measured periods, we confirm that the majority of AGB stars show periods longer than 400 days and large amplitudes (see bottom plot in Fig. 12), as expected in heavily obscured AGB

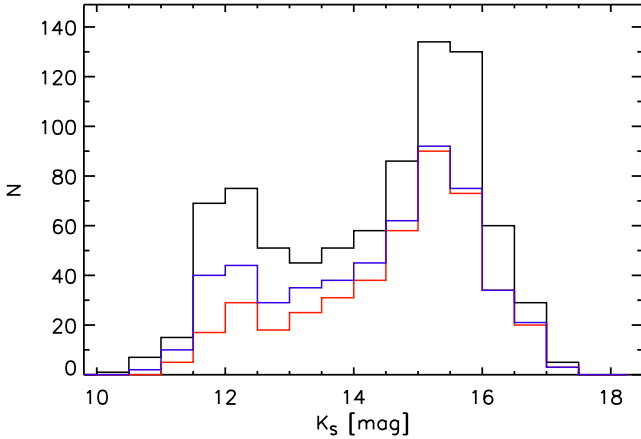


Figure 13. K_s distribution (from 2010 data) of the 816 VVV selected variable stars (solid black line). We show the same distribution for the overall sample of stars found to be likely associated with areas of star formation (blue line) and for the same sample but removing objects that show Mira-like light curves in Sect. 4.1 (red line).

stars. It is interesting to see in the same figure, that variable objects with periods longer than 1500 days show lower amplitudes than expected for their long periods. This is similar to the observed trend in the variable OH/IR stars of Jiménez-Esteban et al. (2006a). According to the authors, these objects correspond to stars at the end of the AGB.

This population of bright pulsating AGB stars can also explain the observed bimodality of the K_s distribution for the full sample of VVV high amplitude variable stars (see Fig. 13). The peaks of the distribution occur at $K_s \sim 11.8$ and $K_s \sim 15.8$. The peak at the bright end is at the same magnitude as the peak for LPVs.

When we only plot objects which are found to be likely associated with areas of star formation, the peak at the bright becomes less evident (see blue histogram in Fig. 13). When we plot only SFR-associated sources that do not have LPV-like light curves (see Sect. 4.1) the bimodality almost disappears, as shown by the red histogram in Fig. 13. AGB stars are probably the main source of contamination in our search for eruptive YSOs in SFRs, especially dust-enshrouded OH/IR stars which can have infrared colours resembling those of YSOs. Hence it is fortunate that we can remove most of this contamination by selecting against LPV-like light curves.

3.6 YSO source density

Our finding in Sect. 3.3 that YSOs constitute about half of the detected population of high amplitude variables in VVV disc fields indicates that they represent the largest single population of high-amplitude infrared variables, at least in the range $11 < K < 17$. Our analysis only considered the VVV disc tiles with $|b| < 1^\circ$, this amounts to 76 tiles, covering each 1.636 deg^2 of the sky. After allowing for the small overlaps between adjacent tiles, the total area covered in this part of the survey is 119.21 deg^2 . Adopting a 50% YSO fraction for the full sample of 816 variables implies a source density of 3.4 deg^{-2} . As noted in Sect. 2.1, the stringent data quality cuts in our selection procedure excluded

$\sim 50\%$ of high amplitude variables down to $K_s=15.5$, and a high fraction at fainter magnitudes where completeness falls (see Fig. 13). The corrected source density is therefore $\sim 7 \text{ deg}^{-2}$.

When considering the source density of high amplitude infrared variables in the UGPS, Contreras Peña et al. (2014) argued that the observed source density under-estimates the actual source density due to three main effects: (1) with only two epochs of K-band data most high amplitude variables will be missed; (2) the source density rises towards the magnitude cut of $K < 16$, indicating that many low luminosity PMS variables that are detected at distances of 1.4 to 2 kpc would be missed at larger distances; and (3) the dataset used in the UGPS search of Contreras Peña et al. excludes the mid-plane and is therefore strongly biased against SFRs. The UGPS YSO source density is estimated to reach 12.7 deg^{-2} when correcting for these 3 factors. In the case of VVV, given the higher number of epochs obtained from this survey, and that this analysis is not biased against areas of star formation, the source density is only likely to be affected by item (2) of the UGPS analysis. Figure 13 shows the magnitude distribution of the VVV variables associated with SFRs, where we can see a similar behaviour to the UGPS results, with the density of sources rising steeply towards faint magnitudes. Contrary to the UGPS search, we do not have a hard magnitude cut in the VVV sample, which includes sources as faint as $K_s \sim 17$. However, the number of sources decreases at $K_s > 16$, so we estimate an effective magnitude detection limit of $K_s = 16.25$ magnitudes. This implies that if typical sources from VVV have similar characteristics to UGPS objects in Cygnus and Serpens ($K=14.8$, $d=1.4\text{-}2$ kpc), then we would not detect them at distances $d > 3.32$ kpc. The complete sample of star forming complexes from Russeil (2003) shows that 83% of them are located beyond these distances. Correcting for this factor we then estimate a true source density of 41 deg^{-2} , though this figure does not include YSOs with low mass and luminosity that are too faint to be sampled by VVV due to the absence of nearby SFRs in the survey area. This figure of 41 deg^{-2} is somewhat larger than the one estimated from the UGPS analysis of Contreras Peña et al. (2014) (12.7 deg^{-2}).

Two effects can account for the somewhat higher source density in VVV than UGPS. (1) High luminosity YSOs are less common, but they can be observed at larger distances. The UGPS study would not find such objects at large distances because the available dataset did not cover the mid-plane of the Galactic disc, in which all distant SFRs are located due to their small scale height. Since VVV does cover the midplane we are able to detect these rare higher luminosity YSOs. This seems to be supported by the slightly larger distances established for members of the spectroscopic subsample in paper II. (2) In the UGPS study, most (23/29) of the variables in SFRs were located in just 2 large SFRs: the Serpens OB2 association and portions of Cygnus X. The much smaller size of the UGPS sample (in number of SFRs and number of variables) meant that there was considerable statistical uncertainty in the area-averaged source density. Moreover, the incidence of high amplitude variability is greater at the earlier stages of YSO evolution (see Sect. 4.3) so the numbers in the UGPS study may have been reduced by a relative lack of YSOs at these stages in the two large SFRs surveyed.

The estimated highly variable YSO source density remains much larger than that estimated for Mira variables in Contreras Peña et al. (2014), indicating a higher average space density for the variable YSOs. The observed variables in SFRs also outnumber the EBs and unclassified variables in the magnitude range of this study. However, we are likely to miss a large part of the population of high amplitude EBs due to the sparse time sampling of VVV.

In Appendix A we attempt to calculate the source density and space density of high amplitude EBs from the OGLE-III Galactic disc sample of Pietrukowicz et al. (2013). In this we are aided by a recent analysis of the physical properties of the large sample of *Kepler* eclipsing binaries (Armstrong et al. 2014), which indicates that EBs with high amplitudes in the VVV K_s and OGLE I passbands are dominated by systems with F to G-type primaries. We use simple calculations to show that while EBs can have very high amplitudes at optical wavelengths, the eclipse depth should not exceed 1.6 mag in K_s . Similarly, we find that eclipse depths should not exceed 3 mag in I . These results are supported by the VVV and OGLE-III datasets (Pietrukowicz et al. 2013) in which the distribution of EB amplitudes falls to zero by these limits. YSOs with $\Delta K_s > 1.6$ mag are very numerous in our sample so we conclude that high amplitude YSOs greatly outnumber EBs above this limit. Below $\Delta K_s = 1.6$ mag it is harder to reach a firm conclusion (see Appendix A). The space densities of EBs and those YSOs massive enough to be sampled by VVV may be comparable at $1 < \Delta K_s < 1.6$ mag. High amplitude YSOs are likely to be more numerous if the variability extends down to the peak of the Initial Mass Function at low masses, given that high amplitude EB systems contain a giant with mass of order $1 M_\odot$.

4 ANALYSIS OF VARIABLES IN STAR FORMATION REGIONS.

The results presented here analyse YSO variability in the K-band. At these wavelengths, variability in typical YSOs is produced by physical mechanisms affecting the stellar photosphere, star-disk interface and the inner edge of the dust disk (see e.g. Rice et al. 2015). Variability in EXors is also thought to occur in the same regions (Lorenzetti et al. 2012). In FUors variability is thought to trace processes occurring in the accretion disk at larger spatial scales beyond 1 AU, such as instabilities leading to outbursts events (see e.g. Audard et al. 2014). At these large spatial scales, overdensities in the disk can lead to fading events (such in the YSO AA Tau, see e.g. Bouvier et al. 2013). Thus, near-infrared variability of YSOs can be caused by different physical mechanisms (or a combination of them), such as cold or hot spots on the stellar photosphere (e.g. Scholz 2012). Meyer et al. (1997) shows that variability in YSOs can be produced by changes in disk parameters such as the location of the inner disk boundary, variable disk inclination and changes in the accretion rate. Variable extinction along the line of sight can also be responsible for the observed changes in the brightness of YSOs. Dust clumps that screen the stellar light have been invoked to explain the variability observed in Herbig Ae/Be stars and early-type Classical T Tauri stars (group also known as UX Ori stars, see e.g. Herbst & Shevchenko

1999; Eiroa et al. 2002). In other scenarios variable extinction can be produced by a warped inner disk, dust that is being uplifted at larger radii by a centrifugally driven wind, azimuthal disc asymmetry produced by the interaction of a planetary mass companion embedded within the disc or by occultations in a binary system with a circumbinary disk (see e.g., Romanova et al. 2013; Bans & Königl 2012; Bouvier et al. 2013; Windemuth & Herbst 2014, and references therein). Finally, sudden and abrupt increases in the accretion rate, going from typical rates of 10^{-7} to $10^{-4} M_\odot \text{ yr}^{-1}$, can produce large changes in the observed luminosity of YSOs (see Audard et al. 2014, for a review of this rarely seen class of eruptive variables).

The amplitude of the variability induced by most of these mechanisms is not expected to be larger than $\Delta K > 1$ magnitude. Table 6 of Wolk et al. (2013) shows the expected amplitude of the K -band variability that would be produced by these different mechanisms. Cold and hot spots, and changes in the size of the inner disk hole are not expected to show ΔK larger than 0.75 magnitudes. We do note that the variability produced by hot spots from accretion depends on the temperature of the spot and the percentage of the photosphere that is covered by such spots, thus sufficiently hot spots can produce larger changes in the magnitude of the system. The range in ΔK from variable extinction is effectively limitless as it depends on the amount of dust that obscures the star. Large changes ($\Delta K > 1$ mag) have been observed from variable extinction in YSOs, e.g. AA Tau, V582 Mon (Bouvier et al. 2013; Windemuth & Herbst 2014). Nevertheless, variable extinction can be inferred from colour variability (see e.g. Sect. 4.2). Wolk et al. (2013) also estimate that a change in the accretion rate of a class II object of $\log \dot{M}$ from -8.5 to $-7 M_\odot \text{ yr}^{-1}$ yields $\Delta K \sim 0.75$ magnitudes. Thus, larger changes as observed in eruptive variables will produce large amplitudes.

Given all of the above, it is reasonable to expect that variability in our YSO sample to be dominated by accretion-related variability and/or events of obscuration by circumstellar dust.

4.1 Light curve morphologies.

We have visually inspected the light curves of our 530 SFR-associated variables in order to gain insight into the physical mechanisms causing the brightness variations. In addition, we used *pdm* in *IRAF* and *LOMBS-CARGLEFAST* in *GATSPY* to search for periodicity in the light curves of our objects. We stress that this is a simple and preliminary classification that is highly influenced by the sparse sampling of VVV. A more detailed study is planned in future, with improved precision by applying the differential photometry method of Huckvale et al. (2014) to the VVV images. We have divided the morphologies in the following classifications.

- **Long-term Periodic Variables.** Defined as objects showing periodic variability with $P > 100$ days. This limit is adopted for consistency with the limit used in the analysis of objects outside of SFRs, with the benefit that contamination by long period AGB stars will be confined to this group. We measure periods for most of these objects, albeit with some difficulty in phase-folding the data in many

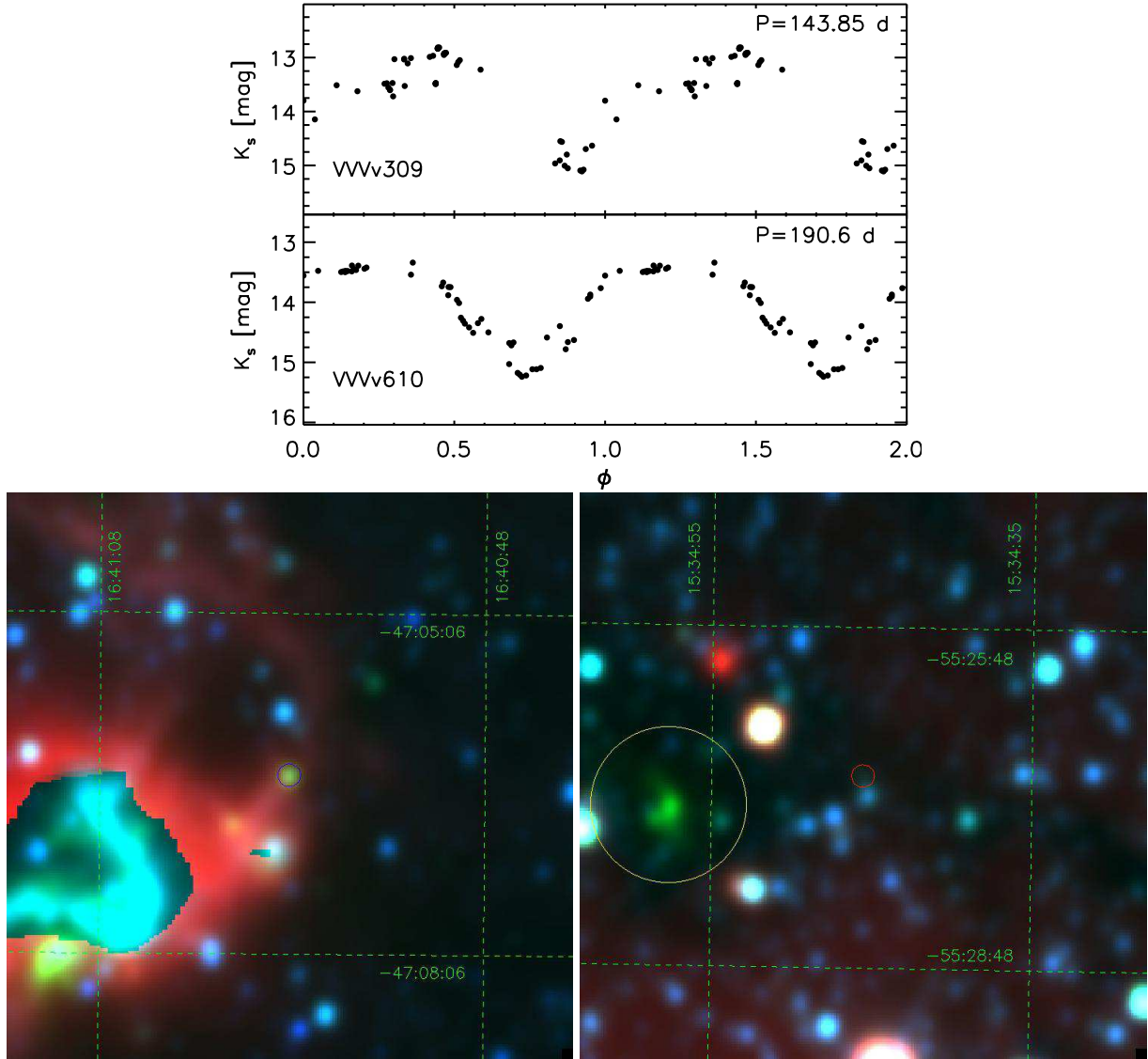


Figure 15. (top) Examples of phased K_s light curves of the long-period variables VVVv309 and VVVv610, which are found in areas of star formation. (bottom) $10' \times 10'$ WISE false colour images (blue=3.5 μm , green=4.6 μm , red=12 μm) centred on VVVv309 (right) and VVVv610 (left). In both images the location of the variable star is marked by ring around the location of the object. VVVv309 is 114'' from HII region GRS G337.90 -00.50 (see e.g. Culverhouse et al. 2011), whilst VVVv610 is located 110'' from EGO G324.72+0.34 (Takami et al. 2012) and outflow likely associated with high-mass star formation. Several masers can be also found in the area that is marked by a yellow ring in the WISE image

of them. In this subsample we find 154 stars, representing 29% of objects spatially associated with SFRs. In Sect. 3.4 we contended that field high-amplitude infrared variables with periodic light curves ($P > 100$ days) are very likely dust-enshrouded AGB stars, these being identifiable by their smooth, approximately sinusoidal light curves. We estimated that $\sim 27\%$ of the 530 SFR-associated variables would be non-YSOs and up to 45% of these would be LPVs, implying that this subsample may contain ~ 64 dusty Miras. Visual inspection of the 154 light curves indicates that while some have a smooth sinusoidal morphology (after allowing for long term trends due to variable extinction in the expanding circumstellar dust shell) others display short timescale scatter superimposed on the high amplitude long

term periodicity. In Fig. 15, we show the examples of objects VVVv309 and VVVv610. The short timescale variability in their light curves is definitely not consistent with the typical light curves of Mira variables and their periods of 143.95 and 190.6 days, respectively, are shorter than those of the dusty Miras detected outside SFRs (see Fig. 12). This short timescale scatter is typical of the scatter observed in normal YSOs due to a combination of hot spots, cold spots, and small variations in accretion rate or extinction, so it is reasonable to think that most of the long period variables with short timescale scatter are in fact YSOs.

To support this interpretation, Fig. 14 shows the period vs ΔK_s and period vs K_s distributions, for objects where we are able to measure a period. The period vs ΔK_s distribution

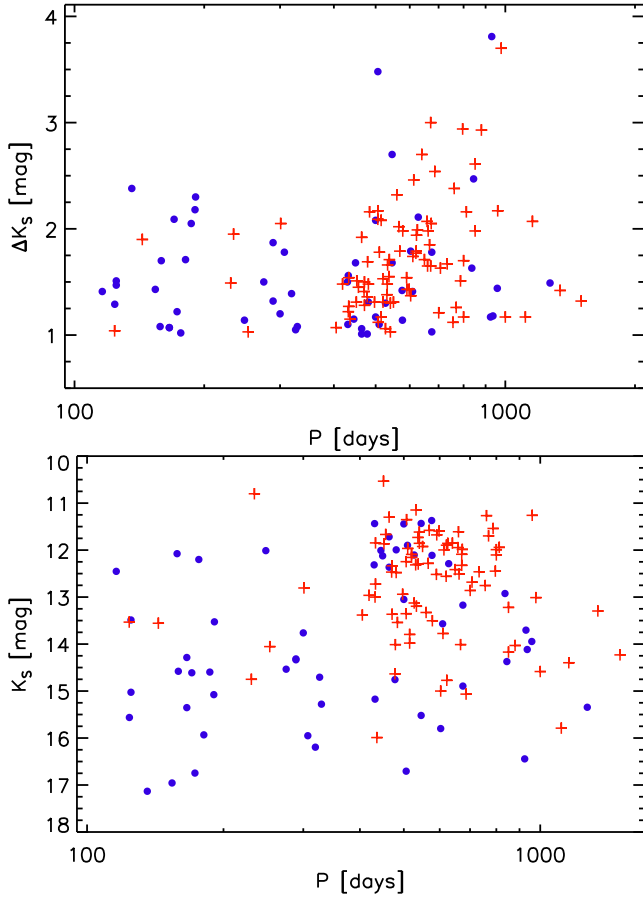


Figure 14. (top) K_s amplitude vs period for stars in SFRs with long-term periodic variability. LPVs that show Mira-like light curves are shown in red plus signs while other sources are shown as blue circles. (bottom) K_s magnitude vs period for the same same of stars.

is similar to that observed in LPVs outside SFRs (Fig. 12) except that there is a larger number of “long-term” periodic variables found with periods, $100 < P < 350$ days. The 65 blue points are the objects with short timescale scatter and the red points are the remaining 89, categorised by careful inspection of the light curves of the 154 long-term periodic variables in SFRs. These clearly dominate the group with $P < 350$ days and they also have a distinctly fainter distribution of K_s magnitudes, similar to that shown in the red histogram in Fig. 13, which represents all objects in SFRs except those with Mira-like light curves. As expected, the red points with Mira-like light curves typically have $K_s \sim 12$, similar to the LPV distribution plotted in Fig. 10. We conclude that inspection of the light curves can separate the evolved star population of LPVs from the YSOs in SFRs with fair success, though we caution that this is an imperfect and somewhat subjective process that can be influenced by outlying data points and our limited knowledge of the time domain behaviour of circumstellar extinction in dusty Mira systems. The limitations are demonstrated by the presence of a number of blue points with $K_s \sim 12$ and $P > 350$ days in the lower panel of Fig. 14 and a hint of bimodality even in the “decontaminated” magnitude distribution in Fig. 13 (red histogram). In the subsequent discussion of YSOs from our

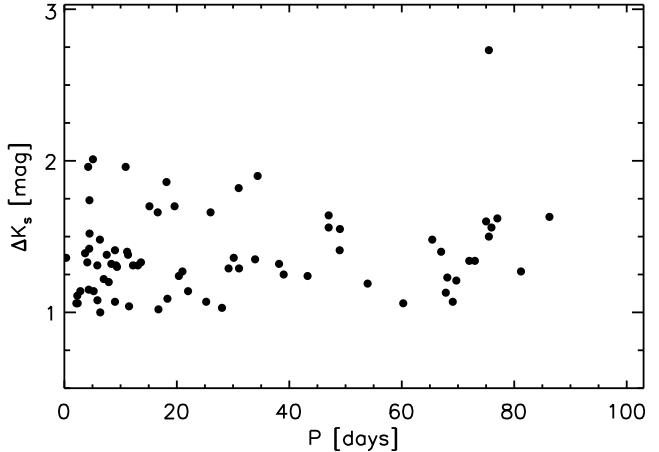


Figure 16. K_s amplitude vs period for stars with short-term variability and with a measured period.

sample we only include the 65 objects with short timescale scatter (called LPV-ysos) and assume the other 89 sources are dusty AGB stars or other types of evolved star (or LPV-Mira).

This decontamination of AGB stars reduces the SFR-associated sample to 441 objects. The long term periodic YSOs represent 15% of this sample.

Periods, $P > 15$ days are longer than the stellar rotation period of YSOs, or the orbital period of their inner discs (Rice et al. 2015). Some YSOs have been observed to show variability with periods longer than even 100 days. WL 4 in ρ Oph shows periodic variability with $P = 130.87$ days (Plavchan et al. 2008), which can be explained by obscuration of the components of a binary system by a circumbinary disk. The K -band amplitude of the variability in that system is somewhat less than 1 magnitude. However, it is possible to think that a similar mechanism might be responsible for the variations in some of our objects. Hodapp et al. (2012) show that variable star V371 Ser, a class I object driving an H_2 outflow, has a periodic light curve with $P = 543$ days. The authors suggest that variability arises from variable accretion modulated by a binary companion. In view of this, the variability in some of the long term periodic variables might be driven by accretion and we discuss this in paper II, based on spectroscopic evidence for a sub-sample of them.

- **Short-term Variability.** This group comprises objects that either have periodic variability and measured periods, $P < 100$ days, (75 objects) or else have light curves that appear to vary continuously over short timescales ($t < 100$ days) but not with an apparent period (87 objects). Their light curves do not resemble those of detached EBs because they vary continuously and cannot be contact binaries (W UMa variables) because their periods are typically longer than 1 day. For objects in this classification that have measured periods, we observe a broad distribution from 1 to 100 days and the amplitudes are in the range $\Delta K_s = 1$ to 2 magnitudes (see Fig. 16). If we join together the long-term periodic variables and the STVs with measured periods, we find that sources with periods, $P > 100$ days show higher amplitudes, on average, and sources with $P > 600$ days have redder SEDs (larger values of the spectral index α). There are no clear gaps in the period distribution, so the 100 day

division between the two groups that we adopted to aid decontamination is as useful as any other. We find 162 stars in the STV group, which represents 37% of the decontaminated SFR-associated sample.

High-amplitude periodic variability has been observed in YSOs over a wide range of periods. RWA1 and RWA26 in Cygnus OB7 (Wolk et al. 2013) vary with periods of 9.11 and 5.8 days respectively. The variability has been explained as arising from extinction and inner disk changes. As mentioned before variability with $P > 15$ days is not expected to arise from the stellar photosphere or changes in the inner disk of YSOs. This is instead could be related to obscuration events from a circumbinary disk, such as in V582 Mon (Windemuth & Herbst 2014), and YSOs ONCvar 149 and 479 in Rice et al. (2015). Variable accretion has been invoked to explain the observed periodic variability ($P \sim 30$ d) of L1634 IRS7 (Hodapp & Chini 2015). The shorter periods within this group may indicate rotational modulation by spots in objects with amplitudes not far above 1 magnitude, see below.

- **Aperiodic Long-term variability.** This category can be divided into three different subclasses: a) Faders. Here the light curves show a continuous decline in magnitude or show a constant magnitude for the first epochs followed by a sudden drop in magnitudes that lasts for a long time (≥ 1 year), continuing until the end of the time series in 2014. This type of objects might be related to either stars going back to quiescent states after an outburst or objects dominated by long-term extinction events similar to the long-lasting deepening event in AA Tau (Bouvier et al. 2013), or some of the faders in Findeisen et al. (2013). b) Objects showing long-lasting fading events and then return to their normal brightness (such as VVVv504 in Fig. 17), which we refer to as dippers. These might also be related to extinction events. Examples of objects in groups (a) and (b) can be seen in Fig. 17.

Group (c) contains sources with outbursts, typically of long duration (≥ 1 yr). In a very small number of objects the outburst duration appear to be much shorter, on the order of weeks. The increases in brightness are also unique or happen no more than twice during the light curve of the object, thus not resembling the light curves of objects in the STV category. An exception is VVVv118, which shows four brief rises on timescales of weeks.

The light curves in this category typically have an increase of ~ 1 magnitude or more. In a small number of cases the rise in the light curve is poorly sampled, starting at or before the beginning of the time series, but the subsequent drop exceeds 1 magnitude. Figure 18 shows four examples of objects falling in the eruptive classification. The examples have been selected in order to illustrate the different temporal behaviour observed in objects belonging to this class. As we have already mentioned, VVVv118 shows multiple short, high-amplitude rises. In general objects show outbursts which last between 1–4 years (see VVVv815 and VVVv322). We also detect a few cases where the outburst duration cannot be measured as it extends beyond 2014 data (e.g. VVVv270).

When comparing to the behaviour of known classes of eruptive variables, VVVv118 would resemble that of EXors and VVVv270 could potentially be a FUor object (based only on photometric data). However most of the objects

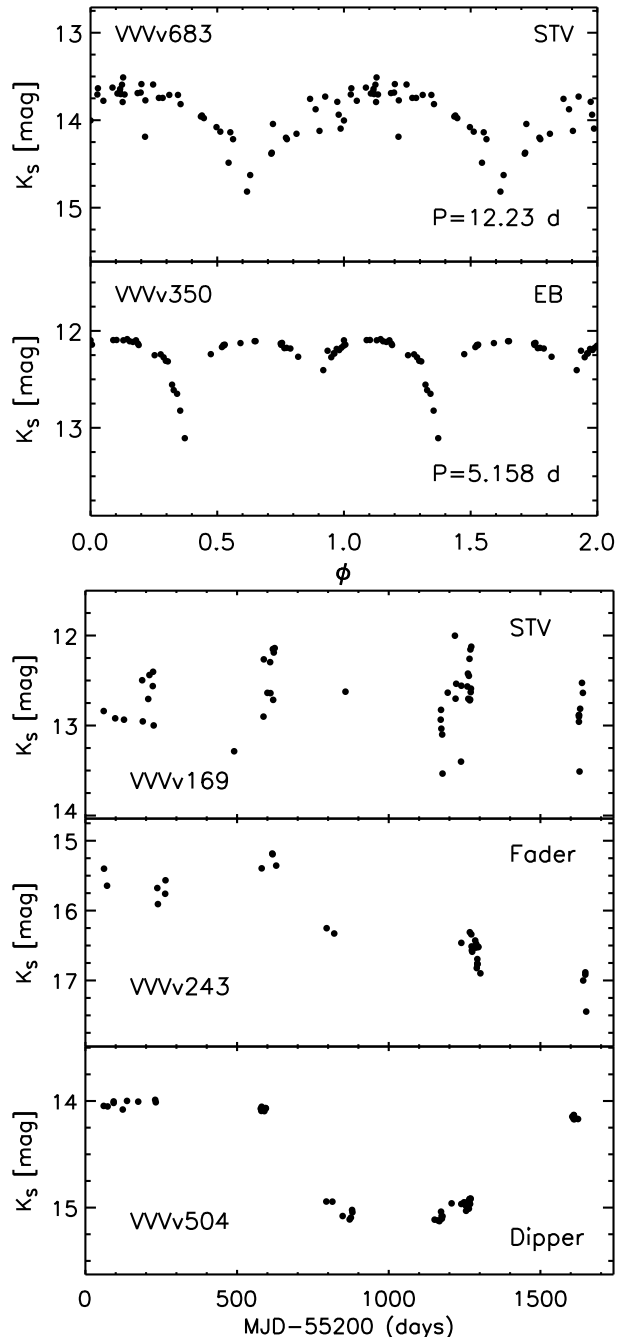


Figure 17. Examples of K_s light curves for the different classifications as explained in the text. (top) Phased light curves of short-term variable star with a measured period, VVVv683 and eclipsing binary VVVv350. (bottom) Light curves of short-term variable star, without a measured period, VVVv169, the fader VVVv243 and the dipper VVVv504.

have outburst durations that are in between the expected duration for EXors and FUors. We note that given the long duration of FUor outbursts we are likely to miss detection of these objects if they went into outburst prior to 2010. Given the sparse VVV time sampling, we also need to test our sensitivity to short, EXor-like eruptions.

We simulate outbursts with timescales from 2 months to 3 yr. First we generate a very rough approximation of an

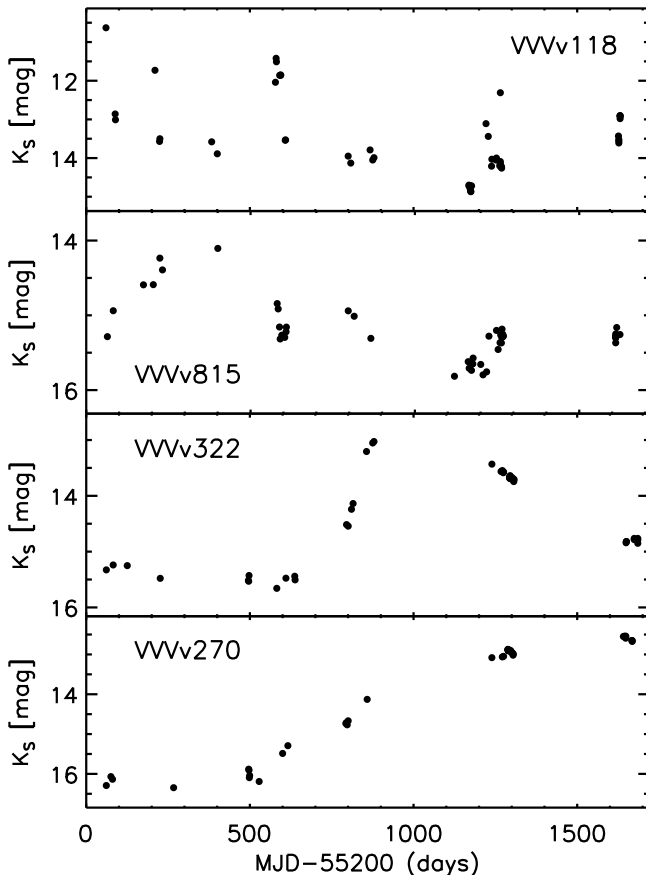


Figure 18. Examples of K_s light curves for different objects in the eruptive classification as explained in the text. From top to bottom we show objects VVVv118, VVVv815, VVVv322 and VVVv270.

eruptive light curve with outburst duration, T_o . The light curve consists of: 1) A quiescent phase of constant magnitude that lasts until the beginning of the outburst, which is set randomly at a point within the 2010–2012 period (between 0 and 1000 d). 2) A rise which is set arbitrarily to have a rate of 0.15 mag/day, lasting $T_{rise} = 10$ d until reaching an outburst amplitude of 1.5 mag, which is a little below the median for the VVV eruptive variable candidates. 3) Plateau phase with a constant magnitude set to the peak of the outburst. This phase lasts for $T_o - T_{rise} - T_{decline} = T_o - 20$ d. 4) The decline, which lasts 10 days and has a rate of 0.15 mag/day. Finally, 5) A second quiescence phase. To every point in the light curve we add a randomly generated scatter of ± 0.2 mag. Once the light curve is generated, we measure the magnitude of the synthetic object at the observation dates of a particular VVV tile. If the synthetic object shows $\Delta K_s \geq 1$ mag then it is marked as a detection. This procedure is repeated 1000 times for each outburst duration (which is set to be between 30 and 900 days). We also repeat this procedure for four different VVV tiles.

The simulation shows that number of detections is very similar ($\sim 80\%$) for $T_o > 7$ months and declines slowly as T_o is reduced, falling by a factor of 2 for $T_o = 2$ months. However, this is not enough to cause the apparent lack of eruptive variables with EXor-like outbursts in our sample. We conclude that the longer (1–4 yr) durations that we ob-

serve are typical values for infrared eruptive variables, rather than a sampling effect.

The characteristics of our eruptive sample agrees with recent discoveries of eruptive variables that show a mixture of characteristics between the known subclasses of eruptive variables (see e.g. Aspin et al. 2009). We note that classification of our sample into the known subclasses becomes even more problematic when taking spectroscopic characteristics into account, as e.g. VVVv270, the potential FUor from its light curve, shows an emission like spectrum, or VVVv322 shows a classical FUor near-infrared spectrum. In Paper II we propose a new class of eruptive variable to describe these intermediate eruptive YSOs.

Sources classified as eruptive are very likely to be eruptive variables, where the changes are explained by an increase of the accretion rate onto the star due to instabilities in the disk of YSOs (see e.g. Audard et al. 2014). We find 39 objects in subgroup (a), 45 in (b) and 106 in (c). The whole class of faders/bursts represent 43% of the likely YSO sample.

• **Eclipsing Binaries.** We find 24 objects with this light curve morphology, representing 5% of the sample. We are able to measure a possible period in 15 of them. The remaining 9 objects are left with this classification given the resemblance of their light curves to the objects with measured periods. We expect that a number of them will be field EBs contaminating our YSO sample. However, inspection of the 2 to 23 μ m spectral index for each object, α , (see Fig. 23), indicates that 12 objects are classified as either Class II or Flat-spectrum sources. If these are in fact YSOs, they would represent a significant discovery as YSO EBs are invaluable anchors for stellar evolutionary models, which generally lack empirical data on stellar radii. Figure 19 shows the light curve and location of one candidate YSO EB, VVVv317, with $P = 6.85$ d and $\alpha = -1.57$. The spectra index places it at the edge of the classification of class II YSOs.

In Fig. 20 we compare the amplitude distributions ($K_{s,max} - K_{s,min}$) of the different categories of variable YSO. We can see that the EBs and STVs typically have the smallest amplitudes (means of 1.18 mag and 1.33 mag, respectively), whereas the faders and eruptive variables have the highest amplitudes (means of 1.95 mag and 1.72 mag, and medians of 1.75 mag and 1.61 mag respectively). The dippers and long-term periodic variables have mean amplitudes of 1.64 mag and 1.57 mag respectively, which are similar to the mean amplitude of 1.56 mag for the full sample. The substantial number of STVs with amplitudes only a little over 1 magnitude is consistent with our suggestion that in the shorter period variables in this category variability may be explained by rotational modulation of dark or bright spots on the photosphere. The relatively high amplitudes of the eruptive variables are not unexpected, whilst the high amplitudes of the faders could be explained if some of these objects are eruptive variables returning to quiescent states.

4.2 Near infrared colour variability

Considering the various class of light curve defined above for SFR-associated variables, it is reasonable to expect that extinction causes the variability in dippers and perhaps some of the STVs. Extinction variability can be observed in erup-

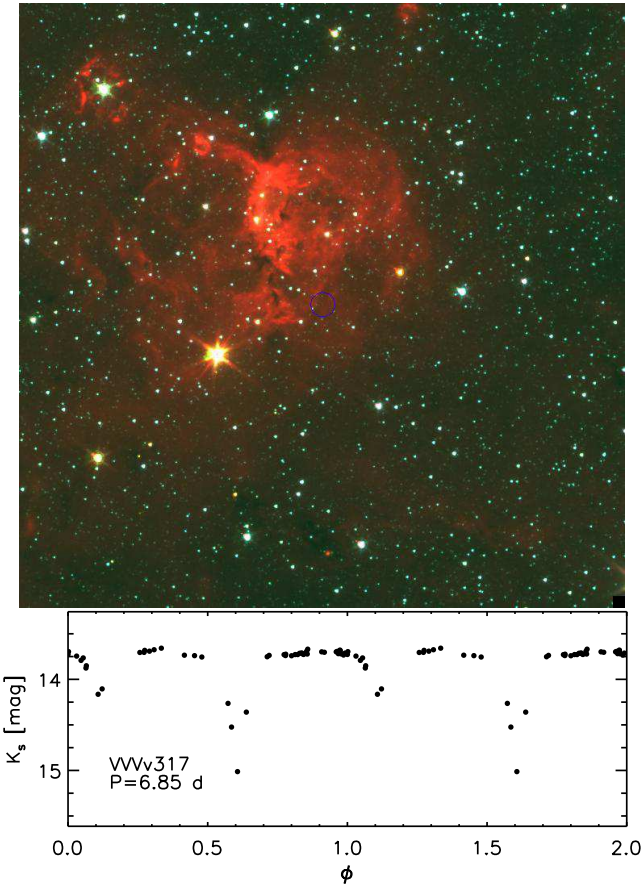


Figure 19. (top) False colour image (blue=3.6 μ m, green=4.5 μ m and red=8 μ m) from Glimpse, showing the location of candidate YSO EB VVVv317 (blue ring). (bottom) Phased light curve of the object.

tive objects. However, we do not expect the main cause of variability in this class to be due to this mechanism. It is less clear what to expect for faders and long-term periodic variables. We can test this by looking at colour variability data.

The VVV survey was initially designed with only 1 epoch of contemporaneous JHKs colour data but a 2nd such epoch was added to the programme for observation in 2015, both to benefit the YSO variability science and to help to understand VVV variables of unknown nature. We note that many objects in the SFR sample are not detected in J- and H-band (see Sect. 4.3), making a colour comparison impossible. Also, in many objects the two epochs do not span a large fraction of the full range of magnitudes in the light curve. E.g. in many eruptive objects we do not have direct comparison between quiescent and outburst states. Nevertheless, comparison of the change in colour vs magnitude still provide some valuable information on the mechanisms driving variability, particularly for those sources in which source magnitudes differ substantially at the 2 epochs.

Following a similar procedure to Lorenzetti et al. (2012) and Antoniucci et al. (2014) we compare the change in colour, ($H - K_s$), vs magnitude, H , between 2010 and 2015 for the different classes of YSOs (see Fig. 21). In the figure we see that in most cases the change in both colour and magnitude are small, thus objects cluster around the

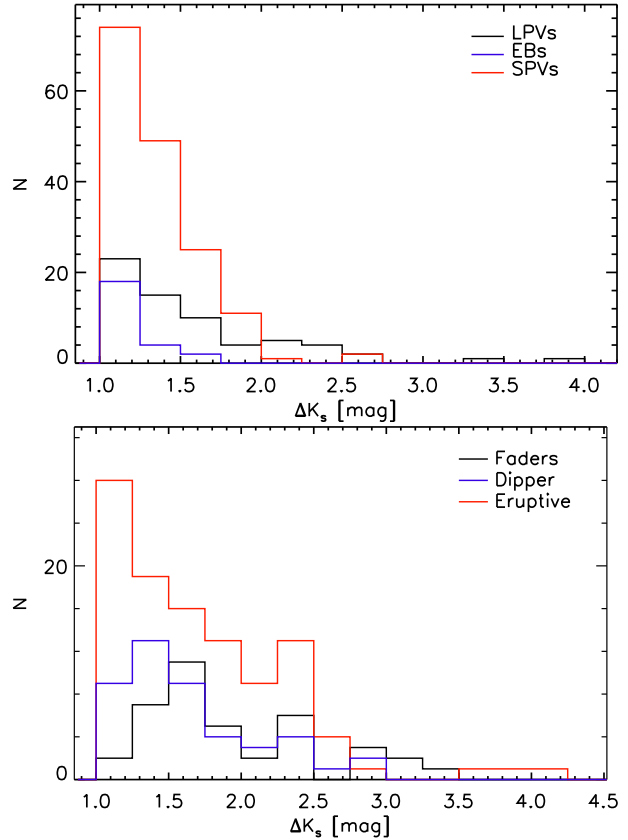


Figure 20. ΔK_s distribution for the different light curve morphology YSO classes. (top) Distribution for LPVs (black line), STVs (red line) and EBs (blue line). (bottom) Distribution for aperiodic variables, faders (black line), dippers (blue line) and eruptive objects (red line).

origin. The latter seems to be true in both EBs and Dippers. The overall distribution of eruptive, LPVs and STVs on the other hand, seems to be elliptical with the major axis passing through the “bluer when brighter” and “redder when fainter” quadrants. This agrees with the behaviour expected from changes due to accretion or extinction in YSOs and resembles the near-infrared variability observed in EXors (Lorenzetti et al. 2009, 2012), the classical T Tauri sample of Lorenzetti et al. (2012), and the mid-infrared variability of candidate EXors from Antoniucci et al. (2014). It is interesting to see that many objects classified as faders fall in the bluer when fading quadrant. This behaviour is still consistent with YSO variability due to changes in disk parameters described by Meyer et al. (1997) and observed in some Cygnus OB7 YSOs (see e.g. Wolk et al. 2013). The different behaviour might also be caused by the different geometry (inclination) of the system with respect to the observer.

Figure 21 also shows the observed change in both ($J - H$) and ($H - K_s$) colours for YSOs detected in the three filters in both epochs. In there we also plot the expected change if the variability occurs parallel to the reddening line or the CTTs locus (independent of the direction of the change). We would expect that variability similar to the observed in EXors (see e.g. fig. 1 in Lorenzetti et al. 2012) would fall in between the reddening and CTTs lines.

It is hard to say much from EBs and dippers as they do not show much variability, although dippers appear to follow the reddening path. The overall change in STVs and dippers could follow either reddening or the CTTs locus depending on the selection of objects from those samples. It is also hard to establish the path followed by LPVs, but it does seem more consistent with being different from reddening. Eruptive variables appear to follow a very different path from reddening. The latter would support that the changes in this group are being driven by accretion variability.

We have checked the individual $(J - H)$ vs. H , $(H - K_s)$ vs K_s and $(J - H)$ vs $(H - K_s)$ color-magnitude and colour-colour diagrams for the 15 eruptive variables that showed changes larger than $\Delta K_s > 0.75$ mag between the two multi-wavelength epochs (this representing a significant fraction of the total amplitude in most systems). From 15 objects, 10 do not show changes consistent with extinction and 5 were found to show variability approximately following the reddening vector. However, the colour behaviour in these 5 objects does not contradict the idea that accretion is the mechanism driving variability because: 1) we are not directly comparing quiescent vs outburst states, as the two near-infrared epochs cover random points in the light curve; 2) As previously mentioned, extinction does play a role in outburst variability. E.g. the near infrared colour variation of V1647 Ori follows the reddening path in fig. 13 of Aspin et al. (2008). Extinction might also be involved in the observed variability or the recent eruptive object V899 Mon (Ninan et al. 2015).

The same analysis of individual CMD and colour-colour diagrams for the remaining classes shows that 3/7 LPV-YSOs, 5/9 STVs, 1/4 dippers and 3/11 faders have colour changes consistent with variable extinction (again considering only systems with $\Delta K_s > 0.75$ between the 2 multi-colour epochs). No results can be derived from EBs as none of the members show changes larger than 0.75 magnitudes between the two epochs. It is interesting to see that the changes in the majority of faders are not consistent with extinction. This supports the idea that variability in many of the objects in this class could be related to accretion changes.

In Appendix B we briefly summarise the colour and magnitude changes detected by the multi-epoch photometry from the WISE satellite. We note that this adds little to the preceding discussion of near-infrared colour changes, though large mid-infrared variability is observed in a minority of sources where the satellite happened to sample both a peak and a trough in the light curve.

4.3 Variability trends with SED class

In order to study the possible evolutionary stage of the variable stars in SFRs, we use the slope of the SEDs of the stars between $2 < \lambda < 24\mu\text{m}$. Following Lada (1987), we define the parameter α as $\alpha = d(\log(\lambda F_\lambda))/d(\log(\lambda))$. The value of α is determined from a linear fit to SED points between $2 < \lambda < 24\mu\text{m}$. Objects are then classified according to their value of α following Greene et al. (1994), also shown in Table 2. We note that this class definition might not necessarily relate to the actual evolutionary stage of the object. As stated in e.g. Robitaille et al. (2006), parameters such as inclination or stellar temperature can affect the shape of the SED at the wavelengths used to classify YSOs. We have

removed numerous objects that showed Mira-like characteristics from their light curves but there may still be some contamination by non-YSOs amongst the remaining objects projected close to an SFR.

We derive α using the photometry arising from VVV and WISE, given that these were taken in the same year (2010). When the objects are not detected in WISE, we use *Spitzer/GLIMPSE* photometry. The use of the latter is more likely to cause errors in the estimation of α due to the time difference between *Spitzer/GLIMPSE* and VVV measurements, but *Spitzer/GLIMPSE* benefits from higher spatial resolution. We find that if we use *Spitzer* instead of WISE the difference in α is on the order of 0.1-0.2 for the majority of the sample detected in both surveys.

The number of objects belonging to different classes are shown in Table 2. We find that the majority (67%) of objects in our sample are either class I or flat spectrum sources (45% and 22%, respectively). Objects belonging to different classes show some differences in their global properties. Figure 22 shows the near-infrared colours of objects in SFRs. As expected the vast majority of objects show colours consistent with them being YSOs. The $H - K_s$ colour tends to be redder for stars belonging to younger evolutionary stages. The fraction of objects detected at J and H bands also decreases with objects belonging to younger stages, as would be expected for typical deeply embedded class I objects. Table 2 shows that 66% of class I objects are not detected in the J band, whilst 23% of them are not detected in either the J nor H bands. These near IR colour trends confirm that, as with typical YSOs, highly variable YSOs whose spectral index indicates an earlier evolutionary stage also have higher extinction by circumstellar matter, along with more infrared emission from circumstellar matter.

It might be thought that the relatively high reddening of most of the YSOs in Fig. 22 is due to foreground extinction, given that in Paper II we derive typical distances of a few kpc for these sources. We measure foreground extinction for a sub-sample of VVV objects (the 28 variable YSOs in Paper II) by estimating the extinction of red clump giants found at distances similar to those of our objects. The distance to VVV objects arises from results of Paper II. The red clump giants are identified in the local K_s vs $(J - K_s)$ colour-magnitude diagrams of the VVV objects ($6' \times 6'$ fields), and distances are estimated from their observed mean $(J - K_s)$ colours using equation 1 in Minniti et al. (2011). The excess of the mean $(J - K_s)$ with respect to the intrinsic colour of red clump giants ($(J - K_s)_0 = 0.70$ mag Minniti et al. 2011), gives us a measure of the foreground extinction to the front of the molecular cloud containing each YSO. In most cases the YSO itself is redder than the red giant branch stars, due to extinction by matter within the cloud and by circumstellar matter. This method yields values of $A_{K_s} \sim 0.8$ to 1.4 mag (i.e. $A_V \sim 7$ to 12 mag) which is higher than the typically very low diffuse interstellar extinction between the sun and nearby molecular clouds. This foreground extinction partially explains why many of these objects are optically very faint. Correcting our values of α accounting for $A_V = 11$ magnitudes, produces changes of 0.2-0.4 in this parameter. These changes would alter the classification of 1/3 of the sample where we can estimate α , mostly in objects where α has a value that is close to the limits set by Greene & Lada (1996). Despite this correction flat-spectrum

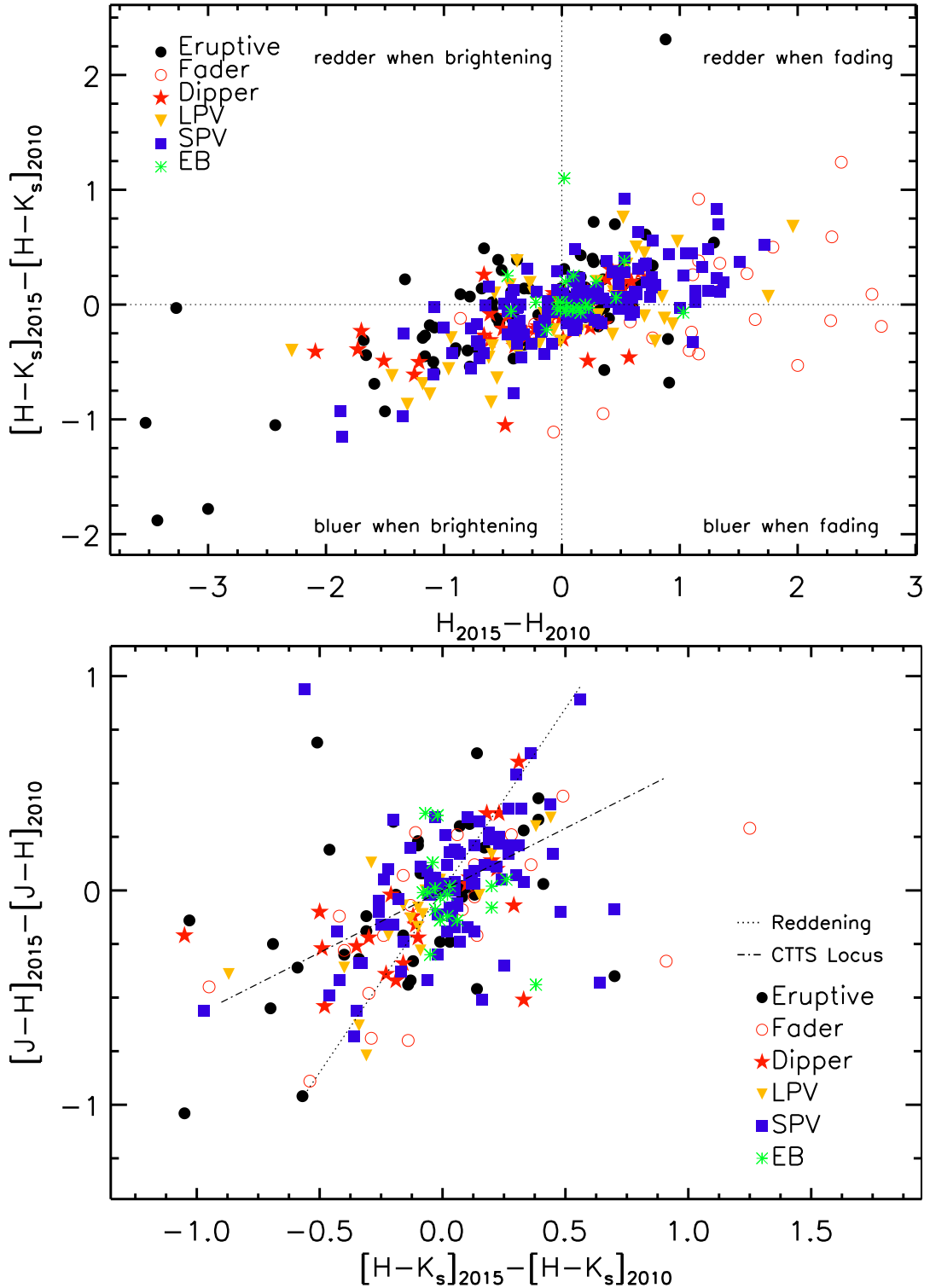


Figure 21. $\Delta(H - K_s)$ vs ΔH (top) and $\Delta(J - H)$ vs $\Delta(H - K_s)$ (bottom) for YSOs with an available second JHK_s epoch from VVV. In the plots we mark the different classes from light curve morphology. Different symbols are explained in the plots. In the bottom plot we mark the expected changes which occur parallel to the reddening vector (dotted line) and to the CTTS locus of Meyer et al. (1997) (dot-dashed line).

Class	α	N	N_{Jdrop}	N_{JHdrop}	$N_{\Delta K_s \geq 2}$
Class I	$\alpha > 0.3$	198	130	45	49
Flat	$-0.3 \leq \alpha \leq 0.3$	95	35	1	12
Class II	$-1.6 < \alpha < -0.3$	83	19	1	6
Class III	$\alpha \leq -1.6$	12	0	0	0
Undefined	n/a	53	10	2	3

Table 2. Number of VVV variable stars belonging to the different evolutionary classes of YSOs, as determined from their SEDs.

and class I sources still dominate the sample of YSOs with a measured value of α : with no correction these represent 76% of the sample, whereas with a correction to α of 0.3 the proportion remains high, at 59%.

We choose not to apply a correction in Table 2 and our subsequent analysis because the extinctions and distances are uncertain (e.g. the red giant branch is not well defined in the CMDs for about a third of sources) and we cannot be sure this method is entirely correct. Our derived extinctions are a factor of ~ 2 higher than indicated by the 3D extinction map of Marshall et al. (2006), which was also based on red clump giants but used 2MASS data on a coarser angular scale. Moreover, in Paper II we compare the ratio of $70 \mu\text{m}$ flux to $24 \mu\text{m}$ flux in the spectroscopic subsample with that found in a nearby sample of YSOs. At these far-infrared wavelengths, where extinction is very low, we find similar flux ratios for class I systems in both datasets, indicating that most VVV class I YSOs have been correctly classified. In the following discussion, we directly compare embedded (Class I and flat spectrum) YSOs with sources in nearby SFRs. We simply ask the reader to note firstly that α may be slightly inflated by interstellar extinction and secondly that this more distant sample will be biased towards more luminous YSOs of intermediate mass (see Paper II).

The distribution of ΔK_s (Fig. 23, upper left panel) shows that peak of the distribution is found at larger ΔK_s for younger objects. We also observe a higher fraction of objects with $\Delta K_s > 2$ mag for class I objects (25%) than for flat-spectrum (13%) and class II (7%) objects. The comparison of α_{class} vs ΔK_s in the bottom panel of the same figure further illustrates the increase in amplitude at younger evolutionary stages, as well as the higher incidence of $\Delta K_s > 1$ variability at the younger stages. The class I and flat spectrum YSOs constitute 87% of the $\Delta K_s > 2$ subsample, dominating it even more than the full SFR-associated sample.

We note that 70 objects with $\Delta K_s > 2$ mag also have redder near infrared colours than the full sample: the proportions of J band non-detections and JH non-detections rises from 44% and 11% in the full SFR-associated sample to 56% and 24% in the $\Delta K_s > 2$ subsample. This further highlights the simple fact that efficient detection of the majority of YSOs with the most extreme variations requires observation at wavelengths $\lambda \geq 2 \mu\text{m}$. Most importantly, this further emphasises that younger objects have higher accretion variations. (Eruptive variables are the largest component of the $\Delta K_s > 2$ sample, comprising 30/70 objects).

In Fig. 23 we also show the mean variability of YSOs belonging to different evolutionary classes as a function of time baseline. This is calculated by averaging the values of r.m.s. variability vs. time interval computed using every pos-

sible pairing of two points within the light curve of each star. In the figure we show the variability over intervals up to 50 days (calculated with time bins of 1 day), and for intervals up to the full 1600 day baseline of the dataset (using time bins of 30 days). The r.m.s. variability over short timescales appears to be larger for more evolved objects than flat and class I sources. The variability increases with time for every YSO class and becomes flat at $t \sim 250 - 350$ days, although this is less clear for class III sources because of noise due to the lower number of objects in this class. Class I and flat sources have higher r.m.s. variability on these longer timescales.

The higher r.m.s variability in class II and III systems on timescales < 25 days can be explained by the fact that in these more evolved YSOs the stellar photosphere contributes a greater proportion of the K-band luminosity of the system, whereas in less evolved YSOs the luminosity is more dominated by the accretion disc. Consequently we may expect a greater contribution to variability from cold and hot spots in the photosphere of class II and class III YSOs, which manifests on the timescale of stellar rotation. We note that variability on rotational timescales of a few days also contributes to the measured mean r.m.s. variability shown in Fig. 23 on all longer timescales, which is why the variation increases rapidly on baselines from zero to 3 days (a typical rotation timescale in YSOs, e.g. Alencar et al. 2010) and then increases more slowly thereafter.

It is also very interesting to see that the 250-350 day timescale at which the maximum of mean r.m.s. variability is reached in all classes of YSO corresponds to variability on spatial scales of 1-2 AU, assuming the timescale is determined by Keplerian rotation about low to intermediate mass YSOs. Connelley & Greene (2014) found from a spectroscopic variability study that mass accretion tracers in their sample of class I YSOs, such as $\text{Br}\gamma$ and CO emission, are highly variable over timescales of 1-3 yrs and they proposed the above explanation of the timescale. We suggest therefore that we are detecting processes in the accretion discs of YSOs on scales up to 1-2 au.

Studies of the optical, near infrared and mid-infrared temporal behaviour of YSOs have shown that the great majority are variable at these wavelengths, with their light curves showing a diversity of amplitudes, timescales and morphologies (see e.g. Findeisen et al. 2013; Cody et al. 2014; Rebull et al. 2014; Rice et al. 2015; Wolk et al. 2015). These studies, and the earlier large scale study of Megeath et al. (2012) showed that the amplitude of the variability increases for younger embedded objects, though these works contained few if any YSOs with $\Delta K_s > 1$. Rice et al. (2012) found indications that amplitudes $\Delta K > 1$ mag are more common amongst class I systems ($13 \pm 7\%$, based on 2 high amplitude objects in a sample of 30 in the Braid Nebula within Cygnus OB7, whereas such high amplitudes are found to be less common in more evolved YSOs (see e.g. Carpenter et al. 2001).

4.4 Eruptive variability.

We have found from the morphological classification that 106 of our SFR-associated high amplitude variables have light curves that show sudden and large increases in brightness. Our near infrared colour variability data, though lim-

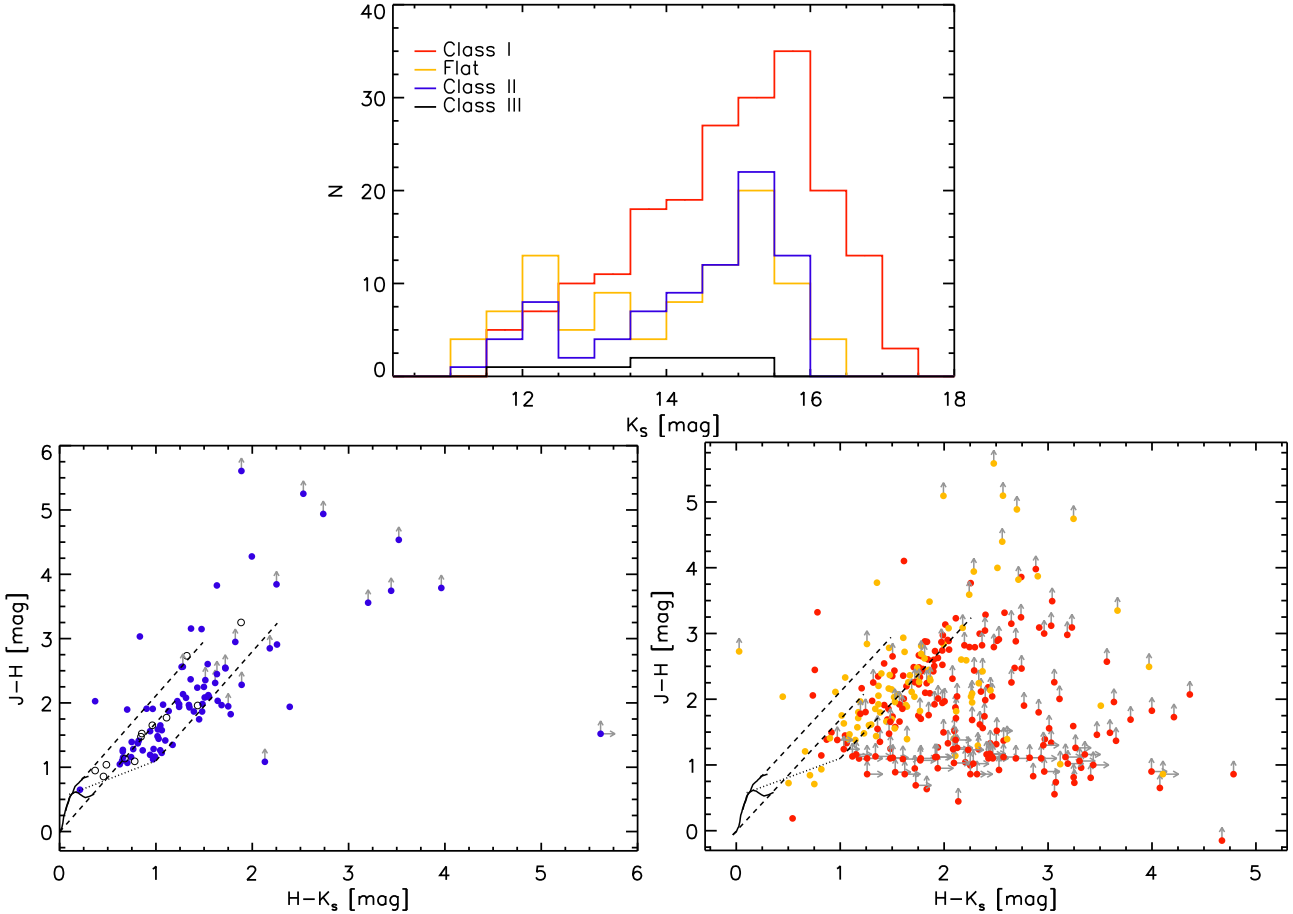


Figure 22. (top) K_s distribution (from 2010 data) of class I (red), flat-spectrum (orange), class II (blue) and class III (black) YSOs. (bottom left) Colour-colour diagram for Class II (blue filled circles) and class III YSOs (black open circles) from VVV. In the figure, lower limits in colour are marked by arrows. The classical T Tauri locus of Meyer et al. (1997) is presented (long-dashed line) along with intrinsic colours of dwarf and giants (solid lines) from Bessell & Brett (1988). Reddening vectors of $A_V = 20$ mag are shown as dotted lines. (bottom right) Colour-colour diagram for class I (red) and flat-spectrum (orange) YSOs.

ited, appears to verify that variability arises from changes in accretion rather than extinction in most cases.

In Fig. 23 (middle panels) we show histograms of the spectral index of the YSOs of each light curve type. We also see that the YSOs classified as eruptive have larger values of α (i.e. redder SEDs) than the other categories of YSO variables. This supports the idea that fluctuations in the accretion rates are larger and much more common at early stages of pre-MS evolution than in the class II stage. This is especially true given that class II YSOs typically outnumber class I YSOs in nearby SFRs by a factor of $\sim 3.7\text{--}4.8$ (see e.g. table 1 in Dunham et al. 2014) due to the greater duration of the class II stage. We have 70 eruptive variables classified as class I YSOs and 5 classified as class II YSOs (the remainder being flat spectrum or class III systems). If we assume that the YSOs classified as eruptive are mainly genuine eruptive variables (which is supported by our spectroscopic follow up in paper II) this tells us that the incidence of eruptive variability is $\sim 50\text{--}70$ times higher in class I YSOs than class II YSOs. If we consider the possible correction to α due to foreground extinction (see 4.3), then we have 52 class I YSOs and 15 class II YSOs in the eruptive category, so eruptive variability is still 13 to 17 times more common in class I

YSOs. We conclude that the difference is at least an order of magnitude.

It is interesting to see that some of the theoretical models that explain the outbursts observed in young stars, predict that luminosity bursts are more common in the Class I stage compared to later stages of stellar evolution. These models mainly involve gravitational instability (GI) in the outer disc, which is most likely to occur during the embedded phase. GI can cause the outer disc to fragment, forming bound fragments that later migrate into the inner disk. The infall of these fragments can lead to mass accretion bursts. GI can also produce a persistent spiral structure which efficiently transfer mass to small radii. The continuous pile up of mass at lower radii can trigger magneto-rotational instabilities (MRI), which lead to sudden disk outbursts (see e.g., Zhu et al. 2009; Audard et al. 2014; Vorobyov & Basu 2015, and references therein). Thus invoking these mechanisms might explain the higher occurrence of eruptive variables at younger stages. However, we note that most mechanisms that explain eruptive variability, such as bursts due to binary interaction (Bonnell & Bastien 1992), MRI activated by layered accretion (Zhu et al. 2009) or thermal instabil-

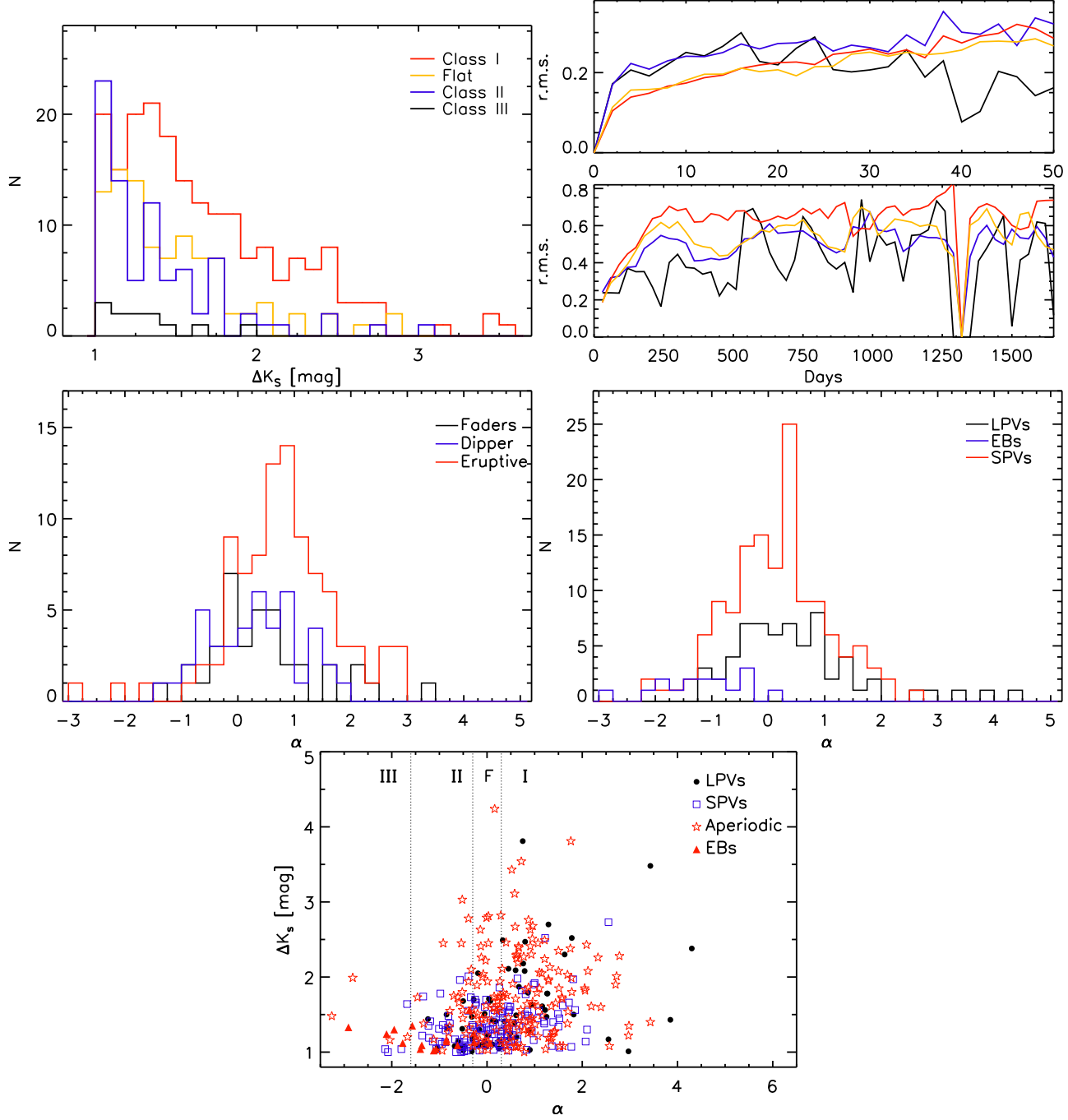


Figure 23. (top, left) ΔK_s distribution of the different YSO classes. (top, right) Mean r.m.s. variability for the different YSO classes over short ($0 < t < 50$ days) and long ($0 < t < 1600$ days) timescales. The colour coding in the top (left and right) figures is the same as in Fig. 22. (middle, left) α distribution for fader (black line), dipper (blue line) and eruptive (red lines) objects. (middle, right) Same distribution but for long-term periodic objects (black lines), stars with short-term variability (red line) and EBs (blue line). (bottom) α vs ΔK_s for objects associated with SFRs. The limits for the different YSO classes are marked by dashed lines. Objects in this figure are divided according to the morphological light curve classification (Sect. 4.1). The different classifications are marked in the plot.

ties (Hartmann & Kenyon 1996), predict outbursts during class I through class II stages of YSO evolution.

The classification as eruptive variables only comes from K_s light curves, and spectroscopic follow up is needed to confirm their YSO nature. However, we note that potentially adding 106 more objects to the YSO eruptive variable class would increase the known members by a factor of five.

Moreover, our survey covers just a portion of the Galactic plane. Therefore eruptive variability in YSOs might be more common than previously thought, especially for the most embedded and young objects. Spectroscopic follow up of a subsample of the objects shows that a large fraction of them are indeed eruptive YSOs (see Paper II).

In paper II we will provide a more detailed discussion on this type of objects

5 SUMMARY AND CONCLUSIONS

We have searched for high amplitude infrared variables in a 119 deg^2 area of the Galactic midplane covered by the VVV survey, using a method that tends to exclude transients and eruptive variables that saturated during outburst or very faint in quiescence, owing to our requirement for a high quality detection at every epoch. We discovered 816 bona fide variables in the 2010–2012 data with $\Delta K_s > 1$ in that time interval. Nearly all of these were previously unknown as variable stars, though a significant minority had been identified as embedded YSO candidates in the Robitaille et al. (2008) catalogue of stars with very red [4.5]–[8.0] *Spitzer*/GLIMPSE colours.

We have presented a fairly simple analysis of the sample using the 2010–2014 VVV light curves, supplemented by a recently obtained 2nd epoch of multi-filter JHK_s data and photometry from *WISE*, and *Spitzer*. Our main conclusions are as follows.

- In agreement with the previous results from searches in the UKIDSS GPS (Contreras Peña et al. 2014), we observe a strong concentration of high-amplitude infrared variables towards areas of star formation. The two point correlation function and nearest neighbour distribution of VVV objects show evidence for clustering on angular scales typical of distant Galactic clusters and SFRs. The variable stars found in SFRs are characterized by having near-infrared colours and SEDs of YSOs.

- The most common types of variable outside SFRs are LPVs (typically dust-obscured Mira variables because other types are saturated in VVV) and EBs. By visual inspection of the light curves of the variables in SFRs we were able to identify and remove most of these contaminating systems and provide a reasonably clean sample of high amplitude YSOs. The YSOs make up about half of the full sample of 816 variables.

- We analysed the light curves of the variables in SFRs, after removal of likely Mira-types, and we classify them as 106 eruptive variables, 39 faders, 45 dippers, 162 short term variables, 65 long-term periodic variables ($P > 100$ days) and 24 eclipsing binaries (EBs) and EB candidates. Individual YSOs may display more than 1 type of variability and the low amplitude variation on short timescales seen in normal YSOs is common in every category.

- Spectroscopic follow up of a substantial subset of the variables with eruptive light curves is presented in the companion paper (Paper II), confirming that the great majority of systems with eruptive light curves are indeed eruptive variables with signatures of strong accretion similar to those seen in EXors or FUors, or a mixture of the two. The 2 epochs of VVV JHK_s multi-colour data indicate that extinction is not the main cause of the variability in systems with eruptive light curves, though there is a trend for the sources to become bluer when brighter, similar to EXors. The faders show a wider range of colour behaviour, with more examples of “bluer when fainter” than the other categories.

- Unsurprisingly, very few of the EBs or dippers showed significant magnitude or colour changes between the two multi-colour epochs. Amongst the STVs, we observe large colour and magnitude changes consistent with the reddening vector in a few systems. It is possible that the flux changes in some of the STVs are caused by extinction, e.g. as has been observed in some binary YSOs with a circumbinary disc (Windemuth & Herbst 2014; Rice et al. 2015).

- The STVs typically have lower amplitudes than any other category except the EBs and EB candidates. Moreover, the STVs have a bluer distribution of spectral indices than the full YSO sample, including a high proportion of class II YSOs with relatively low extinction. It is likely that in many of the STVs with periods $P < 15$ days and K_s amplitudes not far above 1 magnitude the light curve is rotationally modulated by unusually prominent bright or dark spots on the photosphere.

- Variables in the eruptive and fader categories tend to have higher amplitudes than the full YSO sample over the 4 year period, with mean $\Delta K_s = 1.72$ and 1.95 mag, respectively, compared to 1.56 mag for the full YSO sample.

- It is reasonable to suppose that variable accretion is the cause of photometric variability in a proportion of the faders and some of the long-term periodic variables and STVs, although spectroscopic confirmation is limited in these categories as yet. In the periodic variables the accretion rate would presumably be modulated by a companion body (Hodapp et al. 2012). Adding these together with the ~ 100 YSOs with eruptive light curves suggests that the sample contains between 100 and 200 YSOs in which the variability is caused by large changes in accretion. If we take the lower end of this range, this increases the number of probable eruptive variable YSOs available for study by a factor of 5. Some of these systems have K_s amplitudes not far above the 1 mag level, below which variability due to spots and smaller changes in accretion rate and extinction becomes much more common. However, we see no clear argument for a higher threshold given that the amplitudes have a continuous distribution that can be influenced in individual YSOs by the mass and luminosity of the central protostar (Calvet et al. 1991).

- As a whole, the high amplitude variables are a very red sample, dominated by embedded YSOs (i.e. systems with Class I or flat spectrum SEDs that are typically not observable at optical wavelengths). This contrasts with the optical selection of the classical FUors and EXors, the majority of which have a class II or flat spectrum classification. While FUors are often discussed as systems with a remnant envelope, only 3 or 4 deeply embedded eruptive variables were known prior to this study and our recent UGPS 2-epoch study.

- Variables with eruptive light curves tend to have the reddest SEDs. The spectral indices in the eruptive category indicate that this type of variability is at least one order of magnitude more common among class I YSOs than class II YSOs. This demonstrates that eruptive variability is either much more common or recurs much more frequently amongst YSOs at earlier stages of pre-MS evolution, when average accretion rates are higher. We hope this result will inform ongoing efforts to develop a theoretical framework for the phenomenon.

- For the full sample of YSOs, the r.m.s. variability is

higher at earlier evolutionary (SED) classes for time intervals longer than 25 days, and reaches a maximum at 250–350 days for all SED classes. The full duration of the outbursts in eruptive systems is typically 1 to 4 years. Some variables with eruptive light curves show more than 1 outburst. If some of the faders are eruptive variables in decline then a similar or slightly longer duration would apply.

- At time intervals shorter than 25 days the evolutionary dependence is reversed, with class II YSOs showing higher amplitudes than flat spectrum and class I YSOs. This suggests that the shorter timescale variations are dominated by rotational modulation by spots on the photosphere (which are more readily observed in class II systems than embedded YSOs) whereas accretion variations usually take place on longer timescales.

- The 1 to 4 year duration of the eruptions is between that of FUors (> 10 years) and EXors (weeks to months) A small but growing number of eruptive YSOs with these intermediate durations have been found in recent years, some of which have a mixture of the spectroscopic characteristics of FUors and EXors. This has led to the recent concept that FUor and EXors may simply be part of a range of different eruptive behaviours on different timescales, all driven by large variations in accretion rate. Until now it was unclear whether these recent discoveries were rare exceptions, but it now seems clear that they are not. In fact we find that YSOs with intermediate outburst durations outnumber short EXor-like outbursts and are now the majority of known eruptive systems. A much longer duration survey would be required to determine the incidence of FUor-like outbursts amongst embedded systems. In paper II we propose a new class of eruptive variable to describe YSOs with eruptive outbursts of intermediate duration, which are usually optically obscured class I or flat spectrum YSOs and display a variety of the EXor-like and/or FUor-like spectroscopic signatures of strong accretion.

- YSOs are the commonest type of high amplitude infrared variable detected by the VVV survey. We estimate a completeness-corrected source density of 7 deg^{-2} in the mid-plane of quadrant 4, in the approximate mean magnitude range $11 < K_s < 16$. These YSOs are detected at typical distances of a few kpc, there being no very nearby SFRs in the area surveyed, they are therefore likely to be intermediate-mass YSOs. If we were able to detect such objects out to the far edge of the Galactic disc the source density would rise to perhaps $\sim 40 \text{ deg}^{-2}$. This confirms our previous suggestion in Contreras Peña et al. (2014) that high amplitude YSO variables have a higher source density and average space density than Mira variables. EBs are very common at low amplitudes and they may have a comparable space density to YSOs at K_s amplitudes of 1 to 1.6 mag (an approximate upper limit for EBs in *Kepler*). YSOs are more numerous at higher amplitudes and may well be more numerous for all amplitudes over 1 mag if the eruptive phenomenon extends to the lower part of the stellar Initial Mass Function.

ACKNOWLEDGMENTS

This work was supported by the UK's Science and Technology Facilities Council, grant numbers ST/J001333/1, ST/M001008/1 and ST/L001403/1.

We gratefully acknowledge the use of data from the ESO Public Survey program 179.B-2002 taken with the VISTA 4.1m telescope and data products from the Cambridge Astronomical Survey Unit. Support for DM, and CC is provided by the Ministry of Economy, Development, and Tourisms Millennium Science Initiative through grant IC120009, awarded to the Millennium Institute of Astrophysics, MAS. DM is also supported by the Center for Astrophysics and Associated Technologies PFB-06, and Fondecyt Project No. 1130196. This research has made use of the SIMBAD database, operated at CDS, Strasbourg, France; also the SAO/NASA Astrophysics data (ADS). A.C.G. was supported by the Science Foundation of Ireland, grant 13/ERC/I2907.

C. Contreras Peña was supported by a University of Hertfordshire PhD studentship in the earlier stages of this research.

We thank Janet Drew for her helpful comments on the structure of the paper

REFERENCES

- Alencar, S. H. P., et al. 2010, A&A, 519, A88
 Antoniucci, S., Giannini, T., Li Causi, G., & Lorenzetti, D. 2014, ApJ, 782, 51
 Armstrong, D. J., Gómez Maqueo Chew, Y., Faedi, F., & Pollacco, D. 2014, MNRAS, 437, 3473
 Aspin, C., Beck, T. L., & Reipurth, B. 2008, AJ, 135, 423
 Aspin, C., Greene, T. P., & Reipurth, B. 2009, AJ, 137, 2968
 Audard, M., et al. 2014, ArXiv:1401.3368
 Avedisova, V. S. 2002, Astronomy Reports, 46, 193
 Bans, A. & Königl, A. 2012, ApJ, 758, 100
 Baraffe, I., Chabrier, G., & Gallardo, J. 2009, ApJ, 702, L27
 Baraffe, I., Vorobyov, E., & Chabrier, G. 2012, ApJ, 756, 118
 Bate, M. R., Clarke, C. J., & McCaughrean, M. J. 1998, MNRAS, 297, 1163
 Benjamin, R. A., et al. 2003, PASP, 115, 953
 Bessell, M. S. & Brett, J. M. 1988, PASP, 100, 1134
 Bonnell, I. & Bastien, P. 1992, ApJL, 401, L31
 Bouvier, J., Grankin, K., Ellerbroek, L. E., Bouy, H., & Barrado, D. 2013, A&A, 557, A77
 Budding, E., Erdem, A., Çiçek, C., Bulut, I., Soydugan, F., Soydugan, E., Bakiş, V., & Demircan, O. 2004, A&A, 417, 263
 Calvet, N., Patino, A., Magris, G. C., & D'Alessio, P. 1991, ApJ, 380, 617
 Caratti o Garatti, A., et al. 2012, A&A, 538, A64
 Caratti o Garatti, A., et al. 2011, A&A, 526, L1
 Carpenter, J. M., Hillenbrand, L. A., & Skrutskie, M. F. 2001, AJ, 121, 3160
 Catelan, M., et al. 2013, ArXiv:1310.1996
 Cioni, M.-R. L., et al. 2011, A&A, 527, A116
 Cody, A. M., et al. 2014, AJ, 147, 82
 Connelley, M. S. & Greene, T. P. 2014, AJ, 147, 125
 Contreras Peña, C., et al. 2014, MNRAS, 439, 1829
 Culverhouse, T., et al. 2011, ApJS, 195, 8
 Derue, F., et al. 2002, A&A, 389, 149
 Drew, J. E., et al. 2014, MNRAS, 440, 2036

- Dunham, M. M., et al. 2014, ArXiv:1401.1809
- Eiroa, C., et al. 2002, A&A, 384, 1038
- Epcstein, N., et al. 1994, A&SS, 217, 3
- Evans, II, N. J., et al. 2009, ApJS, 181, 321
- Findeisen, K., Hillenbrand, L., Ofek, E., Levitan, D., Sesar, B., Laher, R., & Surace, J. 2013, ApJ, 768, 93
- Gonzalez, O. A., Rejkuba, M., Zoccali, M., Valenti, E., & Minniti, D. 2011, A&A, 534, A3
- Greene, T. P. & Lada, C. J. 1996, AJ, 112, 2184
- Greene, T. P., Wilking, B. A., Andre, P., Young, E. T., & Lada, C. J. 1994, ApJ, 434, 614
- Hartmann, L. & Kenyon, S. J. 1996, ARA&A, 34, 207
- Herbst, W. & Shevchenko, V. S. 1999, AJ, 118, 1043
- Hodapp, K. W. & Chini, R. 2015, ApJ, 813, 107
- Hodapp, K. W., Chini, R., Watermann, R., & Lemke, R. 2012, ApJ, 744, 56
- Hodapp, K.-W., Hora, J. L., Rayner, J. T., Pickles, A. J., & Ladd, E. F. 1996, ApJ, 468, 861
- Huckvale, L., Kerins, E., & Sale, S. E. 2014, MNRAS, 442, 259
- Hughes, J. P., Slane, P., Posselt, B., Charles, P., Rajoelimanana, A., Sefako, R., Halpern, J., & Steeghs, D. 2010, The Astronomer's Telegram, 2771, 1
- Irwin, M. 2009, UKIRT Newsletter, 25, 15
- Ishihara, D., Kaneda, H., Onaka, T., Ita, Y., Matsuura, M., & Matsunaga, N. 2011, A&A, 534, A79
- Jiménez-Esteban, F. M., García-Lario, P., Engels, D., & Manchado, A. 2006a, A&A, 458, 533
- Jiménez-Esteban, F. M., García-Lario, P., Engels, D., & Perea Calderón, J. V. 2006b, A&A, 446, 773
- Kenyon, S. J., Hartmann, L. W., Strom, K. M., & Strom, S. E. 1990, AJ, 99, 869
- Koenig, X. P. & Leisawitz, D. T. 2014, ApJ, 791, 131
- Kóspál, Á., Ábrahám, P., Prusti, T., Acosta-Pulido, J., Hony, S., Moór, A., & Siebenmorgen, R. 2007, A&A, 470, 211
- Lada, C. J. 1987, in IAU Symposium, Vol. 115, Star Forming Regions, ed. M. Peimbert & J. Jugaku, 1–17
- Lawrence, A., et al. 2007, MNRAS, 379, 1599
- López-Morales, M. & Clemens, J. C. 2004, PASP, 116, 22
- Lorenzetti, D., et al. 2012, ApJ, 749, 188
- Lorenzetti, D., Larionov, V. M., Giannini, T., Arkharov, A. A., Antoniucci, S., Nisini, B., & Di Paola, A. 2009, ApJ, 693, 1056
- Lucas, P. W., et al. 2008, MNRAS, 391, 136
- Marshall, D. J., Robin, A. C., Reylé, C., Schultheis, M., & Picaud, S. 2006, A&A, 453, 635
- Megeath, S. T., et al. 2012, AJ, 144, 192
- Meyer, M. R., Calvet, N., & Hillenbrand, L. A. 1997, AJ, 114, 288
- Minniti, D., et al. 2010, NewA, 15, 433
- Minniti, D., Saito, R. K., Alonso-García, J., Lucas, P. W., & Hempel, M. 2011, ApJL, 733, L43
- Murakami, H., et al. 2007, PASJ, 59, 369
- Ninan, J. P., et al. 2015, ArXiv e-prints
- Ochsenbein, F., Bauer, P., & Marcout, J. 2000, A&AS, 143, 23
- Paczynski, B., Szczygiel, D. M., Pilecki, B., & Pojmański, G. 2006, MNRAS, 368, 1311
- Persi, P., Tapia, M., Gómez, M., Whitney, B. A., Marenzi, A. R., & Roth, M. 2007, AJ, 133, 1690
- Pietrukowicz, P., et al. 2013, AcA, 63, 115
- Plavchan, P., Gee, A. H., Stapelfeldt, K., & Becker, A. 2008, ApJL, 684, L37
- Price, S. D., Egan, M. P., Carey, S. J., Mizuno, D. R., & Kuchar, T. A. 2001, AJ, 121, 2819
- Rebull, L. M., et al. 2014, AJ, 148, 92
- Reipurth, B. & Aspin, C. 2010, in Evolution of Cosmic Objects through their Physical Activity, ed. H. A. Harutyunian, A. M. Mickaelian, & Y. Terzian, 19–38
- Rice, T. S., Reipurth, B., Wolk, S. J., Vaz, L. P., & Cross, N. J. G. 2015, ArXiv e-prints
- Rice, T. S., Wolk, S. J., & Aspin, C. 2012, ApJ, 755, 65
- Robitaille, T. P., et al. 2008, AJ, 136, 2413
- Robitaille, T. P., Whitney, B. A., Indebetouw, R., Wood, K., & Denzmore, P. 2006, ApJS, 167, 256
- Romanova, M. M., Ustyugova, G. V., Koldoba, A. V., & Lovelace, R. V. E. 2013, MNRAS, 430, 699
- Russeil, D. 2003, A&A, 397, 133
- Safron, E. J., et al. 2015, ApJL, 800, L5
- Saito, R. K., et al. 2012, A&A, 537, A107
- Saito, R. K., et al. 2013, A&A, 554, A123
- Schechter, P. L., Mateo, M., & Saha, A. 1993, PASP, 105, 1342
- Schlafly, E. F. & Finkbeiner, D. P. 2011, ApJ, 737, 103
- Schlegel, D. J., Finkbeiner, D. P., & Davis, M. 1998, ApJ, 500, 525
- Scholz, A. 2012, MNRAS, 420, 1495
- Scholz, A., Froebrich, D., & Wood, K. 2013, MNRAS, 430, 2910
- Skrutskie, M. F., et al. 2006, AJ, 131, 1163
- Stellingwerf, R. F. 1978, ApJ, 224, 953
- Takami, M., Chen, H.-H., Karr, J. L., Lee, H.-T., Lai, S.-P., & Minh, Y.-C. 2012, ApJ, 748, 8
- Tudose, V., Fender, R. P., Tzioumis, A. K., Spencer, R. E., & van der Klis, M. 2008, MNRAS, 390, 447
- Vorobyov, E. I. & Basu, S. 2015, ApJ, 805, 115
- Wenger, M., et al. 2000, A&AS, 143, 9
- Whitelock, P. A., Feast, M. W., & van Leeuwen, F. 2008, MNRAS, 386, 313
- Windemuth, D. & Herbst, W. 2014, AJ, 147, 9
- Wolk, S. J., et al. 2015, ArXiv e-prints
- Wolk, S. J., Rice, T. S., & Aspin, C. 2013, ApJ, 773, 145
- Wright, E. L., et al. 2010, AJ, 140, 1868
- Zhu, Z., Hartmann, L., & Gammie, C. 2009, ApJ, 694, 1045

APPENDIX A: ECLIPSING BINARIES

In order to compare the YSO and EB space densities, we look at the measured source density of EBs detected in Galactic disc fields by OGLE-III (Pietrukowicz et al. 2013) and estimate their distances with the help of a recent analysis of the physical properties of *Kepler* eclipsing binaries (Armstrong et al. 2014).

Shallow surveys such as the Automated All-Sky Survey (ASAS Paczyński et al. 2006) are sensitive only to the more luminous high amplitude EBs, which are mainly early type Algol systems, similar to the high amplitude EBs in the General Catalogue of Variable Stars (Samus et al. 2010). However, simulations by López-Morales & Clemens (2004) find that EBs seen by deeper surveys such as OGLE-III will be dominated by later type systems. Armstrong et al.

(2014) analysed the large sample of EBs discovered by *Kepler*, providing temperature and radius estimates for the full sample. They note that their results are most accurate for cases where the temperatures of the primary and the secondary are very different, which is fortunate because this is characteristic of high amplitude EBs, in which a hotter main sequence star is eclipsed by a cooler giant star. Inspection of their results shows that high amplitude EBs fall into 2 groups: EBs with early type primaries and EBs with F or early G-type primaries. Simple calculations assuming Planckian SEDs indicate that only the latter group can produce eclipses deeper than 1 magnitude in the K_s passband (and this group also dominates in the OGLE I passband) because early type stars emit little of their total flux in the infrared. The same calculations indicate that no systems with K_s amplitudes above 1.6 mag exist in the *Kepler* sample, whereas YSOs with higher amplitudes are common in our sample, see Sect. 4. Applying this approach in the optical indicates that EBs should exist with amplitudes up to 3 mag in the I passband. This limit is confirmed by the OGLE-III sample of Pietrukowicz et al. (2013), thereby giving confidence that our limit of 1.6 mag at K_s is robust. Indeed our VVV sample of 72 EBs contains no systems with higher amplitude than this. We can assume that the EBs from Pietrukowicz et al. (2013) are mainly composed of F or early G-type stars, based on the *Kepler* results, together with the fact that later type primaries are not expected given the need for these systems to have produced a post-main sequence star within the lifetime of the Galactic disc. Pietrukowicz et al. (2013) reports the discovery of 11589 EBs in area of 7.21 deg^2 across different fields on the Galactic midplane. The catalogue of EBs is reported to be 75% complete to $I=18$. Correcting for the 75% completeness indicates a source density of $2143 \text{ EBs deg}^{-2}$, from which only $\sim 1.6\%$ display $\Delta I > 1$ magnitude. Our Planckian calculations using the results of Armstrong et al. (2014) suggest that this drops to 0.6% at K_s . This implies ~ 12 high amplitude EBs per deg^2 . We can estimate the extinction to the EBs from their observed $V - I$ colours and then roughly estimate their typical distances either using the absolute I magnitudes of F to early G-stars or by converting extinction to distance using the red clump giant branch (as in Sect. 4.3). Both approaches indicate that the EBs from Pietrukowicz et al. (2013) are typically at heliocentric distances of a few kpc, which is similar to the estimated distances to our YSOs based on radial velocities, literature distances to the SFRs and SED fitting (see paper II). Given that the surface density of EBs ($\sim 12 \text{ deg}^{-2}$) is similar to the surface density of the VVV YSO population sampled in this study ($\sim 7 \text{ deg}^{-2}$), the similar distances suggest that the high amplitude EB and YSO populations may have similar average space densities, within an order of magnitude. The YSO population is certainly more numerous at K_s amplitudes over 1.6 mag. If the high amplitude YSO population extends well below a solar mass, which is very possible, then they would probably be more numerous even at our $\Delta K_s = 1$ mag threshold. However, the VVV and OGLE-III data tell us only that both populations are substantial. The number of YSOs rises steeply up to the sensitivity limit and a similar trend is obtained in EBs if we assume that a significant fraction of the unclassified variables shown in Fig. 10 are EBs.

Category	Median $\Delta W1$	Median $\Delta W2$	Median $\Delta(W1 - W2)$	No. in sample
Faders	1.33	0.93	0.37	12
Eruptive	0.72	0.56	0.26	21
lpv-YSOs	0.62	0.67	0.13	23
STVs	0.50	0.38	0.10	11
Dippers	0.59	0.62	0.27	9

Table B1. Colour and megntitude changes measured by WISE.

APPENDIX B: MID-INFRARED COLOUR AND MAGNITUDE VARIABILITY

Photometry from the WISE and NEOWISE missions in the W1 ($3.4 \mu\text{m}$) and W2 ($4.6 \mu\text{m}$) passbands are available at 4 epochs for the whole sky, with simultaneous photometry in the two filters. The WISE satellite scanned the whole sky twice in 2010, at epochs separated by 6 months, and the extended mission, NEOWISE, has repeated the process in 2014. For any given sky location, each epoch is composed of multiple scans taken over a period of several days. For all the high amplitude variables, we downloaded photometry for all these scans from the AllWISE Multiepoch Photometry table (for the 2010 data) and NEOWISE-R Single Exposure L1b Source Table (for the 2014 data), both of which are archived in IRSAs.

Inspection of the W1 and W2 photometry indicated that the uncertainties typically become larger for saturated stars and for faint stars in crowded Galactic fields. For this analysis we therefore considered only sources with $7 < W1 < 11$, and $6 < W2 < 11$ (defining these cuts with the AllWISE Source Catalog). We combined the data from the multiple scans into the 4 widely separated epochs by binning the scans into groups (epochs) with a maximum baseline of 20 days and computing the medians of $W1$, $W2$ and $(W1 - W2)$ at each epoch.

In most cases the WISE data do not sample the full peak to trough variation in the VVV light curves, so changes in $W1$ and $W2$ fluxes are often small. We define $\Delta W1$, $\Delta W2$ and $\Delta(W1 - W2)$ for each source as the largest difference observed at any two epochs (not necessarily the same pair of epochs for each quantity). Then considering each type of VVV light curve category, we present the median of these quantities in Table B1. We see that both magnitude and colour variability are typically larger for faders than the other categories, as is the case in K_s . Eruptive sources, dippers and lpv-YSOs have similar magnitude changes, while STVs have smaller changes (as in K_s). EBs typically show negligible changes since the eclipses are very rarely sampled.

The WISE data are less useful than the JHK_s data for investigating the physical cause of the photometric variability in K_s because the extinction vs. wavelength relation appears to depend strongly on environment (Koenig & Leisawitz 2014). Also, extinction is lower in the WISE passbands than at K_s so extinction may have less effect on the $W1 - W2$ colour than even a modest change in accretion rate.

In most STVs and lpv-YSOs we can confidently state the extinction is not the main cause of the measured $W1$ - $W2$ colour changes because the trend over the 4 epochs is "bluer when fainter", or a negligible colour change, or there is no clear trend. In the eruptive and fader categories about half

the variables (10/21 and 7/12) have a "redder when fainter" trend that might be due to variable accretion, variable extinction, or a combination of the two (in some sources, 1 of the 4 epochs does not follow the trend of the other 3 epochs). The remainder of the eruptive variables and faders show a different trend or no clear result. In some sources with a "redder when fainter" trend in the WISE data, the 2 epochs of JHK_s data appear to rule out extinction as the cause of variability. In dippers, the majority (5/9) sources have a "redder when fainter" trend that might be consistent with extinction.

These results are not very informative because of the limited sampling of the WISE data. In most cases $K_s - W1$, $K_s - W2$ changes cannot be investigated because there are very few sources for which two of the WISE epochs are contemporaneous with VVV K_s epochs.

Fortunately, there are some sources with clear long term trends in the 2010-2014 VVV light curves for which we can usefully compare WISE data from 2010 and 2014. Four examples of such sources are VVVv270, VVVv631, VVV118 and VVVv562, all of which are members of the spectroscopic sub-sample that are discussed individually in Paper II. To bring together those sources here, we note that all four have unusually large amplitudes in K_s , $W1$ and $W2$ ($2.6 < \Delta K_s < 4.2$ mag). The first two show a rising trend (classed as eruptive light curves) whereas the other two show a declining trend: VVVv562 is a fader but VVVv118 is an eruptive variable with several brief eruptions superimposed on a long-term decline. In every case the trend is similar in the 3 wavelengths but the amplitude is larger in K_s than in $W1$ and $W2$, typically by a factor between 1 and 2. Three sources have $\Delta W1 \approx \Delta W2$ (VVVv118, VVVv562, VVVv631), whereas in VVVv270 $\Delta W1 \approx 2\Delta W2$.

The spectroscopic evidence in paper II indicates that these four variables are all bona fide eruptive variables driven by episodic accretion, so the different amplitudes in the different filters presumably reflect differing changes in the luminosity of the different regions of the accretion disc responsible for most of the emission at each wavelength, as well as the effect of temperature changes on the flux emitted by each region at different wavelengths.

APPENDIX C: TABLE 1

Table C1: Parameters of the high-amplitude variables from VVV.

Object ID	VVV Designation	α (J2000)	δ (J2000)	l	b	Z	Z_{err}	Y	Y_{err}	J	J_{err}	H	H_{err}	K_s	$K_{s,err}$	ΔK_s	α_{class}	SFR	Class
VVVv1	VVV J114135.16-622055.51	11:41:35.16	-62:20:55.51	294.92603	-0.56770	—	—	—	—	17.99	0.06	15.95	0.02	14.44	0.01	1.34	-0.29	y	STV
VVVv2	VVV J114412.94-623449.09	11:44:12.94	-62:34:49.09	295.28005	-0.71146	—	—	—	—	—	—	18.78	0.23	15.71	0.03	2.52	1.22	y	STV
VVVv3	VVV J115113.03-623729.29	11:51:13.03	-62:37:29.29	296.07199	-0.55784	13.17	0.01	12.93	0.01	12.90	0.01	12.70	0.01	12.24	0.01	2.21	—	n	Known
VVVv4	VVV J115808.69-630708.60	11:58:08.69	-63:07:08.60	296.95057	-0.86785	—	—	—	—	18.23	0.08	16.62	0.04	15.32	0.02	1.10	-0.24	y	STV
VVVv5	VVV J115959.68-622613.20	11:59:59.68	-62:26:13.20	297.02026	-0.15716	17.69	0.02	16.62	0.01	15.87	0.01	15.25	0.01	13.53	0.01	1.30	—	n	LPV
VVVv6	VVV J115937.81-631109.77	11:59:37.81	-63:11:09.77	297.12836	-0.89953	19.02	0.05	18.08	0.04	16.80	0.02	15.95	0.02	15.50	0.02	1.02	—	n	EB
VVVv7	VVV J120202.67-623615.60	12:02:02.67	-62:36:15.60	297.28472	-0.27538	—	—	—	—	—	—	—	—	17.22	0.12	1.60	2.39	y	Eruptive
VVVv8	VVV J120059.11-631636.18	12:00:59.11	-63:16:36.18	297.29582	-0.95838	—	—	—	—	—	—	—	—	16.86	0.09	1.38	0.64	y	Eruptive
VVVv9	VVV J120217.23-623647.83	12:02:17.23	-62:36:47.83	297.31381	-0.27888	—	—	—	—	18.29	0.08	16.33	0.03	14.64	0.01	2.78	-0.39	y	Dipper
VVVv10	VVV J120250.85-622437.62	12:02:50.85	-62:24:37.62	297.33912	-0.06749	18.57	0.04	18.23	0.05	16.97	0.03	16.35	0.03	16.07	0.04	1.19	—	n	STV
VVVv11	VVV J120436.62-625704.60	12:04:36.62	-62:57:04.60	297.63741	-0.56188	20.20	0.19	19.01	0.13	17.87	0.07	16.79	0.05	16.08	0.08	1.10	—	n	STV
VVVv12	VVV J121033.19-630755.71	12:10:33.19	-63:07:55.71	298.33185	-0.62611	—	—	—	—	—	—	16.30	0.03	15.04	0.03	1.74	0.28	y	Fader
VVVv13	VVV J121216.83-624838.32	12:12:16.83	-62:48:38.32	298.47603	-0.27814	—	—	—	—	—	—	—	—	16.72	0.14	1.40	1.39	y	STV
VVVv14	VVV J121218.13-624904.48	12:12:18.13	-62:49:04.48	298.47958	-0.28495	19.48	0.10	18.88	0.12	17.84	0.06	16.74	0.05	15.56	0.05	1.29	0.88	y	LPV-YSO
VVVv15	VVV J121226.09-624416.97	12:12:26.09	-62:44:16.97	298.48252	-0.20371	19.00	0.07	17.72	0.04	16.57	0.02	15.60	0.02	15.04	0.03	1.09	—	y	EB
VVVv16	VVV J121329.76-624107.74	12:13:29.76	-62:41:07.74	298.59498	-0.13364	18.01	0.03	17.13	0.02	16.06	0.01	14.72	0.01	13.66	0.01	1.29	0.92	y	Eruptive
VVVv17	VVV J121352.08-625549.90	12:13:52.08	-62:55:49.90	298.67278	-0.36986	—	—	—	—	—	—	17.79	0.12	16.41	0.10	1.22	0.44	y	STV
VVVv18	VVV J121950.31-632142.24	12:19:50.31	-63:21:42.24	299.39868	-0.70695	17.82	0.02	17.29	0.02	16.20	0.01	15.52	0.01	15.32	0.02	1.04	—	n	STV
VVVv19	VVV J122255.30-632352.56	12:22:55.30	-63:23:52.56	299.74594	-0.70270	19.56	0.08	18.67	0.06	17.55	0.04	16.40	0.03	15.61	0.03	1.82	—	n	EB
VVVv20	VVV J122827.97-625713.97	12:28:27.97	-62:57:13.97	300.32402	-0.19849	—	—	—	—	17.38	0.04	14.10	0.01	11.70	0.01	1.71	0.60	y	Eruptive
VVVv21	VVV J122902.24-625234.10	12:29:02.24	-62:52:34.10	300.38193	-0.11533	—	—	—	—	—	—	17.12	0.05	15.80	0.03	1.79	0.86	y	LPV-YSO
VVVv22	VVV J123105.60-624457.34	12:31:05.60	-62:44:57.34	300.60547	0.03057	—	—	—	—	18.81	0.14	16.94	0.05	15.55	0.03	1.73	-0.34	y	STV
VVVv23	VVV J123128.53-624433.10	12:31:28.53	-62:44:33.10	300.64855	0.04070	19.44	0.07	18.37	0.05	17.14	0.03	15.57	0.02	14.40	0.01	1.51	-0.20	y	Fader
VVVv24	VVV J123235.68-634319.61	12:32:35.68	-63:43:19.61	300.84794	-0.92662	17.17	0.01	16.13	0.01	14.05	0.01	12.95	0.01	12.23	0.01	1.20	—	n	LPV
VVVv25	VVV J123514.37-624715.63	12:35:14.37	-62:47:15.63	301.08129	0.02587	—	—	—	—	—	—	16.01	0.02	12.34	0.01	1.68	0.22	y	Eruptive
VVVv26	VVV J123845.66-631136.03	12:38:45.66	-63:11:36.03	301.50320	-0.35674	—	—	—	—	19.67	0.29	16.70	0.04	14.71	0.01	2.45	1.07	y	Eruptive
VVVv27	VVV J123848.33-633939.15	12:38:48.33	-63:39:39.15	301.53114	-0.82347	—	—	—	—	—	—	—	—	12.04	0.01	2.73	—	n	LPV
VVVv28	VVV J123911.54-630524.76	12:39:11.54	-63:05:24.76	301.54688	-0.25138	—	—	—	—	—	—	18.91	0.32	16.78	0.09	1.39	0.54	y	STV
VVVv29	VVV J123931.48-630720.38	12:39:31.48	-63:07:20.38	301.58593	-0.28170	—	—	—	—	—	—	—	—	16.94	0.10	2.13	1.32	y	Eruptive
VVVv30	VVV J124140.56-635033.57	12:41:40.56	-63:50:33.57	301.85616	-0.99128	17.92	0.02	17.22	0.02	16.40	0.02	15.66	0.02	15.23	0.02	1.22	—	n	EB
VVVv31	VVV J124140.15-635918.05	12:41:40.15	-63:59:18.05	301.86093	-1.13689	13.91	0.01	13.27	0.01	12.46	0.01	12.08	0.01	11.69	0.01	1.15	—	n	LPV
VVVv32	VVV J124357.15-625445.09	12:43:57.15	-62:54:45.09	302.07991	-0.05314	19.58	0.07	18.08	0.04	16.07	0.01	14.07	0.01	12.45	0.01	2.49	0.33	y	LPV-YSO
VVVv33	VVV J124425.05-631355.76	12:44:25.05	-63:13:55.76	302.14153	-0.37116	—	—	—	—	—	—	18.10	0.16	16.43	0.07	1.37	—	n	STV
VVVv34	VVV J125029.87-625124.93	12:50:29.87	-62:51:24.93	302.82470	0.01465	19.22	0.05	18.32	0.05	17.86	0.06	16.70	0.04	15.71	0.03	1.30	-0.34	y	STV
VVVv35	VVV J125206.52-635711.52	12:52:06.52	-63:57:11.52	303.00557	-1.08152	17.62	0.01	16.85	0.01	17.13	0.03	16.21	0.03	15.97	0.04	1.24	—	n	EB
VVVv36	VVV J125917.72-633008.44	12:59:17.72	-63:30:08.44	303.80825	-0.64394	14.38	0.01	13.84	0.01	13.27	0.01	12.56	0.01	11.81	0.01	1.03	-0.11	y	Eruptive
VVVv37	VVV J130243.05-631130.00	13:02:43.05	-63:11:30.00	304.20331	-0.34774	18.80	0.03	17.75	0.03	16.74	0.02	15.89	0.02	15.38	0.03	1.34	—	n	STV
VVVv38	VVV J130311.38-631439.09	13:03:11.38	-63:14:39.09	304.25411	-0.40259	—	—	—	—	—	—	17.79	0.13	16.32	0.07	1.41	1.20	y	STV
VVVv39	VVV J130440.98-635313.45	13:04:40.98	-63:53:13.45	304.38893	-1.05277	18.67	0.03	17.89	0.03	17.57	0.05	16.38	0.04	15.49	0.03	1.51	—	n	STV
VVVv40	VVV J130600.43-630144.40	13:06:00.43	-63:01:44.40	304.58298	-0.20394	20.71	0.20	19.49	0.14	16.52	0.02	15.42	0.02	14.69	0.01	1.24	—	n	EB
VVVv41	VVV J130944.05-634431.38	13:09:44.05	-63:44:31.38	304.95408	-0.94214	18.09	0.02	17.50	0.03	15.83	0.01	15.22	0.01	14.90	0.02	1.20	—	n	EB

Continued on next page

Table C1 – *Continued from previous page*

Object ID	VVV Designation	α (J2000)	δ (J2000)	l (degrees)	b (degrees)	Z (mag)	Z_{err} (mag)	Y (mag)	Y_{err} (mag)	J (mag)	J_{err} (mag)	H (mag)	H_{err} (mag)	K_s (mag)	$K_{s,err}$ (mag)	ΔK_s (mag)	α_{class}	SFR	Class
VVVv42	VVV J130934.64-624932.52	13:09:34.64	-62:49:32.52	305.00126	-0.02683	–	–	–	–	18.45	0.10	14.26	0.01	11.94	0.01	2.16	–	n	EB
VVVv43	VVV J131044.06-625541.32	13:10:44.06	-62:55:41.32	305.12535	-0.13858	–	–	–	–	–	–	17.62	0.11	16.14	0.06	1.23	0.53	y	STV
VVVv44	VVV J131054.29-625604.36	13:10:54.29	-62:56:04.36	305.14420	-0.14642	–	–	–	–	19.34	0.23	16.83	0.05	15.15	0.02	1.27	–	y	STV
VVVv45	VVV J131143.07-624854.77	13:11:43.07	-62:48:54.77	305.24579	-0.03459	–	–	–	–	–	–	–	–	13.33	0.01	2.32	1.27	y	LPV-Mira
VVVv46	VVV J131246.62-625628.58	13:12:46.62	-62:56:28.58	305.35595	-0.16998	–	–	–	–	–	–	17.32	0.09	15.80	0.04	1.31	0.12	y	STV
VVVv47	VVV J131313.97-624429.31	13:13:13.97	-62:44:29.31	305.42449	0.02477	–	–	–	–	19.12	0.19	17.27	0.08	15.93	0.05	1.71	0.04	y	LPV-YSO
VVVv48	VVV J131545.37-625244.45	13:15:45.37	-62:52:44.45	305.69929	-0.13798	–	–	–	–	19.53	0.28	17.39	0.09	16.09	0.05	1.30	–	y	Dipper
VVVv49	VVV J131816.29-633743.65	13:18:16.29	-63:37:43.65	305.90658	-0.91211	19.98	0.13	–	–	18.35	0.09	–	–	12.48	0.01	1.76	–	n	LPV
VVVv50	VVV J131843.99-632716.96	13:18:43.99	-63:27:16.96	305.97598	-0.74438	17.60	0.02	17.30	0.02	16.24	0.01	15.81	0.02	15.60	0.03	1.14	–	n	STV
VVVv51	VVV J131942.87-630101.88	13:19:42.87	-63:01:01.88	306.13293	-0.32129	–	–	–	–	–	–	16.86	0.05	14.49	0.01	2.82	0.29	y	Dipper
VVVv52	VVV J132308.94-624835.13	13:23:08.94	-62:48:35.13	306.54533	-0.16068	14.49	0.01	13.64	0.01	12.75	0.01	12.66	0.01	12.16	0.01	1.11	–	n	EB
VVVv53	VVV J132702.40-630622.47	13:27:02.40	-63:06:22.47	306.94521	-0.51222	–	–	–	–	–	–	16.61	0.06	14.53	0.02	2.41	0.66	y	Eruptive
VVVv54	VVV J132758.65-631448.97	13:27:58.65	-63:14:48.97	307.03032	-0.66629	12.89	0.01	12.51	0.01	–	–	12.49	0.01	12.12	0.01	1.02	–	n	Known
VVVv55	VVV J133403.43-625325.69	13:34:03.43	-62:53:25.69	307.76515	-0.41933	20.11	0.21	18.92	0.15	16.87	0.03	15.93	0.03	15.39	0.03	1.15	–	n	STV
VVVv56	VVV J133746.01-622807.54	13:37:46.01	-62:28:07.54	308.25687	-0.07694	19.21	0.08	17.48	0.03	15.52	0.01	13.41	0.01	12.45	0.01	1.41	0.18	y	LPV-YSO
VVVv57	VVV J134041.89-631440.96	13:40:41.89	-63:14:40.96	308.44250	-0.90120	–	–	–	–	18.10	0.06	16.69	0.04	15.85	0.04	1.62	–	n	EB
VVVv58	VVV J134213.00-621825.35	13:42:13.00	-62:18:25.35	308.79362	-0.01457	17.48	0.02	16.46	0.01	15.04	0.01	13.79	0.01	12.61	0.01	1.20	–	n	LPV
VVVv59	VVV J134330.94-623719.95	13:43:30.94	-62:37:19.95	308.87836	-0.35323	–	–	–	–	17.64	0.04	14.68	0.01	12.62	0.01	1.11	–	n	LPV
VVVv60	VVV J134452.75-631740.41	13:44:52.75	-63:17:40.41	308.89356	-1.04304	–	–	18.78	0.09	16.98	0.02	15.82	0.02	15.15	0.02	1.13	–	n	EB
VVVv61	VVV J134406.00-624932.88	13:44:06.00	-62:49:32.88	308.90289	-0.56614	–	–	–	–	–	–	18.27	0.17	15.54	0.03	1.04	–	n	STV
VVVv62	VVV J134550.28-622827.70	13:45:50.28	-62:28:27.70	309.17062	-0.26336	–	–	–	–	–	–	–	–	14.01	0.01	1.85	1.13	y	LPV-Mira
VVVv63	VVV J134620.48-622530.81	13:46:20.48	-62:25:30.81	309.23785	-0.22755	–	–	–	–	18.53	0.09	15.79	0.02	13.81	0.01	1.44	0.90	y	Eruptive
VVVv64	VVV J134623.81-622003.09	13:46:23.81	-62:20:03.09	309.26338	-0.13994	–	–	–	–	–	–	14.96	0.01	11.44	0.01	1.17	-0.31	y	LPV-YSO
VVVv65	VVV J134751.09-624237.46	13:47:51.09	-62:42:37.46	309.34673	-0.54335	–	–	–	–	18.75	0.10	15.85	0.02	13.59	0.01	1.36	-0.31	y	STV
VVVv66	VVV J134820.90-624309.74	13:48:20.90	-62:43:09.74	309.40035	-0.56451	–	–	–	–	18.12	0.06	16.64	0.03	15.41	0.03	1.24	0.02	y	STV
VVVv67	VVV J134838.70-624627.31	13:48:38.70	-62:46:27.31	309.42145	-0.62550	–	–	–	–	19.33	0.17	16.98	0.05	15.61	0.03	1.08	0.40	y	Eruptive
VVVv68	VVV J134843.51-624549.42	13:48:43.51	-62:45:49.42	309.43271	-0.61725	–	–	–	–	19.90	0.28	16.42	0.03	14.56	0.01	1.03	0.14	y	STV
VVVv69	VVV J134759.94-622011.92	13:47:59.94	-62:20:11.92	309.44451	-0.18221	–	–	–	–	19.69	0.24	17.55	0.08	16.34	0.06	1.36	–	n	LPV
VVVv70	VVV J135020.05-624524.09	13:50:20.05	-62:45:24.09	309.61377	-0.65149	–	–	20.14	0.21	18.05	0.05	16.35	0.03	15.31	0.02	1.15	–	n	EB
VVVv71	VVV J135332.54-623724.91	13:53:32.54	-62:37:24.91	310.00262	-0.60748	–	–	–	–	19.15	0.14	16.79	0.04	15.23	0.02	1.15	–	n	LPV
VVVv72	VVV J135328.30-623001.48	13:53:28.30	-62:30:01.48	310.02404	-0.48591	21.20	0.33	19.39	0.11	17.77	0.04	16.53	0.03	15.83	0.04	1.03	–	n	EB
VVVv73	VVV J135517.97-630055.44	13:55:17.97	-63:00:55.44	310.10271	-1.03615	16.43	0.01	15.27	0.01	15.21	0.01	14.29	0.01	13.64	0.01	1.02	–	n	EB
VVVv74	VVV J135625.78-630003.44	13:56:25.78	-63:00:03.44	310.23056	-1.05383	17.69	0.02	17.21	0.02	16.50	0.01	15.91	0.02	15.57	0.03	1.04	–	n	STV
VVVv75	VVV J135613.31-623609.30	13:56:13.31	-62:36:09.30	310.30662	-0.66206	–	–	–	–	18.81	0.10	17.09	0.05	15.86	0.04	1.17	–	n	Rare
VVVv76	VVV J135547.01-621233.21	13:55:47.01	-62:12:33.21	310.35477	-0.26837	–	–	–	–	19.88	0.28	15.35	0.01	11.94	0.01	1.65	–	n	LPV
VVVv77	VVV J135706.18-620016.61	13:57:06.18	-62:00:16.61	310.55520	-0.10865	–	–	19.74	0.16	18.83	0.11	17.63	0.08	16.87	0.10	1.06	–	y	STV
VVVv78	VVV J135733.86-615736.39	13:57:33.86	-61:57:36.39	310.61885	-0.07926	20.79	0.23	19.14	0.09	17.59	0.04	16.04	0.02	15.13	0.02	1.01	–	n	LPV
VVVv79	VVV J135935.30-621036.12	13:59:35.30	-62:10:36.12	310.79224	-0.34949	–	–	–	–	–	–	18.68	0.25	16.75	0.15	1.12	–	y	Eruptive
VVVv80	VVV J135903.61-614733.53	13:59:03.61	-61:47:33.53	310.83213	0.03749	–	–	–	–	18.87	0.12	16.74	0.04	15.45	0.05	1.14	-0.99	y	STV
VVVv81	VVV J140700.55-615115.98	14:07:00.55	-61:51:15.98	311.71777	-0.27860	–	–	–	–	–	–	17.32	0.07	13.20	0.01	1.66	0.67	y	LPV-Mira
VVVv82	VVV J140719.19-613717.46	14:07:19.19	-61:37:17.46	311.82022	-0.06621	–	–	–	–	–	–	15.71	0.02	11.75	0.01	1.47	-0.32	y	LPV-YSO
VVVv83	VVV J141056.71-622513.45	14:10:56.71	-62:25:13.45	311.98995	-0.95514	–	–	17.99	0.03	16.39	0.01	14.44	0.01	12.75	0.01	1.12	0.22	y	LPV-Mira

Continued on next page

Table C1 – *Continued from previous page*

Object ID	VVV Designation	α (J2000)	δ (J2000)	l (degrees)	b (degrees)	Z (mag)	Z_{err} (mag)	Y (mag)	Y_{err} (mag)	J (mag)	J_{err} (mag)	H (mag)	H_{err} (mag)	K_s (mag)	$K_{s,err}$ (mag)	ΔK_s (mag)	α_{class}	SFR	Class
VVVv84	VVV J140911.55-613224.31	14:09:11.55	-61:32:24.31	312.05712	-0.05358	20.05	0.13	19.33	0.11	17.10	0.03	14.02	0.01	11.97	0.01	2.81	0.03	y	Fader
VVVv85	VVV J141046.67-615734.01	14:10:46.67	-61:57:34.01	312.11070	-0.50985	19.81	0.10	18.86	0.07	17.68	0.04	16.20	0.03	15.39	0.04	1.32	–	n	LPV
VVVv86	VVV J141028.74-614946.06	14:10:28.74	-61:49:46.06	312.11632	-0.37530	–	–	–	–	18.34	0.08	13.78	0.01	10.78	0.01	2.10	–	n	LPV
VVVv87	VVV J141254.98-614527.53	14:12:54.98	-61:45:27.53	312.41250	-0.39486	–	–	–	–	–	–	18.52	0.22	15.40	0.04	1.73	0.23	y	Fader
VVVv88	VVV J141227.76-613027.81	14:12:27.76	-61:30:27.81	312.43848	-0.14052	–	–	–	–	18.42	0.08	16.68	0.04	15.71	0.06	1.52	–	y	STV
VVVv89	VVV J141534.31-621945.07	14:15:34.31	-62:19:45.07	312.52810	-1.03528	–	–	–	–	–	–	15.71	0.02	12.28	0.01	2.52	–	n	LPV
VVVv90	VVV J141730.13-615054.83	14:17:30.13	-61:50:54.83	312.89716	-0.65337	–	–	–	–	–	–	17.68	0.10	16.08	0.08	2.05	1.15	y	Eruptive
VVVv91	VVV J141649.12-611516.58	14:16:49.12	-61:15:16.58	313.01334	-0.06523	–	–	–	–	–	–	17.82	0.11	15.71	0.06	1.97	1.29	y	Dipper
VVVv92	VVV J141848.92-614133.03	14:18:48.92	-61:41:33.03	313.09512	-0.55705	19.94	0.09	18.67	0.05	17.28	0.03	16.11	0.02	15.60	0.05	1.16	–	n	EB
VVVv93	VVV J142239.35-620248.52	14:22:39.35	-62:02:48.52	313.40139	-1.04353	21.05	0.25	20.11	0.21	18.77	0.11	17.10	0.06	15.98	0.07	2.10	–	n	Rare
VVVv94	VVV J142257.76-610547.03	14:22:57.76	-61:05:47.03	313.76407	-0.16427	–	–	–	–	–	–	16.42	0.03	13.39	0.01	1.91	0.54	y	Eruptive
VVVv95	VVV J142517.08-613042.02	14:25:17.08	-61:30:42.02	313.87973	-0.65086	–	–	20.11	0.25	18.07	0.06	16.66	0.04	15.98	0.04	1.09	–	n	STV
VVVv96	VVV J142634.45-613900.61	14:26:34.45	-61:39:00.61	313.97367	-0.83496	–	–	19.91	0.21	18.48	0.08	16.78	0.04	15.92	0.04	1.05	–	n	EB
VVVv97	VVV J142422.62-605320.62	14:24:22.62	-60:53:20.62	313.99705	-0.02970	–	–	–	–	19.21	0.16	17.04	0.05	15.71	0.03	1.09	–	y	STV
VVVv98	VVV J142500.68-605448.20	14:25:00.68	-60:54:48.20	314.06065	-0.07963	–	–	–	–	–	–	18.08	0.14	14.61	0.01	2.09	0.60	y	LPV-YSO
VVVv99	VVV J142701.20-612525.27	14:27:01.20	-61:25:25.27	314.10472	-0.64275	13.48	0.01	13.04	0.01	12.74	0.01	12.78	0.01	12.39	0.01	1.03	–	n	EB
VVVv100	VVV J142807.13-613816.91	14:28:07.13	-61:38:16.91	314.14907	-0.88999	18.30	0.03	17.51	0.02	16.63	0.02	15.71	0.02	15.33	0.02	1.12	–	n	Rare
VVVv101	VVV J142538.25-604811.19	14:25:38.25	-60:48:11.19	314.17103	-0.00354	–	–	–	–	–	–	17.60	0.09	15.61	0.03	1.32	0.43	y	STV
VVVv102	VVV J142852.17-612217.27	14:28:52.17	-61:22:17.27	314.32991	-0.67464	–	–	–	–	19.05	0.14	15.27	0.01	12.37	0.01	2.17	–	n	LPV
VVVv103	VVV J143227.49-603942.58	14:32:27.49	-60:39:42.58	314.99820	-0.17868	–	–	–	–	19.78	0.28	16.83	0.04	14.75	0.01	1.49	0.94	y	LPV-Mira
VVVv104	VVV J143404.67-610609.65	14:34:04.67	-61:06:09.65	315.01158	-0.66137	18.20	0.02	17.57	0.03	16.64	0.02	15.64	0.01	14.77	0.01	1.06	–	n	STV
VVVv105	VVV J143437.21-611023.13	14:34:37.21	-61:10:23.13	315.04474	-0.75160	18.29	0.03	17.92	0.03	16.94	0.02	16.29	0.03	15.99	0.04	1.15	–	n	STV
VVVv106	VVV J143357.09-604737.87	14:33:57.09	-60:47:37.87	315.11639	-0.37046	–	–	–	–	–	–	14.88	0.01	11.91	0.01	2.35	–	n	LPV
VVVv107	VVV J144044.97-610704.39	14:40:44.97	-61:07:04.39	315.74517	-0.99527	–	–	–	–	16.35	0.02	12.93	0.01	11.32	0.01	1.54	–	n	LPV
VVVv108	VVV J143853.29-601007.32	14:38:53.29	-60:10:07.32	315.92142	-0.03511	–	–	–	–	17.74	0.05	15.05	0.01	13.44	0.01	1.12	–	n	LPV
VVVv109	VVV J144212.43-604125.50	14:42:12.43	-60:41:25.50	316.08250	-0.67847	–	–	19.33	0.11	16.66	0.02	14.21	0.01	12.36	0.01	1.35	0.12	y	STV
VVVv110	VVV J144351.27-602150.93	14:43:51.27	-60:21:50.93	316.40259	-0.46621	–	–	–	–	19.44	0.26	16.64	0.05	14.40	0.01	1.19	1.29	y	Eruptive
VVVv111	VVV J144444.70-602616.44	14:44:44.70	-60:26:16.44	316.47132	-0.57939	–	–	–	–	–	–	–	–	13.22	0.01	1.98	1.23	y	LPV-Mira
VVVv112	VVV J144427.29-595924.99	14:44:27.29	-59:59:24.99	316.62747	-0.15834	–	–	–	–	18.79	0.13	14.92	0.01	12.02	0.01	1.32	-0.10	y	STV
VVVv113	VVV J144523.82-595209.70	14:45:23.82	-59:52:09.70	316.78555	-0.09868	–	–	–	–	–	–	18.58	0.27	15.72	0.04	1.56	1.85	y	STV
VVVv114	VVV J144906.82-604557.11	14:49:06.82	-60:45:57.11	316.81448	-1.10592	–	–	–	–	–	–	–	–	15.78	0.04	3.02	–	n	LPV
VVVv115	VVV J144802.41-600427.26	14:48:02.41	-60:04:27.26	316.99634	-0.42561	20.02	0.11	18.86	0.07	17.71	0.05	16.40	0.04	15.47	0.03	1.26	–	n	STV
VVVv116	VVV J144812.64-600310.10	14:48:12.64	-60:03:10.10	317.02482	-0.41553	19.66	0.08	18.49	0.05	17.41	0.04	16.50	0.04	15.96	0.05	1.39	–	n	STV
VVVv117	VVV J145003.98-594734.18	14:50:03.98	-59:47:34.18	317.34758	-0.28338	–	–	20.39	0.27	18.14	0.07	16.55	0.04	15.49	0.03	1.15	–	y	STV
VVVv118	VVV J145120.97-600027.40	14:51:20.97	-60:00:27.40	317.39680	-0.54718	16.61	0.01	15.98	0.01	16.09	0.01	14.54	0.01	13.01	0.01	4.24	0.16	y	Eruptive
VVVv119	VVV J145253.28-600452.73	14:52:53.28	-60:04:52.73	317.53562	-0.69901	–	–	–	–	18.30	0.08	15.49	0.02	13.71	0.01	1.22	0.02	y	LPV-YSO
VVVv120	VVV J145300.70-591443.50	14:53:00.70	-59:14:43.50	317.92578	0.04041	17.94	0.02	17.71	0.02	17.37	0.04	16.55	0.04	15.94	0.05	1.50	–	n	STV
VVVv121	VVV J145521.85-593709.11	14:55:21.85	-59:37:09.11	318.02247	-0.42844	18.58	0.03	16.84	0.01	15.06	0.01	13.65	0.01	12.76	0.01	1.11	–	n	LPV
VVVv122	VVV J145630.67-594925.77	14:56:30.67	-59:49:25.77	318.05670	-0.67663	–	–	–	–	19.39	0.19	17.03	0.05	15.42	0.03	1.08	0.55	y	STV
VVVv123	VVV J145731.64-593810.86	14:57:31.64	-59:38:10.86	318.25710	-0.56991	–	–	–	–	–	–	14.17	0.01	11.27	0.01	2.38	0.78	y	LPV-Mira
VVVv124	VVV J145531.30-590703.08	14:55:31.30	-59:07:03.08	318.27027	0.00823	20.32	0.16	19.24	0.11	17.59	0.04	15.89	0.02	14.12	0.01	1.18	0.47	y	LPV-YSO
VVVv125	VVV J145940.19-595943.02	14:59:40.19	-59:59:43.02	318.32666	-1.01321	–	–	–	–	18.32	0.07	16.83	0.04	16.04	0.05	1.20	–	n	STV

Continued on next page

Table C1 – *Continued from previous page*

Object ID	VVV Designation	α (J2000)	δ (J2000)	l (degrees)	b (degrees)	Z (mag)	Z_{err} (mag)	Y (mag)	Y_{err} (mag)	J (mag)	J_{err} (mag)	H (mag)	H_{err} (mag)	K_s (mag)	$K_{s,err}$ (mag)	ΔK_s (mag)	α_{class}	SFR	Class
VVVv126	VVV J150007.69-595334.83	15:00:07.69	-59:53:34.83	318.42562	-0.95026	–	–	19.24	0.11	16.50	0.01	14.04	0.01	12.18	0.01	1.70	–	n	LPV
VVVv127	VVV J145747.25-591424.34	14:57:47.25	-59:14:24.34	318.47092	-0.23466	–	–	–	–	–	–	–	–	16.93	0.11	1.13	2.03	y	LPV-Mira
VVVv128	VVV J145829.67-590940.29	14:58:29.67	-59:09:40.29	318.58781	-0.20720	–	–	–	–	19.62	0.24	17.15	0.06	14.47	0.01	2.51	0.95	y	Eruptive
VVVv129	VVV J150213.13-595904.80	15:02:13.13	-59:59:04.80	318.61195	-1.15579	16.90	0.01	16.49	0.01	15.92	0.01	15.25	0.01	15.00	0.02	1.39	–	n	Rare
VVVv130	VVV J150043.33-592229.68	15:00:43.33	-59:22:29.68	318.73777	-0.52997	–	–	20.34	0.31	17.07	0.02	14.40	0.01	12.65	0.01	1.02	0.42	y	Eruptive
VVVv131	VVV J150310.44-595120.55	15:03:10.44	-59:51:20.55	318.77903	-1.10056	19.84	0.10	18.72	0.07	18.30	0.07	17.40	0.07	16.78	0.09	1.31	–	n	EB
VVVv132	VVV J150201.88-584927.58	15:02:01.88	-58:49:27.58	319.14859	-0.12671	–	–	–	–	19.08	0.15	17.31	0.07	16.38	0.06	1.02	–	n	STV
VVVv133	VVV J150620.36-592544.52	15:06:20.36	-59:25:44.52	319.33663	-0.92401	19.89	0.11	19.01	0.10	17.88	0.05	16.61	0.04	15.78	0.04	1.11	–	n	STV
VVVv134	VVV J150738.24-585138.25	15:07:38.24	-58:51:38.25	319.76324	-0.51313	–	–	–	–	18.57	0.11	16.04	0.03	14.32	0.01	1.32	-0.83	y	LPV-YSO
VVVv135	VVV J150738.65-582404.65	15:07:38.65	-58:24:04.65	319.99291	-0.11534	–	–	–	–	–	–	17.57	0.11	15.18	0.02	1.06	1.52	y	STV
VVVv136	VVV J151216.89-590331.54	15:12:16.89	-59:03:31.54	320.17950	-0.98686	19.05	0.05	18.04	0.04	17.15	0.03	16.36	0.04	15.97	0.05	1.39	–	n	STV
VVVv137	VVV J151252.81-591036.72	15:12:52.81	-59:10:36.72	320.18465	-1.12765	17.29	0.01	16.34	0.01	15.04	0.01	13.95	0.01	13.06	0.01	1.27	–	n	Rare
VVVv138	VVV J151007.47-582209.73	15:10:07.47	-58:22:09.73	320.29002	-0.25102	17.81	0.02	16.83	0.01	15.92	0.01	15.03	0.01	14.60	0.01	1.22	–	n	EB
VVVv139	VVV J150932.71-581345.47	15:09:32.71	-58:13:45.47	320.29513	-0.09169	–	–	–	–	–	–	18.17	0.19	16.06	0.05	2.22	-0.03	y	Eruptive
VVVv140	VVV J151338.45-585243.48	15:13:38.45	-58:52:43.48	320.42244	-0.92288	–	–	–	–	–	–	16.06	0.03	13.32	0.01	2.30	0.63	y	Dipper
VVVv141	VVV J151120.96-582222.07	15:11:20.96	-58:22:22.07	320.42657	-0.33559	18.01	0.02	17.19	0.02	17.28	0.03	15.54	0.02	14.09	0.01	1.01	-0.48	y	STV
VVVv142	VVV J151430.54-585847.00	15:14:30.54	-58:58:47.00	320.46581	-1.06733	–	–	–	–	–	–	17.99	0.16	16.23	0.06	1.24	–	n	LPV
VVVv143	VVV J151523.39-585404.60	15:15:23.39	-58:54:04.60	320.60367	-1.05966	20.83	0.25	19.81	0.19	18.15	0.08	15.62	0.02	12.63	0.01	1.98	–	n	LPV
VVVv144	VVV J151636.38-580912.14	15:16:36.38	-58:09:12.14	321.13146	-0.50643	–	–	18.88	0.09	17.80	0.07	16.62	0.06	16.00	0.07	1.19	–	n	STV
VVVv145	VVV J151656.42-580326.30	15:16:56.42	-58:03:26.30	321.21961	-0.44808	–	–	–	–	–	–	16.94	0.08	14.59	0.02	1.04	1.23	y	Eruptive
VVVv146	VVV J152110.72-582125.91	15:21:10.72	-58:21:25.91	321.53117	-0.99990	18.06	0.02	17.44	0.03	16.93	0.03	16.39	0.05	15.87	0.06	1.12	–	n	STV
VVVv147	VVV J151837.80-574504.85	15:18:37.80	-57:45:04.85	321.57219	-0.30779	–	–	–	–	–	–	18.65	0.40	15.90	0.06	1.95	–	n	Rare
VVVv148	VVV J151906.61-573927.84	15:19:06.61	-57:39:27.84	321.67639	-0.26286	–	–	–	–	–	–	–	–	16.23	0.08	1.70	–	n	STV
VVVv149	VVV J152100.25-575153.34	15:21:00.25	-57:51:53.34	321.77808	-0.57327	–	–	–	–	–	–	–	–	15.53	0.04	2.03	1.69	y	Eruptive
VVVv150	VVV J151958.89-571807.48	15:19:58.89	-57:18:07.48	321.96587	-0.02536	–	–	–	–	18.52	0.13	16.44	0.05	15.13	0.03	1.14	-0.58	y	STV
VVVv151	VVV J152447.81-580940.66	15:24:47.81	-58:09:40.66	322.03681	-1.09599	–	–	–	–	–	–	–	–	16.19	0.07	1.07	1.77	y	STV
VVVv152	VVV J152040.85-571000.26	15:20:40.85	-57:10:00.26	322.11848	0.03774	15.65	0.01	14.44	0.01	13.46	0.01	12.50	0.01	11.82	0.01	2.21	–	n	Known
VVVv153	VVV J152128.41-571847.88	15:21:28.41	-57:18:47.88	322.12944	-0.14352	–	–	–	–	–	–	–	–	16.70	0.13	1.27	0.30	y	STV
VVVv154	VVV J152405.24-574954.21	15:24:05.24	-57:49:54.21	322.13999	-0.76917	18.33	0.03	17.19	0.02	16.27	0.02	16.07	0.04	14.94	0.03	1.08	–	n	EB
VVVv155	VVV J152308.09-571712.94	15:23:08.09	-57:17:12.94	322.33200	-0.24357	–	–	–	–	–	–	17.10	0.10	14.99	0.03	2.13	–	n	LPV
VVVv156	VVV J152511.24-571946.17	15:25:11.24	-57:19:46.17	322.54002	-0.43158	18.96	0.05	17.81	0.03	16.69	0.02	15.61	0.02	14.99	0.02	1.30	–	n	Rare
VVVv157	VVV J152548.43-565949.91	15:25:48.43	-56:59:49.91	322.79413	-0.20156	–	–	19.32	0.12	17.70	0.05	16.32	0.04	15.37	0.03	1.05	–	n	STV
VVVv158	VVV J152542.31-564529.64	15:25:42.31	-56:45:29.64	322.91517	0.00496	–	–	19.12	0.10	16.70	0.02	15.28	0.01	14.52	0.01	1.15	–	n	EB
VVVv159	VVV J152729.60-565854.70	15:27:29.60	-56:58:54.70	322.99331	-0.31691	–	–	–	–	18.82	0.14	17.09	0.08	16.04	0.06	1.02	–	n	STV
VVVv160	VVV J152734.81-565811.76	15:27:34.81	-56:58:11.76	323.00980	-0.31367	16.66	0.01	15.19	0.01	13.74	0.01	12.91	0.01	12.32	0.01	1.09	–	n	EB
VVVv161	VVV J152939.43-571119.22	15:29:39.43	-57:11:19.22	323.11960	-0.65341	–	–	–	–	–	–	18.35	0.24	16.64	0.10	1.42	0.90	y	Eruptive
VVVv162	VVV J152917.51-565411.95	15:29:17.51	-56:54:11.95	323.24023	-0.39007	–	–	–	–	–	–	–	–	14.01	0.01	1.69	0.31	y	LPV-Mira
VVVv163	VVV J152934.08-565225.52	15:29:34.08	-56:52:25.52	323.28806	-0.38705	–	–	–	–	18.71	0.13	16.17	0.03	14.74	0.02	1.79	0.34	y	Fader
VVVv164	VVV J152921.67-563902.13	15:29:21.67	-56:39:02.13	323.39104	-0.18706	19.50	0.09	18.25	0.05	17.19	0.03	16.02	0.03	15.55	0.04	1.06	–	n	STV
VVVv165	VVV J152941.48-564020.33	15:29:41.48	-56:40:20.33	323.41614	-0.23066	–	–	–	–	17.99	0.07	15.56	0.02	13.78	0.01	1.08	1.53	y	Eruptive
VVVv166	VVV J152940.33-563823.01	15:29:40.33	-56:38:23.01	323.43245	-0.20232	–	–	–	–	18.87	0.15	17.00	0.07	16.10	0.06	1.12	–	n	EB
VVVv167	VVV J153021.60-563844.55	15:30:21.60	-56:38:44.55	323.50687	-0.26093	20.18	0.16	18.26	0.05	15.70	0.01	13.34	0.01	11.84	0.01	1.33	0.46	y	Eruptive

Continued on next page

Table C1 – *Continued from previous page*

Object ID	VVV Designation	α (J2000)	δ (J2000)	l (degrees)	b (degrees)	Z (mag)	Z_{err} (mag)	Y (mag)	Y_{err} (mag)	J (mag)	J_{err} (mag)	H (mag)	H_{err} (mag)	K_s (mag)	$K_{s,err}$ (mag)	ΔK_s (mag)	α_{class}	SFR	Class
VVVv168	VVV J153200.86-563842.58	15:32:00.86	-56:38:42.58	323.69382	-0.39040	–	–	–	–	–	–	16.45	0.04	14.27	0.01	1.96	-0.57	y	STV
VVVv169	VVV J153157.36-563609.37	15:31:57.36	-56:36:09.37	323.71166	-0.35094	–	–	–	–	–	–	15.32	0.02	12.44	0.01	1.53	0.33	y	STV
VVVv170	VVV J153647.49-565210.20	15:36:47.49	-56:52:10.20	324.09644	-0.95330	–	–	–	–	–	–	17.67	0.17	15.17	0.03	1.56	1.22	y	LPV-YSO
VVVv171	VVV J153706.12-563233.54	15:37:06.12	-56:32:33.54	324.32323	-0.71408	–	–	19.42	0.15	17.33	0.05	16.24	0.04	15.61	0.05	1.30	–	n	EB
VVVv172	VVV J153640.80-555258.91	15:36:40.80	-55:52:58.91	324.66374	-0.14610	20.61	0.23	18.66	0.07	18.03	0.09	16.60	0.06	15.86	0.06	1.04	–	n	EB
VVVv173	VVV J153746.87-560415.21	15:37:46.87	-56:04:15.21	324.67753	-0.38864	–	–	–	–	18.23	0.10	17.26	0.11	16.10	0.07	1.11	–	n	STV
VVVv174	VVV J153815.79-553951.62	15:38:15.79	-55:39:51.62	324.97249	-0.10080	–	–	–	–	19.19	0.26	17.11	0.10	16.03	0.07	1.22	–	n	STV
VVVv175	VVV J153939.81-555046.92	15:39:39.81	-55:50:46.92	325.02281	-0.36427	–	–	–	–	19.40	0.31	17.16	0.10	15.73	0.05	1.55	-0.40	y	STV
VVVv176	VVV J153837.25-552821.44	15:38:37.25	-55:28:21.44	325.12683	0.02366	–	–	–	–	–	–	–	–	14.56	0.02	1.22	2.97	y	Eruptive
VVVv177	VVV J154007.59-553015.85	15:40:07.59	-55:30:15.85	325.27927	-0.12884	–	–	19.58	0.17	18.22	0.11	17.22	0.11	16.75	0.13	1.47	–	n	STV
VVVv178	VVV J154249.38-560011.63	15:42:49.38	-56:00:11.63	325.28237	-0.75552	19.84	0.11	18.92	0.10	17.76	0.07	16.91	0.08	16.43	0.10	1.21	–	n	EB
VVVv179	VVV J154502.34-555807.95	15:45:02.34	-55:58:07.95	325.54925	-0.91681	–	–	–	–	18.45	0.11	16.58	0.05	15.45	0.04	1.56	-0.51	y	Dipper
VVVv180	VVV J154252.38-552311.07	15:42:52.38	-55:23:11.07	325.66138	-0.26881	–	–	–	–	–	–	–	–	12.18	0.01	1.74	–	n	LPV
VVVv181	VVV J154639.17-555028.27	15:46:39.17	-55:50:28.27	325.80621	-0.95485	20.42	0.17	19.40	0.14	17.81	0.06	15.02	0.01	12.72	0.01	3.54	0.72	y	Eruptive
VVVv182	VVV J154309.19-550153.01	15:43:09.19	-55:01:53.01	325.90823	-0.01055	–	–	–	–	19.08	0.19	16.98	0.08	15.16	0.03	1.56	0.47	y	STV
VVVv183	VVV J154307.07-550119.87	15:43:07.07	-55:01:19.87	325.90979	-0.00017	–	–	–	–	–	–	16.80	0.07	14.51	0.02	1.42	0.76	y	Dipper
VVVv184	VVV J154513.00-552251.04	15:45:13.00	-55:22:51.04	325.92885	-0.46700	–	–	19.84	0.23	17.35	0.04	15.58	0.02	14.54	0.02	1.07	–	n	EB
VVVv185	VVV J154605.44-551957.68	15:46:05.44	-55:19:57.68	326.05649	-0.50513	–	–	–	–	19.42	0.26	17.33	0.11	15.46	0.04	1.50	0.80	y	STV
VVVv186	VVV J154758.12-552938.44	15:47:58.12	-55:29:38.44	326.16666	-0.79655	14.57	0.01	13.99	0.01	13.43	0.01	12.91	0.01	12.55	0.01	1.26	–	n	EB
VVVv187	VVV J154617.80-550439.61	15:46:17.80	-55:04:39.61	326.23646	-0.32207	–	–	–	–	–	–	–	–	12.88	0.01	1.77	–	n	LPV
VVVv188	VVV J154635.47-545846.03	15:46:35.47	-54:58:46.03	326.33016	-0.27062	–	–	–	–	–	–	14.19	0.01	11.68	0.01	1.43	0.11	y	LPV-Mira
VVVv189	VVV J154905.50-552236.60	15:49:05.50	-55:22:36.60	326.36429	-0.80370	19.67	0.08	18.92	0.10	18.80	0.15	17.60	0.14	16.65	0.11	1.49	–	n	LPV
VVVv190	VVV J154703.56-544310.15	15:47:03.56	-54:43:10.15	326.54350	-0.10750	–	–	–	–	18.83	0.15	15.60	0.02	13.49	0.01	1.47	1.25	y	LPV-YSO
VVVv191	VVV J154707.98-544302.68	15:47:07.98	-54:43:02.68	326.55314	-0.11242	–	–	–	–	–	–	–	–	15.63	0.04	1.08	2.57	y	Eruptive
VVVv192	VVV J155121.51-545723.34	15:51:21.51	-54:57:23.34	326.87990	-0.67856	–	–	–	–	–	–	18.10	0.17	14.45	0.01	1.18	0.64	y	STV
VVVv193	VVV J154914.34-543423.66	15:49:14.34	-54:34:23.66	326.88153	-0.18832	–	–	–	–	–	–	16.59	0.04	13.90	0.01	1.25	0.86	y	Eruptive
VVVv194	VVV J154957.50-543838.27	15:49:57.50	-54:38:38.27	326.91875	-0.30860	–	–	–	–	–	–	–	–	15.54	0.04	1.16	0.98	y	STV
VVVv195	VVV J155314.61-551333.40	15:53:14.61	-55:13:33.40	326.91871	-1.05781	19.67	0.11	18.83	0.09	18.55	0.10	16.97	0.06	15.91	0.05	2.10	-0.33	y	Fader
VVVv196	VVV J154932.40-542534.67	15:49:32.40	-54:25:34.67	327.00734	-0.10072	–	–	–	–	–	–	18.14	0.18	16.10	0.06	1.14	2.07	y	STV
VVVv197	VVV J155122.71-542010.52	15:51:22.71	-54:20:10.52	327.27238	-0.19829	–	–	–	–	–	–	16.78	0.05	12.50	0.01	1.37	0.56	y	LPV-Mira
VVVv198	VVV J155307.15-543639.89	15:53:07.15	-54:36:39.89	327.29485	-0.57106	20.53	0.23	19.49	0.16	19.11	0.16	17.72	0.12	14.75	0.02	1.82	2.06	y	Fader
VVVv199	VVV J155256.17-542852.83	15:52:56.17	-54:28:52.83	327.35655	-0.45388	–	–	–	–	19.24	0.18	16.80	0.05	15.28	0.03	1.08	0.72	y	Eruptive
VVVv200	VVV J155302.80-542708.40	15:53:02.80	-54:27:08.40	327.38735	-0.44161	–	–	–	–	–	–	–	–	12.68	0.01	1.63	1.00	y	LPV-Mira
VVVv201	VVV J155211.02-541051.16	15:52:11.02	-54:10:51.16	327.46158	-0.15176	–	–	–	–	–	–	–	–	14.62	0.02	2.54	–	n	LPV
VVVv202	VVV J155426.41-540829.40	15:54:26.41	-54:08:29.40	327.74188	-0.33087	–	–	–	–	17.38	0.03	13.28	0.01	11.66	0.01	1.61	1.16	y	LPV-YSO
VVVv203	VVV J155643.05-542945.28	15:56:43.05	-54:29:45.28	327.76983	-0.81574	–	–	18.26	0.05	16.65	0.02	15.19	0.01	14.39	0.01	1.09	–	n	EB
VVVv204	VVV J155450.66-540315.87	15:54:50.66	-54:03:15.87	327.84307	-0.30161	–	–	–	–	–	–	–	–	14.17	0.01	2.61	2.39	y	LPV-Mira
VVVv205	VVV J155628.83-541406.86	15:56:28.83	-54:14:06.86	327.91112	-0.59397	19.69	0.11	18.78	0.09	16.31	0.01	14.97	0.01	13.79	0.01	1.78	-0.98	y	STV
VVVv206	VVV J155608.75-535525.81	15:56:08.75	-53:55:25.81	328.07362	-0.32383	–	–	–	–	–	–	16.24	0.03	11.62	0.01	1.30	-0.25	y	LPV-Mira
VVVv207	VVV J155544.14-533732.94	15:55:44.14	-53:37:32.94	328.21834	-0.05636	–	–	–	–	–	–	16.12	0.03	12.28	0.01	2.02	0.18	y	LPV-Mira
VVVv208	VVV J155641.55-534553.75	15:56:41.55	-53:45:53.75	328.23755	-0.25395	–	–	19.61	0.18	–	–	16.79	0.05	12.52	0.01	1.54	0.20	y	LPV-Mira
VVVv209	VVV J155758.41-535807.08	15:57:58.41	-53:58:07.08	328.25034	-0.53142	–	–	–	–	19.17	0.17	16.68	0.05	15.34	0.03	1.31	–	y	LPV-YSO

Continued on next page

Table C1 – *Continued from previous page*

Object ID	VVV Designation	α (J2000)	δ (J2000)	l (degrees)	b (degrees)	Z (mag)	Z_{err} (mag)	Y (mag)	Y_{err} (mag)	J (mag)	J_{err} (mag)	H (mag)	H_{err} (mag)	K_s (mag)	$K_{s,err}$ (mag)	ΔK_s (mag)	α_{class}	SFR	Class
VVVv210	VVV J155819.39-540133.97	15:58:19.39	-54:01:33.97	328.25230	-0.60849	–	–	–	–	–	–	15.47	0.02	11.67	0.01	1.45	-0.37	y	LPV-Mira
VVVv211	VVV J155807.52-535714.66	15:58:07.52	-53:57:14.66	328.27680	-0.53478	–	–	–	–	–	–	–	–	15.51	0.04	1.40	3.43	y	Fader
VVVv212	VVV J155558.91-533219.30	15:55:58.91	-53:32:19.30	328.30224	-0.01294	–	–	19.38	0.15	16.56	0.02	14.07	0.01	12.36	0.01	3.11	0.58	y	Fader
VVVv213	VVV J155617.48-532950.20	15:56:17.48	-53:29:50.20	328.36411	-0.01074	–	–	–	–	17.79	0.07	14.54	0.01	12.65	0.01	1.99	-2.82	y	Eruptive
VVVv214	VVV J155741.02-534347.63	15:57:41.02	-53:43:47.63	328.37212	-0.32167	–	–	–	–	–	–	16.26	0.05	14.06	0.01	1.02	0.45	y	STV
VVVv215	VVV J155916.48-540006.12	15:59:16.48	-54:00:06.12	328.37445	-0.68067	–	–	–	–	19.15	0.23	14.52	0.01	11.65	0.01	2.36	–	n	LPV
VVVv216	VVV J155844.58-535337.80	15:58:44.58	-53:53:37.80	328.38508	-0.54785	–	–	–	–	18.88	0.18	16.95	0.09	15.60	0.05	1.73	-0.61	y	Eruptive
VVVv217	VVV J155902.40-534116.97	15:59:02.40	-53:41:16.97	328.55209	-0.41986	17.70	0.02	16.69	0.01	15.30	0.01	14.04	0.01	12.99	0.01	3.03	-0.52	y	Fader
VVVv218	VVV J155807.87-532943.96	15:58:07.87	-53:29:43.96	328.57433	-0.18588	–	–	19.25	0.14	17.54	0.06	15.48	0.02	12.12	0.01	1.55	–	n	LPV
VVVv219	VVV J155938.19-533959.95	15:59:38.19	-53:39:59.95	328.63309	-0.46109	–	–	–	–	–	–	16.95	0.08	14.50	0.02	1.49	-0.28	y	Dipper
VVVv220	VVV J155954.74-534027.71	15:59:54.74	-53:40:27.71	328.65906	-0.49357	–	–	–	–	–	–	17.79	0.18	15.46	0.04	1.30	0.07	y	STV
VVVv221	VVV J160046.60-534036.32	16:00:46.60	-53:40:36.32	328.75440	-0.57900	–	–	–	–	–	–	15.93	0.03	12.29	0.01	2.22	–	n	LPV
VVVv222	VVV J160448.76-535412.84	16:04:48.76	-53:54:12.84	329.05271	-1.14271	–	–	–	–	18.39	0.11	14.95	0.01	12.21	0.01	1.78	–	n	LPV
VVVv223	VVV J160202.72-532218.87	16:02:02.72	-53:22:18.87	329.09671	-0.47265	–	–	–	–	17.53	0.05	13.46	0.01	11.69	0.01	1.15	–	n	LPV
VVVv224	VVV J160347.48-533418.99	16:03:47.48	-53:34:18.99	329.15985	-0.79441	–	–	–	–	–	–	16.64	0.06	13.31	0.01	2.46	–	n	LPV
VVVv225	VVV J160528.47-534420.45	16:05:28.47	-53:44:20.45	329.23518	-1.08499	17.16	0.01	16.09	0.01	14.89	0.01	13.99	0.01	13.31	0.01	1.14	–	n	LPV
VVVv226	VVV J160206.29-530850.39	16:02:06.29	-53:08:50.39	329.25116	-0.30937	–	–	–	–	–	–	16.82	0.08	14.18	0.01	1.82	0.73	y	STV
VVVv227	VVV J160133.14-525521.83	16:01:33.14	-52:55:21.83	329.33616	-0.08550	18.05	0.02	17.13	0.02	17.38	0.05	16.44	0.06	15.68	0.05	1.23	–	n	EB
VVVv228	VVV J160335.44-531414.20	16:03:35.44	-53:14:14.20	329.35903	-0.52381	–	–	–	–	–	–	16.82	0.08	13.76	0.01	1.20	0.62	y	LPV-YSO
VVVv229	VVV J160424.48-530114.01	16:04:24.48	-53:01:14.01	329.59450	-0.44282	–	–	–	–	–	–	–	–	13.01	0.01	3.70	–	n	LPV-YSO
VVVv230	VVV J161006.42-525119.46	16:10:06.42	-52:51:19.46	330.34185	-0.89679	–	–	–	–	17.43	0.05	15.94	0.03	14.93	0.03	1.30	–	n	EB
VVVv231	VVV J160825.89-521333.77	16:08:25.89	-52:13:33.77	330.57989	-0.26091	–	–	–	–	–	–	15.52	0.02	12.81	0.01	2.05	-0.21	y	LPV-Mira
VVVv232	VVV J161004.42-521301.46	16:10:04.42	-52:13:01.46	330.77123	-0.42439	–	–	–	–	–	–	16.75	0.07	14.81	0.02	2.49	1.21	y	Eruptive
VVVv233	VVV J161240.47-523302.72	16:12:40.47	-52:33:02.72	330.83416	-0.93907	–	–	–	–	19.04	0.23	17.09	0.10	15.76	0.06	1.18	–	n	LPV
VVVv234	VVV J161146.65-521915.53	16:11:46.65	-52:19:15.53	330.89153	-0.67793	18.15	0.03	17.73	0.04	17.15	0.04	15.68	0.03	11.95	0.01	1.20	–	n	LPV
VVVv235	VVV J160935.53-515414.08	16:09:35.53	-51:54:14.08	330.92907	-0.14398	–	–	–	–	–	–	17.95	0.22	11.70	0.01	1.26	1.15	y	LPV-Mira
VVVv236	VVV J160937.74-514027.52	16:09:37.74	-51:40:27.52	331.08873	0.02112	19.43	0.08	17.88	0.04	16.45	0.02	15.36	0.02	14.58	0.02	1.04	-1.80	y	STV
VVVv237	VVV J161048.22-514245.01	16:10:48.22	-51:42:45.01	331.19651	-0.13049	–	–	19.46	0.21	18.44	0.15	16.25	0.05	13.83	0.01	1.85	1.10	y	Eruptive
VVVv238	VVV J161210.99-515417.23	16:12:10.99	-51:54:17.23	331.22135	-0.41654	–	–	–	–	19.20	0.31	16.71	0.07	14.95	0.03	2.11	0.32	y	Eruptive
VVVv239	VVV J161153.85-513059.51	16:11:53.85	-51:30:59.51	331.45432	-0.10280	–	–	–	–	–	–	–	–	15.71	0.06	1.27	1.42	y	Dipper
VVVv240	VVV J161303.44-514151.91	16:13:03.44	-51:41:51.91	331.46161	-0.35819	–	–	–	–	–	–	16.35	0.05	12.10	0.01	1.17	0.74	y	LPV-Mira
VVVv241	VVV J161706.22-511730.81	16:17:06.22	-51:17:30.81	332.19736	-0.49979	18.35	0.04	16.72	0.02	15.33	0.01	14.19	0.01	13.51	0.01	1.24	-2.11	y	EB
VVVv242	VVV J161703.71-510640.99	16:17:03.71	-51:06:40.99	332.31823	-0.36556	–	–	–	–	–	–	15.26	0.02	12.06	0.01	2.45	-0.54	y	Dipper
VVVv243	VVV J161802.02-511439.85	16:18:02.02	-51:14:39.85	332.33479	-0.56710	–	–	–	–	–	–	–	–	15.64	0.05	2.26	2.33	y	Fader
VVVv244	VVV J162001.99-512602.11	16:20:01.99	-51:26:02.11	332.42494	-0.92108	–	–	–	–	17.62	0.07	14.99	0.01	13.05	0.01	2.08	0.79	y	LPV-YSO
VVVv245	VVV J161920.93-511107.06	16:19:20.93	-51:11:07.06	332.52333	-0.66895	–	–	–	–	–	–	17.48	0.14	15.61	0.05	1.08	–	n	STV
VVVv246	VVV J161841.84-505702.76	16:18:41.84	-50:57:02.76	332.61452	-0.42986	–	–	–	–	–	–	17.76	0.18	16.27	0.10	1.23	–	n	LPV
VVVv247	VVV J161713.24-503845.65	16:17:13.24	-50:38:45.65	332.66002	-0.04874	17.47	0.01	16.71	0.01	15.93	0.01	14.87	0.01	12.46	0.01	1.67	0.84	y	LPV-Mira
VVVv248	VVV J162051.74-511336.09	16:20:51.74	-51:13:36.09	332.66283	-0.86504	–	–	–	–	19.68	0.30	17.17	0.08	15.27	0.03	1.54	0.85	y	STV
VVVv249	VVV J161724.00-503658.01	16:17:24.00	-50:36:58.01	332.70127	-0.04709	–	–	20.04	0.22	18.10	0.07	15.86	0.02	14.83	0.02	1.27	–	y	Eruptive
VVVv250	VVV J161819.35-503227.95	16:18:19.35	-50:32:27.95	332.85853	-0.09549	–	–	–	–	–	–	15.79	0.02	12.30	0.01	1.71	0.47	y	LPV-Mira
VVVv251	VVV J162034.52-505106.31	16:20:34.52	-50:51:06.31	332.89495	-0.56713	–	–	–	–	–	–	17.29	0.09	15.03	0.02	1.51	-0.05	y	LPV-YSO

Continued on next page

Table C1 – *Continued from previous page*

Object ID	VVV Designation	α (J2000)	δ (J2000)	l (degrees)	b (degrees)	Z (mag)	Z_{err} (mag)	Y (mag)	Y_{err} (mag)	J (mag)	J_{err} (mag)	H (mag)	H_{err} (mag)	K_s (mag)	$K_{s,err}$ (mag)	ΔK_s (mag)	α_{class}	SFR	Class
VVVv252	VVV J161920.52-502317.47	16:19:20.52	-50:23:17.47	333.08142	-0.09980	–	–	–	–	–	–	–	–	17.13	0.17	2.38	4.30	y	LPV-YSO
VVVv253	VVV J162115.82-504027.98	16:21:15.82	-50:40:27.98	333.09714	-0.51808	–	–	–	–	19.72	0.30	17.97	0.16	13.77	0.01	1.74	2.16	y	LPV-Mira
VVVv254	VVV J161943.16-502401.84	16:19:43.16	-50:24:01.84	333.11563	-0.15078	–	–	–	–	18.62	0.11	16.36	0.04	14.71	0.02	1.05	0.25	y	LPV-YSO
VVVv255	VVV J162122.89-503514.65	16:21:22.89	-50:35:14.65	333.17183	-0.46962	–	–	–	–	–	–	18.05	0.18	15.61	0.04	1.38	1.20	y	STV
VVVv256	VVV J161935.14-501640.86	16:19:35.14	-50:16:40.86	333.18641	-0.04855	–	–	–	–	–	–	18.57	0.29	15.16	0.03	1.12	0.37	y	Dipper
VVVv257	VVV J162101.87-502912.99	16:21:01.87	-50:29:12.99	333.20324	-0.35914	–	–	–	–	–	–	17.76	0.13	15.42	0.04	1.66	1.72	y	STV
VVVv258	VVV J162153.24-503407.34	16:21:53.24	-50:34:07.34	333.24186	-0.51312	–	–	–	–	–	–	17.70	0.13	15.43	0.04	1.62	1.59	y	STV
VVVv259	VVV J162141.05-502857.12	16:21:41.05	-50:28:57.12	333.27994	-0.42935	–	–	–	–	–	–	–	–	16.91	0.14	2.08	2.12	y	Eruptive
VVVv260	VVV J162105.71-501916.41	16:21:05.71	-50:19:16.41	333.32734	-0.24884	14.41	0.01	13.52	0.01	13.20	0.01	13.02	0.01	12.47	0.01	1.37	1.01	y	Eruptive
VVVv261	VVV J162136.83-502407.96	16:21:36.83	-50:24:07.96	333.32877	-0.36459	–	–	–	–	–	–	17.38	0.09	14.27	0.01	1.61	2.19	y	Fader
VVVv262	VVV J162159.58-502620.59	16:21:59.58	-50:26:20.59	333.34544	-0.43335	19.02	0.05	18.23	0.04	17.30	0.03	16.32	0.04	15.67	0.05	1.03	–	y	Eruptive
VVVv263	VVV J162144.17-502041.41	16:21:44.17	-50:20:41.41	333.38312	-0.33779	–	–	–	–	–	–	16.81	0.06	13.24	0.01	2.24	1.21	y	Eruptive
VVVv264	VVV J162120.67-501547.33	16:21:20.67	-50:15:47.33	333.39653	-0.23577	–	–	–	–	–	–	–	–	15.07	0.03	2.54	1.31	y	LPV-Mira
VVVv265	VVV J162047.39-500359.42	16:20:47.39	-50:03:59.42	333.47223	-0.03372	–	–	–	–	17.09	0.03	14.72	0.01	13.05	0.01	1.13	-0.02	y	Eruptive
VVVv266	VVV J162052.46-500415.80	16:20:52.46	-50:04:15.80	333.47864	-0.04650	–	–	20.13	0.25	18.13	0.07	16.15	0.03	15.08	0.03	1.13	-0.88	y	STV
VVVv267	VVV J162217.53-501402.98	16:22:17.53	-50:14:02.98	333.52419	-0.32240	–	–	–	–	–	–	–	–	14.77	0.02	1.94	2.41	y	LPV-Mira
VVVv268	VVV J162255.11-495757.37	16:22:55.11	-49:57:57.37	333.78515	-0.20438	–	–	–	–	–	–	17.99	0.17	15.38	0.04	1.29	-0.11	y	STV
VVVv269	VVV J162330.97-495006.51	16:23:30.97	-49:50:06.51	333.94581	-0.18068	–	–	–	–	–	–	16.89	0.06	12.92	0.01	2.00	-0.10	y	Dipper
VVVv270	VVV J162327.14-494443.96	16:23:27.14	-49:44:43.96	334.00225	-0.11033	–	–	–	–	–	–	18.34	0.23	16.14	0.07	3.81	1.76	y	Eruptive
VVVv271	VVV J162733.92-495537.61	16:27:33.92	-49:55:37.61	334.33558	-0.71174	–	–	–	–	18.25	0.08	16.58	0.05	15.47	0.04	1.06	–	n	STV
VVVv272	VVV J162841.05-495311.78	16:28:41.05	-49:53:11.78	334.48953	-0.81370	18.97	0.05	18.14	0.04	16.85	0.02	15.78	0.02	15.08	0.03	1.22	-1.36	y	STV
VVVv273	VVV J163010.37-495319.51	16:30:10.37	-49:53:19.51	334.65324	-0.98893	17.95	0.02	17.07	0.02	15.63	0.01	14.35	0.01	13.37	0.01	1.00	-0.65	y	STV
VVVv274	VVV J162618.97-491433.07	16:26:18.97	-49:14:33.07	334.68700	-0.09031	–	–	–	–	–	–	17.05	0.08	13.38	0.01	1.07	0.99	y	LPV-Mira
VVVv275	VVV J162951.29-493754.93	16:29:51.29	-49:37:54.93	334.80437	-0.77501	20.31	0.16	18.71	0.07	17.26	0.03	16.14	0.03	15.47	0.04	1.00	–	n	STV
VVVv276	VVV J162917.42-492231.45	16:29:17.42	-49:22:31.45	334.92721	-0.53187	–	–	–	–	–	–	17.97	0.17	13.81	0.01	1.25	–	n	LPV
VVVv277	VVV J162708.30-490019.80	16:27:08.30	-49:00:19.80	334.95085	-0.02207	–	–	–	–	–	–	–	–	15.95	0.06	1.80	1.78	y	Eruptive
VVVv278	VVV J162856.75-491343.89	16:28:56.75	-49:13:43.89	334.99454	-0.39010	–	–	19.73	0.17	17.67	0.05	16.02	0.03	15.06	0.03	1.00	-2.08	y	STV
VVVv279	VVV J162939.57-492006.48	16:29:39.57	-49:20:06.48	334.99782	-0.54768	–	–	–	–	–	–	17.97	0.17	15.40	0.04	1.92	1.00	y	STV
VVVv280	VVV J162952.41-491102.80	16:29:52.41	-49:11:02.80	335.13140	-0.46904	–	–	–	–	19.11	0.18	16.24	0.04	14.42	0.02	2.30	0.93	y	Dipper
VVVv281	VVV J162749.92-485144.00	16:27:49.92	-48:51:44.00	335.13307	-0.00469	–	–	–	–	17.08	0.03	15.61	0.02	14.52	0.02	1.23	-0.23	y	Eruptive
VVVv282	VVV J162953.95-490948.69	16:29:53.95	-49:09:48.69	335.14921	-0.45791	–	–	–	–	19.92	0.38	17.14	0.08	15.67	0.05	1.39	-0.16	y	Eruptive
VVVv283	VVV J162904.28-485908.99	16:29:04.28	-48:59:08.99	335.18456	-0.23722	–	–	–	–	–	–	–	–	13.37	0.01	1.28	-0.09	y	LPV-Mira
VVVv284	VVV J162820.68-484917.24	16:28:20.68	-48:49:17.24	335.22089	-0.03732	–	–	–	–	–	–	15.07	0.01	12.09	0.01	1.53	0.76	y	LPV-Mira
VVVv285	VVV J162959.38-484955.29	16:29:59.38	-48:49:55.29	335.40001	-0.24062	–	–	20.24	0.27	18.15	0.08	15.26	0.01	12.75	0.01	1.76	0.41	y	Eruptive
VVVv286	VVV J163051.43-484356.65	16:30:51.43	-48:43:56.65	335.57057	-0.27605	18.21	0.04	17.23	0.03	17.29	0.04	15.60	0.03	14.15	0.02	1.07	0.64	y	Dipper
VVVv287	VVV J163317.78-490138.74	16:33:17.78	-49:01:38.74	335.62893	-0.77046	–	–	–	–	17.51	0.05	16.07	0.04	15.04	0.03	1.19	-1.22	y	STV
VVVv288	VVV J163058.02-482220.40	16:30:58.02	-48:22:20.40	335.84512	-0.04237	–	–	19.02	0.14	17.18	0.04	16.00	0.04	15.20	0.04	1.21	–	y	EB
VVVv289	VVV J163232.83-483609.97	16:32:32.83	-48:36:09.97	335.85597	-0.39099	–	–	–	–	17.82	0.07	15.51	0.02	14.23	0.02	1.32	-0.87	y	LPV-Mira
VVVv290	VVV J163231.47-480227.03	16:32:31.47	-48:02:27.03	336.26444	-0.00508	–	–	–	–	–	–	15.39	0.02	12.56	0.01	1.77	1.10	y	LPV-Mira
VVVv291	VVV J163441.08-482000.21	16:34:41.08	-48:20:00.21	336.29434	-0.46802	–	–	18.49	0.08	16.28	0.02	13.56	0.01	12.04	0.01	1.19	–	n	LPV
VVVv292	VVV J163252.77-475717.93	16:32:52.77	-47:57:17.93	336.36776	0.00997	–	–	–	–	16.62	0.02	14.66	0.01	13.23	0.01	1.64	-1.68	y	STV
VVVv293	VVV J163455.76-481324.47	16:34:55.76	-48:13:24.47	336.40284	-0.42364	18.78	0.06	18.31	0.07	17.54	0.06	16.80	0.08	16.33	0.11	1.60	–	n	STV

Continued on next page

Table C1 – *Continued from previous page*

Object ID	VVV Designation	α (J2000)	δ (J2000)	l (degrees)	b (degrees)	Z (mag)	Z_{err} (mag)	Y (mag)	Y_{err} (mag)	J (mag)	J_{err} (mag)	H (mag)	H_{err} (mag)	K_s (mag)	$K_{s,err}$ (mag)	ΔK_s (mag)	α_{class}	SFR	Class
VVVv294	VVV J163257.43-475355.83	16:32:57.43	-47:53:55.83	336.41772	0.03868	–	–	–	–	–	–	17.13	0.11	15.22	0.04	1.60	0.49	y	STV
VVVv295	VVV J163657.31-482731.22	16:36:57.31	-48:27:31.22	336.45585	-0.83088	–	–	–	–	16.45	0.02	13.15	0.01	11.67	0.01	2.51	–	n	LPV
VVVv296	VVV J163559.12-475138.62	16:35:59.12	-47:51:38.62	336.78964	-0.30906	–	–	–	–	17.80	0.08	16.18	0.04	15.25	0.04	1.10	–	y	EB
VVVv297	VVV J163510.88-473943.17	16:35:10.88	-47:39:43.17	336.84518	-0.07525	17.74	0.03	17.20	0.03	16.97	0.03	16.49	0.06	16.06	0.09	1.12	–	y	STV
VVVv298	VVV J163506.52-473750.51	16:35:06.52	-47:37:50.51	336.85998	-0.04508	19.92	0.18	18.40	0.08	17.07	0.04	16.17	0.04	15.43	0.05	1.04	–	y	STV
VVVv299	VVV J163549.32-474139.27	16:35:49.32	-47:41:39.27	336.89416	-0.17660	–	–	19.65	0.25	17.36	0.05	16.07	0.04	15.29	0.05	1.06	–	y	STV
VVVv300	VVV J163520.86-473509.87	16:35:20.86	-47:35:09.87	336.92010	-0.04465	–	–	–	–	–	–	16.79	0.08	12.72	0.01	1.54	0.27	y	LPV-Mira
VVVv301	VVV J163815.13-474825.10	16:38:15.13	-47:48:25.10	337.08476	-0.55507	–	–	–	–	16.50	0.02	13.82	0.01	11.90	0.01	1.79	0.77	y	LPV-Mira
VVVv302	VVV J163716.53-473816.00	16:37:16.53	-47:38:16.00	337.10049	-0.31979	–	–	–	–	18.75	0.18	16.58	0.07	15.37	0.05	1.61	1.07	y	Fader
VVVv303	VVV J163909.57-473235.02	16:39:09.57	-47:32:35.02	337.38326	-0.49277	–	–	–	–	–	–	15.59	0.03	12.47	0.01	1.41	-0.07	y	LPV-Mira
VVVv304	VVV J164056.68-474302.70	16:40:56.68	-47:43:02.70	337.45259	-0.83342	–	–	18.90	0.10	17.32	0.05	14.86	0.01	13.06	0.01	1.09	0.37	y	STV
VVVv305	VVV J163942.31-473033.43	16:39:42.31	-47:30:33.43	337.46978	-0.53905	–	–	–	–	–	–	15.97	0.04	13.57	0.01	1.48	0.87	y	STV
VVVv306	VVV J164057.54-471531.45	16:40:57.54	-47:15:31.45	337.79806	-0.53166	–	–	–	–	–	–	17.51	0.17	15.52	0.06	1.21	0.42	y	STV
VVVv307	VVV J164113.16-471747.09	16:41:13.16	-47:17:47.09	337.79902	-0.58970	–	–	–	–	–	–	16.28	0.05	16.26	0.11	1.12	0.06	y	EB
VVVv308	VVV J164220.97-471911.31	16:42:20.97	-47:19:11.31	337.90787	-0.74909	–	–	–	–	16.95	0.03	14.45	0.01	12.36	0.01	1.62	–	n	LPV
VVVv309	VVV J164058.19-470631.93	16:40:58.19	-47:06:31.93	337.91164	-0.43387	–	–	–	–	–	–	17.32	0.14	13.53	0.01	2.30	1.63	y	LPV-YSO
VVVv310	VVV J164118.44-470744.80	16:41:18.44	-47:07:44.80	337.93443	-0.49032	–	–	–	–	–	–	–	–	15.55	0.06	1.51	1.49	y	STV
VVVv311	VVV J164222.77-463204.23	16:42:22.77	-46:32:04.23	338.50224	-0.23581	–	–	–	–	18.84	0.18	16.87	0.08	15.53	0.05	1.07	-0.51	y	STV
VVVv312	VVV J164336.63-463555.56	16:43:36.63	-46:35:55.56	338.59283	-0.43754	–	–	–	–	–	–	16.26	0.05	11.86	0.01	1.99	0.50	y	LPV-Mira
VVVv313	VVV J164322.08-463031.47	16:43:22.08	-46:30:31.47	338.63345	-0.34702	–	–	–	–	–	–	–	–	16.44	0.11	1.17	2.55	y	LPV-YSO
VVVv314	VVV J164436.13-462642.81	16:44:36.13	-46:26:42.81	338.82057	-0.46604	19.29	0.08	19.03	0.11	16.14	0.02	14.11	0.01	12.39	0.01	1.29	0.03	y	STV
VVVv315	VVV J164319.07-460818.16	16:43:19.07	-46:08:18.16	338.90723	-0.09744	–	–	–	–	16.91	0.03	14.88	0.01	13.66	0.01	1.35	-1.57	y	EB
VVVv316	VVV J164517.96-462415.96	16:45:17.96	-46:24:15.96	338.92986	-0.53047	–	–	–	–	19.38	0.29	16.64	0.07	14.73	0.02	2.25	0.62	y	Fader
VVVv317	VVV J164447.36-461634.12	16:44:47.36	-46:16:34.12	338.96971	-0.38009	–	–	–	–	–	–	15.91	0.03	13.27	0.01	1.77	0.81	y	STV
VVVv318	VVV J164542.89-461737.70	16:45:42.89	-46:17:37.70	339.06053	-0.51288	–	–	–	–	–	–	14.66	0.01	12.10	0.01	1.30	-0.16	y	LPV-YSO
VVVv319	VVV J164517.04-460555.44	16:45:17.04	-46:05:55.44	339.16005	-0.32929	–	–	–	–	17.35	0.05	14.75	0.01	12.58	0.01	1.94	0.01	y	Eruptive
VVVv320	VVV J164541.05-460645.91	16:45:41.05	-46:06:45.91	339.19456	-0.39105	20.04	0.16	19.33	0.14	18.33	0.11	16.88	0.08	15.84	0.06	1.39	0.31	y	STV
VVVv321	VVV J164703.25-461214.67	16:47:03.25	-46:12:14.67	339.27907	-0.63080	18.01	0.03	17.58	0.03	17.67	0.06	16.09	0.04	14.56	0.02	1.30	0.61	y	STV
VVVv322	VVV J164624.57-455921.04	16:46:24.57	-45:59:21.04	339.37029	-0.40641	–	–	–	–	18.48	0.13	16.82	0.08	15.25	0.04	2.63	0.91	y	Eruptive
VVVv323	VVV J164925.09-461955.83	16:49:25.09	-46:19:55.83	339.44450	-1.02573	–	–	–	–	–	–	16.19	0.04	14.22	0.01	1.28	0.94	y	STV
VVVv324	VVV J164711.61-455737.06	16:47:11.61	-45:57:37.06	339.48056	-0.49144	–	–	–	–	17.83	0.07	15.98	0.03	14.51	0.02	1.47	0.70	y	Fader
VVVv325	VVV J164916.71-461417.94	16:49:16.71	-46:14:17.94	339.50098	-0.94697	15.95	0.01	15.38	0.01	13.46	0.01	12.62	0.01	11.91	0.01	1.24	0.28	y	STV
VVVv326	VVV J164528.77-453801.97	16:45:28.77	-45:38:01.97	339.53491	-0.05229	–	–	–	–	–	–	17.89	0.20	13.35	0.01	2.09	1.04	y	LPV-Mira
VVVv327	VVV J164746.43-455444.92	16:47:46.43	-45:54:44.92	339.58225	-0.53750	–	–	–	–	17.29	0.04	15.42	0.02	13.94	0.01	1.02	-0.94	y	Eruptive
VVVv328	VVV J164737.86-453948.08	16:47:37.86	-45:39:48.08	339.75637	-0.35759	–	–	–	–	18.32	0.11	15.59	0.03	14.27	0.02	1.16	-2.04	y	Eruptive
VVVv329	VVV J164623.58-452459.68	16:46:23.58	-45:24:59.68	339.80405	-0.03261	–	–	–	–	–	–	13.38	0.01	10.66	0.01	2.16	–	n	LPV
VVVv330	VVV J164925.34-454635.09	16:49:25.34	-45:46:35.09	339.87121	-0.66959	–	–	–	–	–	–	16.35	0.05	12.57	0.01	2.43	–	n	LPV
VVVv331	VVV J164654.11-451521.92	16:46:54.11	-45:15:21.92	339.98421	0.00338	–	–	–	–	19.84	0.30	16.52	0.06	15.74	0.07	2.67	0.59	y	Eruptive
VVVv332	VVV J165142.03-455238.00	16:51:42.03	-45:52:38.00	340.04734	-1.03927	–	–	–	–	–	–	16.85	0.08	15.35	0.05	1.49	0.61	y	LPV-YSO
VVVv333	VVV J164815.42-452141.77	16:48:15.42	-45:21:41.77	340.05765	-0.24663	–	–	–	–	–	–	–	–	15.99	0.09	1.15	6.22	y	LPV-Mira
VVVv334	VVV J164809.91-451905.07	16:48:09.91	-45:19:05.07	340.08052	-0.20624	–	–	–	–	–	–	15.21	0.02	12.16	0.01	1.31	0.42	y	LPV-Mira
VVVv335	VVV J165209.73-455249.55	16:52:09.73	-45:52:49.55	340.09595	-1.10332	17.20	0.01	16.11	0.01	14.61	0.01	12.55	0.01	11.82	0.01	3.43	0.52	y	Fader

Continued on next page

Table C1 – *Continued from previous page*

Object ID	VVV Designation	α (J2000)	δ (J2000)	l (degrees)	b (degrees)	Z (mag)	Z_{err} (mag)	Y (mag)	Y_{err} (mag)	J (mag)	J_{err} (mag)	H (mag)	H_{err} (mag)	K_s (mag)	$K_{s,err}$ (mag)	ΔK_s (mag)	α_{class}	SFR	Class
VVVv336	VVV J165106.53-454324.24	16:51:06.53	-45:43:24.24	340.10021	-0.86179	–	–	–	–	–	–	–	–	15.47	0.06	2.27	0.77	y	Eruptive
VVVv337	VVV J165207.12-454634.45	16:52:07.12	-45:46:34.45	340.17162	-1.03128	–	–	–	–	18.55	0.09	14.78	0.01	13.43	0.01	1.66	-0.23	y	STV
VVVv338	VVV J164900.46-451559.95	16:49:00.46	-45:15:59.95	340.21527	-0.28650	–	–	19.42	0.20	17.99	0.06	12.88	0.01	10.53	0.01	1.31	-0.27	y	LPV-Mira
VVVv339	VVV J164856.73-451230.02	16:48:56.73	-45:12:30.02	340.25289	-0.24062	–	–	–	–	–	–	16.88	0.08	15.07	0.04	1.06	0.28	y	STV
VVVv340	VVV J164831.39-450636.17	16:48:31.39	-45:06:36.17	340.28023	-0.12039	18.31	0.03	17.56	0.04	17.33	0.03	15.72	0.03	12.86	0.01	1.21	0.02	y	LPV-Mira
VVVv341	VVV J164936.97-451216.30	16:49:36.97	-45:12:16.30	340.33168	-0.32873	–	–	–	–	–	–	15.76	0.03	12.31	0.01	1.50	-0.85	y	LPV-YSO
VVVv342	VVV J165400.57-452249.43	16:54:00.57	-45:22:49.43	340.68757	-1.03674	20.10	0.17	18.46	0.09	17.58	0.04	15.68	0.03	14.98	0.04	1.29	-0.87	y	STV
VVVv343	VVV J165207.50-450636.51	16:52:07.50	-45:06:36.51	340.68672	-0.60889	17.01	0.01	15.91	0.01	15.60	0.01	14.42	0.01	14.43	0.02	1.17	–	n	EB
VVVv344	VVV J165408.46-451939.80	16:54:08.46	-45:19:39.80	340.74304	-1.02144	20.70	0.30	18.73	0.11	17.96	0.06	15.93	0.03	15.48	0.06	1.15	-0.22	y	Eruptive
VVVv345	VVV J165128.98-445511.43	16:51:28.98	-44:55:11.43	340.76133	-0.40026	–	–	–	–	–	–	17.12	0.10	12.97	0.01	3.69	–	n	LPV
VVVv346	VVV J165412.34-451756.95	16:54:12.34	-45:17:56.95	340.77239	-1.01226	–	–	19.58	0.24	18.05	0.06	15.73	0.03	14.95	0.04	1.55	–	y	Dipper
VVVv347	VVV J164957.30-443856.10	16:49:57.30	-44:38:56.10	340.79657	-0.01860	–	–	–	–	–	–	–	–	12.36	0.01	1.06	-1.04	y	LPV-YSO
VVVv348	VVV J165357.35-451050.19	16:53:57.35	-45:10:50.19	340.83662	-0.90334	–	–	–	–	–	–	14.76	0.01	11.60	0.01	1.43	0.41	y	LPV-Mira
VVVv349	VVV J165453.41-451345.52	16:54:53.41	-45:13:45.52	340.90250	-1.06184	19.43	0.09	17.57	0.04	16.20	0.01	–	–	13.38	0.01	1.02	-0.16	y	STV
VVVv350	VVV J165030.84-442939.22	16:50:30.84	-44:29:39.22	340.97914	0.00390	–	–	19.03	0.14	15.96	0.01	12.93	0.01	12.10	0.01	1.02	-1.12	y	EB
VVVv351	VVV J165149.25-444006.46	16:51:49.25	-44:40:06.46	340.99336	-0.28646	–	–	–	–	–	–	14.25	0.01	11.72	0.01	1.01	-0.32	y	LPV-YSO
VVVv352	VVV J165153.69-443850.98	16:51:53.69	-44:38:50.98	341.01790	-0.28327	–	–	–	–	–	–	16.94	0.08	15.66	0.07	1.33	-0.38	y	Eruptive
VVVv353	VVV J165209.03-444046.25	16:52:09.03	-44:40:46.25	341.02208	-0.33871	–	–	–	–	–	–	14.41	0.01	11.35	0.01	1.12	-0.47	y	LPV-Mira
VVVv354	VVV J165049.33-442228.30	16:50:49.33	-44:22:28.30	341.10638	0.03805	18.16	0.03	17.42	0.03	16.97	0.02	15.62	0.03	14.77	0.03	2.25	–	y	Eruptive
VVVv355	VVV J165113.82-442732.78	16:51:13.82	-44:27:32.78	341.08776	-0.07202	–	–	–	–	–	–	13.91	0.01	11.44	0.01	1.10	0.12	y	LPV-YSO
VVVv356	VVV J165240.98-443802.07	16:52:40.98	-44:38:02.07	341.11746	-0.38295	–	–	–	–	–	–	16.13	0.04	12.00	0.01	2.46	1.00	y	LPV-Mira
VVVv357	VVV J165238.49-443632.52	16:52:38.49	-44:36:32.52	341.13199	-0.36144	–	–	18.44	0.08	17.19	0.03	15.16	0.02	14.79	0.03	1.13	-0.47	y	STV
VVVv358	VVV J165433.46-445023.87	16:54:33.46	-44:50:23.87	341.16816	-0.77117	–	–	–	–	–	–	14.04	0.01	11.84	0.01	1.22	–	n	LPV
VVVv359	VVV J165329.81-443421.75	16:53:29.81	-44:34:21.75	341.25655	-0.45631	–	–	19.22	0.17	17.54	0.04	15.09	0.02	14.33	0.02	1.21	1.07	y	Fader
VVVv360	VVV J165643.64-445641.92	16:56:43.64	-44:56:41.92	341.32737	-1.13632	–	–	–	–	–	–	–	–	16.81	0.20	3.71	–	n	LPV
VVVv361	VVV J165454.74-443841.67	16:54:54.74	-44:38:41.67	341.35939	-0.69735	–	–	–	–	–	–	15.48	0.02	12.65	0.01	1.38	–	n	LPV
VVVv362	VVV J165304.23-442234.26	16:53:04.23	-44:22:34.26	341.36060	-0.27305	–	–	–	–	–	–	17.46	0.13	15.33	0.05	1.61	1.35	y	Eruptive
VVVv363	VVV J165300.74-441028.62	16:53:00.74	-44:10:28.62	341.50999	-0.13733	–	–	–	–	18.32	0.09	15.47	0.02	12.17	0.01	1.85	–	n	LPV
VVVv364	VVV J165432.55-440446.80	16:54:32.55	-44:04:46.80	341.75703	-0.29022	–	–	–	–	18.40	0.10	14.12	0.01	12.12	0.01	1.68	-0.50	y	LPV-YSO
VVVv365	VVV J165521.41-440217.92	16:55:21.41	-44:02:17.92	341.88120	-0.37796	17.33	0.01	16.61	0.01	15.83	0.01	15.08	0.01	14.65	0.02	1.08	–	n	EB
VVVv366	VVV J165644.69-433017.90	16:56:44.69	-43:30:17.90	342.45393	-0.23927	–	–	–	–	18.10	0.07	15.84	0.03	14.59	0.02	1.17	0.03	y	LPV-Mira
VVVv367	VVV J170029.61-435300.34	17:00:29.61	-43:53:00.34	342.57740	-1.00550	–	–	–	–	–	–	17.32	0.11	13.69	0.01	2.35	1.50	y	Fader
VVVv368	VVV J165755.54-432803.82	16:57:55.54	-43:28:03.82	342.61656	-0.38353	–	–	–	–	–	–	17.72	0.16	16.09	0.08	1.23	–	n	STV
VVVv369	VVV J165641.41-431129.86	16:56:41.41	-43:11:29.86	342.69237	-0.03573	–	–	18.66	0.08	17.41	0.04	16.33	0.04	15.79	0.06	1.07	–	n	STV
VVVv370	VVV J165748.65-430442.53	16:57:48.65	-43:04:42.53	342.90831	-0.12502	–	–	–	–	–	–	14.57	0.01	12.01	0.01	1.15	0.25	y	LPV-YSO
VVVv371	VVV J165950.04-431721.62	16:59:50.04	-43:17:21.62	342.97146	-0.54512	–	–	19.26	0.11	17.75	0.04	15.79	0.02	14.60	0.01	2.05	-0.19	y	LPV-YSO
VVVv372	VVV J165834.31-425647.04	16:58:34.31	-42:56:47.04	343.09823	-0.15194	–	–	–	–	–	–	14.73	0.01	11.99	0.01	1.31	-0.52	y	LPV-YSO
VVVv373	VVV J170242.77-432514.46	17:02:42.77	-43:25:14.46	343.18920	-1.03878	–	–	–	–	–	–	14.23	0.01	11.66	0.01	1.63	–	n	LPV
VVVv374	VVV J165833.99-424955.25	16:58:33.99	-42:49:55.25	343.18734	-0.08021	–	–	–	–	17.12	0.02	13.99	0.01	11.98	0.01	2.41	0.91	y	Eruptive
VVVv375	VVV J165916.71-425325.43	16:59:16.71	-42:53:25.43	343.22235	-0.21877	–	–	–	–	17.47	0.03	13.64	0.01	12.01	0.01	1.14	-0.61	y	LPV-YSO
VVVv376	VVV J165844.44-424736.58	16:58:44.44	-42:47:36.58	343.23737	-0.08137	–	–	–	–	17.28	0.03	14.67	0.01	12.83	0.01	1.74	0.34	y	Fader
VVVv377	VVV J170123.56-430945.16	17:01:23.56	-43:09:45.16	343.24620	-0.69078	–	–	–	–	20.17	0.34	16.56	0.03	14.40	0.01	2.07	0.13	y	LPV-Mira

Continued on next page

Table C1 – *Continued from previous page*

Object ID	VVV Designation	α (J2000)	δ (J2000)	l (degrees)	b (degrees)	Z (mag)	Z_{err} (mag)	Y (mag)	Y_{err} (mag)	J (mag)	J_{err} (mag)	H (mag)	H_{err} (mag)	K_s (mag)	$K_{s,err}$ (mag)	ΔK_s (mag)	α_{class}	SFR	Class
VVVv378	VVV J165846.18-424637.73	16:58:46.18	-42:46:37.73	343.25349	-0.07541	–	–	–	–	–	–	15.94	0.02	12.32	0.01	1.65	0.82	y	LPV-Mira
VVVv379	VVV J170043.40-430219.08	17:00:43.40	-43:02:19.08	343.26885	-0.51826	–	–	–	–	–	–	–	–	17.09	0.14	1.79	1.05	y	Eruptive
VVVv380	VVV J170128.15-430612.43	17:01:28.15	-43:06:12.43	343.30142	-0.66553	14.12	0.01	14.11	0.01	12.84	0.01	12.79	0.01	12.46	0.01	1.04	–	n	STV
VVVv381	VVV J170056.90-425637.41	17:00:56.90	-42:56:37.41	343.36899	-0.49231	–	–	–	–	–	–	16.67	0.04	13.71	0.01	2.76	0.87	y	Fader
VVVv382	VVV J170206.05-425926.64	17:02:06.05	-42:59:26.64	343.46124	-0.68763	19.48	0.08	19.13	0.10	18.62	0.09	17.83	0.11	14.32	0.01	3.29	–	n	LPV
VVVv383	VVV J170340.88-431135.78	17:03:40.88	-43:11:35.78	343.47692	-1.03981	–	–	19.97	0.21	16.54	0.01	12.98	0.01	11.24	0.01	2.02	–	n	LPV
VVVv384	VVV J170024.90-423701.24	17:00:24.90	-42:37:01.24	343.56623	-0.21407	–	–	–	–	19.28	0.16	14.46	0.01	11.96	0.01	1.78	0.48	y	LPV-Mira
VVVv385	VVV J165952.37-422429.44	16:59:52.37	-42:24:29.44	343.66897	-0.00661	17.24	0.01	16.78	0.01	16.25	0.01	15.70	0.02	15.50	0.03	1.30	–	n	STV
VVVv386	VVV J170105.37-423008.44	17:01:05.37	-42:30:08.44	343.73305	-0.24140	–	–	–	–	19.55	0.19	17.41	0.07	16.45	0.08	1.06	–	y	Eruptive
VVVv387	VVV J170300.08-423144.81	17:03:00.08	-42:31:44.81	343.92764	-0.53630	20.31	0.18	19.18	0.10	17.55	0.03	16.39	0.03	15.74	0.04	1.08	–	y	STV
VVVv388	VVV J170302.23-422515.48	17:03:02.23	-42:25:15.48	344.01736	-0.47555	–	–	–	–	–	–	–	–	16.10	0.06	1.64	0.84	y	Eruptive
VVVv389	VVV J170317.18-422549.88	17:03:17.18	-42:25:49.88	344.03782	-0.51780	–	–	–	–	–	–	16.69	0.04	13.51	0.01	1.56	0.71	y	Eruptive
VVVv390	VVV J170203.10-420332.27	17:02:03.10	-42:03:32.27	344.19236	-0.10990	–	–	–	–	19.49	0.19	17.46	0.08	15.82	0.05	1.06	-0.58	y	LPV-YSO
VVVv391	VVV J170430.33-422215.38	17:04:30.33	-42:22:15.38	344.22202	-0.66025	–	–	–	–	–	–	–	–	15.88	0.05	1.35	0.39	y	STV
VVVv392	VVV J170310.35-415131.99	17:03:10.35	-41:51:31.99	344.47807	-0.15256	–	–	–	–	–	–	16.19	0.04	12.31	0.01	1.38	-0.20	y	LPV-Mira
VVVv393	VVV J170436.13-415410.75	17:04:36.13	-41:54:10.75	344.60491	-0.39061	–	–	–	–	18.08	0.07	16.71	0.06	15.74	0.05	1.05	–	n	STV
VVVv394	VVV J170507.70-414631.38	17:05:07.70	-41:46:31.38	344.76581	-0.39125	–	–	–	–	–	–	15.65	0.02	13.89	0.01	1.02	–	n	LPV
VVVv395	VVV J170724.60-415541.50	17:07:24.60	-41:55:41.50	344.89996	-0.82239	–	–	–	–	18.92	0.15	17.27	0.11	16.35	0.09	2.68	–	n	Rare
VVVv396	VVV J170347.02-412326.48	17:03:47.02	-41:23:26.48	344.91895	0.04206	–	–	–	–	–	–	14.23	0.01	12.23	0.01	1.16	-0.15	y	Eruptive
VVVv397	VVV J170501.10-413310.92	17:05:01.10	-41:33:10.92	344.93032	-0.24027	–	–	–	–	–	–	–	–	13.98	0.01	1.17	0.33	y	LPV-Mira
VVVv398	VVV J170818.57-414440.23	17:08:18.57	-41:44:40.23	345.14743	-0.84651	–	–	–	–	18.91	0.15	16.52	0.05	15.12	0.03	1.11	-0.11	y	STV
VVVv399	VVV J170523.37-411925.23	17:05:23.37	-41:19:25.23	345.15502	-0.15685	–	–	–	–	18.42	0.10	16.98	0.08	15.64	0.05	1.24	0.10	y	STV
VVVv400	VVV J170805.25-414002.24	17:08:05.25	-41:40:02.24	345.18452	-0.76711	–	–	–	–	19.27	0.21	17.03	0.08	15.53	0.04	1.02	-0.43	y	STV
VVVv401	VVV J170528.32-411709.21	17:05:28.32	-41:17:09.21	345.19448	-0.14634	–	–	–	–	–	–	17.39	0.12	12.09	0.01	3.00	0.35	y	LPV-Mira
VVVv402	VVV J170533.12-411547.18	17:05:33.12	-41:15:47.18	345.22171	-0.14452	–	–	–	–	–	–	–	–	15.07	0.03	1.19	1.34	y	Eruptive
VVVv403	VVV J170645.11-412444.47	17:06:45.11	-41:24:44.47	345.23847	-0.41420	–	–	–	–	18.76	0.13	16.84	0.07	15.39	0.04	1.12	–	n	Rare
VVVv404	VVV J170936.20-414740.73	17:09:36.20	-41:47:40.73	345.25111	-1.07003	–	–	–	–	–	–	16.23	0.04	13.00	0.01	1.49	1.15	y	Eruptive
VVVv405	VVV J170938.62-413851.81	17:09:38.62	-41:38:51.81	345.37370	-0.98868	–	–	–	–	–	–	17.50	0.13	13.50	0.01	1.99	1.77	y	Dipper
VVVv406	VVV J170957.47-413548.87	17:09:57.47	-41:35:48.87	345.44947	-1.00565	–	–	18.89	0.12	17.51	0.04	14.61	0.01	12.57	0.01	2.06	1.10	y	Dipper
VVVv407	VVV J171014.46-413159.13	17:10:14.46	-41:31:59.13	345.53228	-1.01036	–	–	–	–	18.73	0.13	17.24	0.11	16.32	0.10	1.07	0.60	y	Eruptive
VVVv408	VVV J170719.60-405954.28	17:07:19.60	-40:59:54.28	345.63430	-0.25183	–	–	19.75	0.25	18.82	0.14	16.90	0.08	15.27	0.04	1.40	0.13	y	STV
VVVv409	VVV J170633.12-405257.01	17:06:33.12	-40:52:57.01	345.63897	-0.06526	19.08	0.07	18.26	0.06	17.05	0.03	15.95	0.03	15.30	0.04	1.41	-1.19	y	STV
VVVv410	VVV J170951.32-410424.87	17:09:51.32	-41:04:24.87	345.85893	-0.67912	–	–	–	–	–	–	17.42	0.20	13.37	0.01	1.89	–	n	LPV
VVVv411	VVV J170714.78-403616.02	17:07:14.78	-40:36:16.02	345.94021	-0.00312	–	–	–	–	–	–	17.43	0.20	15.95	0.09	1.78	1.27	y	LPV-YSO
VVVv412	VVV J170719.21-403041.54	17:07:19.21	-40:30:41.54	346.02292	0.04146	–	–	–	–	–	–	14.86	0.02	12.15	0.01	1.29	0.20	y	Eruptive
VVVv413	VVV J171244.60-405917.67	17:12:44.60	-40:59:17.67	346.24984	-1.06791	–	–	–	–	–	–	15.76	0.04	11.66	0.01	1.97	–	n	LPV
VVVv414	VVV J170826.92-402011.77	17:08:26.92	-40:20:11.77	346.29166	-0.02571	–	–	–	–	–	–	15.64	0.04	12.14	0.01	1.83	–	n	LPV
VVVv415	VVV J170913.65-401051.69	17:09:13.65	-40:10:51.69	346.50518	-0.05205	19.34	0.09	18.22	0.07	16.90	0.04	15.06	0.02	11.55	0.01	1.89	–	n	LPV
VVVv416	VVV J170954.59-395612.24	17:09:54.59	-39:56:12.24	346.77920	-0.01154	19.12	0.07	18.20	0.07	17.17	0.06	14.73	0.02	11.69	0.01	1.79	–	n	LPV
VVVv417	VVV J171002.75-395634.95	17:10:02.75	-39:56:34.95	346.78961	-0.03624	–	–	–	–	–	–	16.04	0.06	14.38	0.02	1.35	–	n	LPV
VVVv418	VVV J170950.73-395404.21	17:09:50.73	-39:54:04.21	346.80045	0.01953	–	–	–	–	–	–	14.71	0.02	11.64	0.01	1.22	–	n	LPV
VVVv419	VVV J171322.75-394816.82	17:13:22.75	-39:48:16.82	347.27891	-0.47067	16.34	0.01	15.86	0.01	15.25	0.01	14.68	0.02	14.42	0.03	1.07	–	n	EB

Continued on next page

Table C1 – *Continued from previous page*

Object ID	VVV Designation	α (J2000)	δ (J2000)	l (degrees)	b (degrees)	Z (mag)	Z_{err} (mag)	Y (mag)	Y_{err} (mag)	J (mag)	J_{err} (mag)	H (mag)	H_{err} (mag)	K_s (mag)	$K_{s,err}$ (mag)	ΔK_s (mag)	α_{class}	SFR	Class
VVVv420	VVV J171234.47-393812.04	17:12:34.47	-39:38:12.04	347.32392	-0.24676	–	–	19.20	0.21	17.73	0.12	16.48	0.10	15.65	0.09	1.12	–	n	LPV
VVVv421	VVV J171416.64-385217.39	17:14:16.64	-38:52:17.39	348.13698	-0.06482	–	–	17.63	0.05	14.03	0.01	12.47	0.01	11.49	0.01	1.77	–	n	LPV
VVVv422	VVV J171910.90-390227.06	17:19:10.90	-39:02:27.06	348.55130	-0.94006	–	–	–	–	–	–	–	–	15.42	0.07	1.85	2.05	y	Eruptive
VVVv423	VVV J171803.97-385228.88	17:18:03.97	-38:52:28.88	348.56253	-0.66712	–	–	–	–	–	–	17.23	0.19	15.09	0.05	1.34	-0.79	y	Fader
VVVv424	VVV J171929.84-390253.81	17:19:29.84	-39:02:53.81	348.58037	-0.99454	–	–	–	–	17.53	0.11	15.63	0.05	14.66	0.03	1.00	-0.54	y	STV
VVVv425	VVV J171717.53-382435.22	17:17:17.53	-38:24:35.22	348.85491	-0.27532	–	–	–	–	–	–	14.52	0.01	11.58	0.01	1.79	0.18	y	LPV-Mira
VVVv426	VVV J171901.66-381856.10	17:19:01.66	-38:18:56.10	349.12795	-0.49911	–	–	18.90	0.10	16.98	0.04	15.58	0.04	14.68	0.03	1.10	0.28	y	STV
VVVv427	VVV J171751.37-375720.53	17:17:51.37	-37:57:20.53	349.28963	-0.10357	–	–	–	–	16.82	0.03	13.67	0.01	12.20	0.01	1.02	-0.50	y	LPV-YSO
VVVv428	VVV J172200.73-382816.84	17:22:00.73	-38:28:16.84	349.33401	-1.06811	–	–	18.71	0.08	17.30	0.05	15.42	0.03	14.63	0.03	1.16	–	n	Rare
VVVv429	VVV J171737.48-375148.58	17:17:37.48	-37:51:48.58	349.33859	-0.01309	–	–	–	–	–	–	14.71	0.02	11.99	0.01	2.05	0.33	y	LPV-Mira
VVVv430	VVV J172258.00-381855.60	17:22:58.00	-38:18:55.60	349.56849	-1.13389	–	–	–	–	–	–	15.33	0.03	12.29	0.01	2.11	0.45	y	LPV-YSO
VVVv431	VVV J172237.25-380642.48	17:22:37.25	-38:06:42.48	349.69794	-0.96261	19.01	0.05	17.96	0.04	17.59	0.07	15.50	0.03	13.95	0.02	1.44	-1.24	y	LPV-YSO
VVVv432	VVV J171827.35-373153.62	17:18:27.35	-37:31:53.62	349.70459	0.04393	–	–	–	–	17.99	0.10	15.12	0.02	11.85	0.01	2.70	0.88	y	LPV-Mira
VVVv433	VVV J172230.65-373952.40	17:22:30.65	-37:39:52.40	350.05420	-0.69131	–	–	–	–	–	–	15.49	0.03	12.48	0.01	1.48	0.05	y	LPV-Mira
VVVv434	VVV J172412.71-375231.53	17:24:12.71	-37:52:31.53	350.07010	-1.08782	19.70	0.09	18.91	0.10	16.96	0.04	15.64	0.04	14.78	0.03	1.20	–	y	STV
VVVv435	VVV J114449.44-612030.53	11:44:49.44	-61:20:30.53	295.03186	0.50402	–	–	–	–	19.31	0.23	17.01	0.06	15.27	0.02	1.59	0.13	y	Dipper
VVVv436	VVV J114920.18-612533.85	11:49:20.18	-61:25:33.85	295.57625	0.55563	20.07	0.13	18.87	0.08	17.62	0.05	15.29	0.01	13.54	0.01	2.16	0.10	y	LPV-Mira
VVVv437	VVV J120800.72-612716.02	12:08:00.72	-61:27:16.02	297.76730	0.98110	18.82	0.06	18.10	0.05	17.07	0.02	16.27	0.02	15.82	0.03	1.10	–	n	STV
VVVv438	VVV J121458.74-623509.84	12:14:58.74	-62:35:09.84	298.74931	-0.01075	–	–	–	–	–	–	17.52	0.07	15.26	0.02	1.59	0.16	y	Dipper
VVVv439	VVV J121555.97-623408.87	12:15:55.97	-62:34:08.87	298.85571	0.02130	–	–	–	–	–	–	17.74	0.08	15.97	0.03	1.08	0.26	y	STV
VVVv440	VVV J121710.81-622317.02	12:17:10.81	-62:23:17.02	298.97406	0.22016	18.52	0.04	17.68	0.03	16.76	0.02	16.00	0.02	15.56	0.02	1.14	–	y	STV
VVVv441	VVV J122130.75-621939.83	12:21:30.75	-62:19:39.83	299.46516	0.34244	19.72	0.11	17.82	0.04	16.08	0.01	14.63	0.01	13.73	0.01	1.49	–	n	LPV
VVVv442	VVV J122346.20-621804.25	12:23:46.20	-62:18:04.25	299.72280	0.39807	20.09	0.15	18.57	0.07	16.88	0.02	15.30	0.01	14.42	0.01	1.91	–	n	LPV
VVVv443	VVV J122758.25-624255.21	12:27:58.25	-62:42:55.21	300.24623	0.03400	18.78	0.05	18.01	0.05	17.28	0.03	16.12	0.02	15.33	0.02	1.00	–	n	STV
VVVv444	VVV J123511.19-624550.01	12:35:11.19	-62:45:50.01	301.07374	0.04923	19.92	0.14	18.70	0.07	17.32	0.03	15.93	0.02	15.18	0.02	1.26	-0.81	y	Dipper
VVVv445	VVV J123605.64-614556.40	12:36:05.64	-61:45:56.40	301.11794	1.05205	–	–	–	–	19.01	0.13	16.42	0.03	14.20	0.01	1.63	-0.24	y	STV
VVVv446	VVV J123659.77-622732.15	12:36:59.77	-62:27:32.15	301.26334	0.36604	18.77	0.05	18.21	0.05	17.44	0.03	16.45	0.03	16.42	0.05	1.08	–	n	STV
VVVv447	VVV J123745.17-622536.29	12:37:45.17	-62:25:36.29	301.34896	0.40295	19.14	0.06	18.24	0.05	17.00	0.02	16.22	0.02	15.75	0.03	1.36	–	n	STV
VVVv448	VVV J123746.96-623154.07	12:37:46.96	-62:31:54.07	301.35798	0.29835	18.95	0.06	17.96	0.04	16.98	0.02	16.02	0.02	14.05	0.01	1.68	–	n	LPV
VVVv449	VVV J124055.13-615710.28	12:40:55.13	-61:57:10.28	301.69559	0.89366	20.57	0.25	18.94	0.09	17.01	0.02	14.70	0.01	12.84	0.01	2.45	0.03	y	Dipper
VVVv450	VVV J124124.20-614717.91	12:41:24.20	-61:47:17.91	301.74609	1.06035	–	–	–	–	18.65	0.09	17.04	0.05	15.77	0.03	1.11	0.24	y	STV
VVVv451	VVV J124115.97-623337.44	12:41:15.97	-62:33:37.44	301.76038	0.28823	–	–	–	–	–	–	18.97	0.27	14.89	0.01	1.78	1.26	y	LPV-YSO
VVVv452	VVV J124158.06-621342.90	12:41:58.06	-62:13:42.90	301.82894	0.62290	–	–	–	–	18.10	0.06	15.68	0.01	13.78	0.01	2.46	0.40	y	Eruptive
VVVv453	VVV J124205.43-621621.45	12:42:05.43	-62:16:21.45	301.84484	0.57941	–	–	–	–	18.48	0.08	16.85	0.04	15.81	0.03	1.18	-0.26	y	STV
VVVv454	VVV J124228.93-620929.37	12:42:28.93	-62:09:29.37	301.88639	0.69543	–	–	–	–	–	–	17.72	0.08	14.95	0.01	1.15	1.34	y	Dipper
VVVv455	VVV J124251.78-621810.74	12:42:51.78	-62:18:10.74	301.93566	0.55220	–	–	–	–	–	–	15.21	0.01	11.92	0.01	1.31	0.22	y	LPV-Mira
VVVv456	VVV J124303.86-621246.44	12:43:03.86	-62:12:46.44	301.95610	0.64300	–	–	–	–	18.96	0.12	17.16	0.05	15.77	0.03	1.60	-0.05	y	STV
VVVv457	VVV J124316.34-621127.15	12:43:16.34	-62:11:27.15	301.97963	0.66580	–	–	18.19	0.05	14.86	0.01	12.31	0.01	11.26	0.01	2.17	-0.54	y	LPV-Mira
VVVv458	VVV J124352.55-615134.62	12:43:52.55	-61:51:34.62	302.04027	0.99906	14.96	0.01	14.27	0.01	13.67	0.01	12.47	0.01	11.80	0.01	1.70	-0.02	y	STV
VVVv459	VVV J124349.50-625419.27	12:43:49.50	-62:54:19.27	302.06520	-0.04639	20.62	0.21	19.11	0.09	18.21	0.07	17.26	0.06	16.75	0.09	1.22	–	y	LPV-YSO
VVVv460	VVV J124452.97-623402.84	12:44:52.97	-62:34:02.84	302.17700	0.29470	–	–	19.22	0.10	17.82	0.05	16.30	0.02	15.10	0.02	1.62	–	n	STV
VVVv461	VVV J124841.99-623046.38	12:48:41.99	-62:30:46.38	302.61596	0.35721	19.97	0.12	18.81	0.07	17.54	0.04	16.38	0.03	15.79	0.04	1.34	–	n	Rare

Continued on next page

Table C1 – *Continued from previous page*

Object ID	VVV Designation	α (J2000)	δ (J2000)	l (degrees)	b (degrees)	Z (mag)	Z_{err} (mag)	Y (mag)	Y_{err} (mag)	J (mag)	J_{err} (mag)	H (mag)	H_{err} (mag)	K_s (mag)	$K_{s,err}$ (mag)	ΔK_s (mag)	α_{class}	SFR	Class
VVVv462	VVV J124951.84-620038.13	12:49:51.84	-62:00:38.13	302.74722	0.86061	20.92	0.27	19.78	0.17	18.73	0.11	17.33	0.07	16.75	0.09	3.33	–	n	LPV
VVVv463	VVV J125455.60-623638.34	12:54:55.60	-62:36:38.34	303.33315	0.25840	–	–	20.05	0.22	18.14	0.06	16.66	0.03	15.40	0.03	1.78	–	n	LPV
VVVv464	VVV J125658.47-622019.66	12:56:58.47	-62:20:19.66	303.57447	0.52607	18.17	0.03	17.22	0.02	16.24	0.01	15.32	0.01	14.79	0.01	1.21	–	n	STV
VVVv465	VVV J125710.56-622245.50	12:57:10.56	-62:22:45.50	303.59696	0.48506	18.47	0.03	17.85	0.03	17.05	0.02	16.22	0.02	15.80	0.03	1.04	–	n	STV
VVVv466	VVV J125936.70-622418.69	12:59:36.70	-62:24:18.69	303.87834	0.45156	–	–	–	–	–	–	–	–	14.58	0.01	2.41	-0.13	y	Fader
VVVv467	VVV J130113.23-622527.93	13:01:13.23	-62:25:27.93	304.06381	0.42584	–	–	–	–	17.05	0.02	14.65	0.01	12.90	0.01	2.26	-0.12	y	Fader
VVVv468	VVV J130237.59-623928.81	13:02:37.59	-62:39:28.81	304.21624	0.18586	–	–	–	–	–	–	16.46	0.03	14.29	0.01	1.07	-0.02	y	LPV-YSO
VVVv469	VVV J130402.14-621003.89	13:04:02.14	-62:10:03.89	304.40186	0.66806	–	–	18.54	0.07	17.63	0.04	16.31	0.02	13.15	0.01	2.78	–	n	LPV
VVVv470	VVV J130653.37-622408.51	13:06:53.37	-62:24:08.51	304.72042	0.41574	13.93	0.01	13.51	0.01	13.08	0.01	12.85	0.01	12.51	0.01	1.01	–	n	LPV
VVVv471	VVV J130819.74-623121.15	13:08:19.74	-62:31:21.15	304.87894	0.28536	–	–	–	–	–	–	17.99	0.11	15.62	0.03	1.30	0.78	y	Dipper
VVVv472	VVV J130834.09-621741.78	13:08:34.09	-62:17:41.78	304.92159	0.51064	–	–	–	–	18.47	0.09	16.56	0.04	15.66	0.03	1.04	-0.56	y	STV
VVVv473	VVV J131057.49-623522.34	13:10:57.49	-62:35:22.34	305.17637	0.19714	–	–	–	–	–	–	–	–	14.53	0.01	1.50	1.82	y	LPV-YSO
VVVv474	VVV J131102.14-623513.07	13:11:02.14	-62:35:13.07	305.18548	0.19903	–	–	–	–	–	–	18.11	0.15	16.36	0.06	1.07	–	y	STV
VVVv475	VVV J131129.71-623426.91	13:11:29.71	-62:34:26.91	305.23920	0.20774	–	–	–	–	–	–	18.08	0.14	16.18	0.06	1.82	–	y	STV
VVVv476	VVV J131204.60-623457.16	13:12:04.60	-62:34:57.16	305.30528	0.19408	–	–	–	–	–	–	–	–	15.57	0.03	1.30	2.10	y	STV
VVVv477	VVV J131309.69-624330.96	13:13:09.69	-62:43:30.96	305.41772	0.04161	–	–	–	–	–	–	17.88	0.12	16.52	0.07	1.42	0.79	y	STV
VVVv478	VVV J131415.24-622300.25	13:14:15.24	-62:23:00.25	305.57265	0.37133	14.13	0.01	13.80	0.01	12.20	0.01	12.66	0.01	12.05	0.01	1.05	–	n	EB
VVVv479	VVV J131546.03-624155.02	13:15:46.03	-62:41:55.02	305.71754	0.04149	–	–	19.76	0.20	18.65	0.11	17.41	0.08	16.65	0.08	1.24	–	y	STV
VVVv480	VVV J131650.32-622341.61	13:16:50.32	-62:23:41.61	305.86975	0.33190	16.94	0.01	16.46	0.01	15.81	0.01	15.08	0.01	14.58	0.01	1.70	-0.28	y	LPV-YSO
VVVv481	VVV J131723.85-623904.20	13:17:23.85	-62:39:04.20	305.90837	0.07049	18.85	0.05	18.40	0.06	18.08	0.06	16.93	0.05	16.11	0.05	1.15	0.39	y	STV
VVVv482	VVV J131832.04-624000.36	13:18:32.04	-62:40:00.36	306.03658	0.04155	–	–	–	–	19.19	0.18	17.45	0.08	15.95	0.04	1.35	0.68	y	STV
VVVv483	VVV J131954.87-623001.95	13:19:54.87	-62:30:01.95	306.21246	0.18971	18.42	0.03	17.63	0.03	16.21	0.01	15.06	0.01	14.40	0.01	1.94	-0.39	y	Fader
VVVv484	VVV J132049.78-623750.56	13:20:49.78	-62:37:50.56	306.30262	0.04855	15.78	0.01	15.14	0.01	14.37	0.01	13.66	0.01	12.84	0.01	1.42	–	n	Known
VVVv485	VVV J132015.07-615257.98	13:20:15.07	-61:52:57.98	306.32004	0.79931	–	–	19.16	0.12	17.33	0.03	15.92	0.02	15.08	0.02	1.00	–	n	STV
VVVv486	VVV J132223.72-622522.25	13:22:23.72	-62:25:22.25	306.50625	0.23389	20.13	0.16	18.57	0.07	16.66	0.02	14.44	0.01	12.68	0.01	1.38	0.43	y	Fader
VVVv487	VVV J132325.88-622610.52	13:23:25.88	-62:26:10.52	306.62359	0.20597	–	–	–	–	–	–	–	–	17.27	0.15	1.18	–	n	STV
VVVv488	VVV J132631.34-621727.54	13:26:31.34	-62:17:27.54	306.99787	0.30349	–	–	–	–	–	–	18.31	0.20	16.07	0.05	1.11	–	n	LPV
VVVv489	VVV J132654.40-620318.49	13:26:54.40	-62:03:18.49	307.07449	0.53101	–	–	–	–	18.50	0.10	15.84	0.02	14.06	0.01	1.29	0.67	y	Eruptive
VVVv490	VVV J133104.45-622318.47	13:31:04.45	-62:23:18.47	307.50652	0.13074	16.26	0.01	15.82	0.01	15.65	0.01	14.84	0.01	13.72	0.01	1.24	–	n	Rare
VVVv491	VVV J133031.03-615116.55	13:30:31.03	-61:51:16.55	307.52336	0.66830	17.70	0.02	17.00	0.02	16.44	0.02	15.76	0.02	15.39	0.03	1.04	–	n	STV
VVVv492	VVV J133044.67-614803.84	13:30:44.67	-61:48:03.84	307.55799	0.71714	20.30	0.19	19.21	0.13	17.91	0.06	16.44	0.04	15.61	0.03	1.09	–	n	STV
VVVv493	VVV J133425.10-612855.50	13:34:25.10	-61:28:55.50	308.03945	0.96273	19.27	0.06	18.20	0.04	17.10	0.03	16.10	0.02	15.57	0.03	1.10	–	n	EB
VVVv494	VVV J134038.29-614700.31	13:40:38.29	-61:47:00.31	308.71294	0.53487	–	–	–	–	–	–	19.59	0.58	14.92	0.02	1.35	2.98	y	Eruptive
VVVv495	VVV J134030.34-613514.32	13:40:30.34	-61:35:14.32	308.73464	0.73041	–	–	–	–	–	–	18.52	0.21	15.99	0.04	2.43	2.09	y	Eruptive
VVVv496	VVV J134148.93-620635.35	13:41:48.93	-62:06:35.35	308.78618	0.18798	–	–	–	–	–	–	17.15	0.06	15.28	0.02	1.55	0.20	y	Eruptive
VVVv497	VVV J134202.43-613911.50	13:42:02.43	-61:39:11.50	308.90099	0.63073	19.05	0.05	18.34	0.05	17.63	0.04	16.50	0.03	15.66	0.03	1.25	–	y	STV
VVVv498	VVV J134449.97-621446.41	13:44:49.97	-62:14:46.41	309.10389	-0.01601	–	–	–	–	–	–	14.42	0.01	11.30	0.01	1.92	0.61	y	LPV-Mira
VVVv499	VVV J134500.58-620616.25	13:45:00.58	-62:06:16.25	309.15326	0.11842	–	–	–	–	–	–	18.45	0.20	16.19	0.05	1.39	0.58	y	LPV-YSO
VVVv500	VVV J134346.56-611919.69	13:43:46.56	-61:19:19.69	309.16963	0.91417	–	–	–	–	–	–	17.66	0.10	15.07	0.02	1.10	–	n	STV
VVVv501	VVV J134540.86-620350.24	13:45:40.86	-62:03:50.24	309.23854	0.14180	–	–	–	–	–	–	18.05	0.14	16.40	0.06	1.32	-0.15	y	STV
VVVv502	VVV J134536.57-614435.04	13:45:36.57	-61:44:35.04	309.29723	0.45739	19.24	0.06	18.31	0.05	17.26	0.03	16.44	0.03	16.01	0.04	1.07	–	n	STV
VVVv503	VVV J134816.19-615819.55	13:48:16.19	-61:58:19.55	309.55482	0.16669	–	–	–	–	18.97	0.11	17.21	0.05	16.23	0.05	1.40	–	y	STV

Continued on next page

Table C1 – *Continued from previous page*

Object ID	VVV Designation	α (J2000)	δ (J2000)	l (degrees)	b (degrees)	Z (mag)	Z_{err} (mag)	Y (mag)	Y_{err} (mag)	J (mag)	J_{err} (mag)	H (mag)	H_{err} (mag)	K_s (mag)	$K_{s,err}$ (mag)	ΔK_s (mag)	α_{class}	SFR	Class
VVVv504	VVV J135017.97-614106.77	13:50:17.97	-61:41:06.77	309.85215	0.39315	–	–	–	–	20.07	0.30	16.31	0.02	14.05	0.01	1.14	0.56	y	Dipper
VVVv505	VVV J135241.63-613622.63	13:52:41.63	-61:36:22.63	310.14697	0.40440	–	–	20.10	0.20	17.74	0.04	16.32	0.02	15.22	0.02	1.74	-1.34	y	STV
VVVv506	VVV J135317.06-611021.46	13:53:17.06	-61:10:21.46	310.31808	0.80910	20.08	0.11	18.79	0.06	17.71	0.04	16.28	0.02	15.12	0.02	1.18	–	n	STV
VVVv507	VVV J135543.10-615844.13	13:55:43.10	-61:58:44.13	310.40415	-0.04330	20.04	0.10	17.59	0.02	15.39	0.01	13.20	0.01	11.70	0.01	2.08	–	n	LPV
VVVv508	VVV J135631.54-613714.61	13:56:31.54	-61:37:14.61	310.58535	0.28008	–	–	–	–	19.53	0.18	17.90	0.10	16.47	0.06	1.89	–	n	LPV
VVVv509	VVV J135541.73-605333.65	13:55:41.73	-60:53:33.65	310.66909	1.01015	12.69	0.01	12.60	0.01	13.90	0.01	13.10	0.01	12.91	0.01	1.23	–	n	Known
VVVv510	VVV J135741.61-611127.48	13:57:41.61	-61:11:27.48	310.82869	0.66087	–	–	19.24	0.09	17.87	0.06	16.39	0.03	15.37	0.03	1.33	-0.82	y	STV
VVVv511	VVV J135826.40-611522.53	13:58:26.40	-61:15:22.53	310.89890	0.57482	17.48	0.01	17.17	0.02	16.33	0.02	15.86	0.02	15.61	0.03	1.08	–	n	STV
VVVv512	VVV J135943.90-614155.63	13:59:43.90	-61:41:55.63	310.93326	0.10746	–	–	–	–	–	–	15.27	0.01	11.79	0.01	1.95	–	n	LPV
VVVv513	VVV J135935.48-612208.31	13:59:35.48	-61:22:08.31	311.00322	0.43020	19.07	0.04	18.23	0.04	17.00	0.03	15.84	0.02	15.10	0.02	1.17	-0.85	y	EB
VVVv514	VVV J140045.37-613339.95	14:00:45.37	-61:33:39.95	311.08692	0.20826	–	–	–	–	17.40	0.04	14.80	0.01	13.26	0.01	1.73	-1.46	y	Fader
VVVv515	VVV J135923.70-605422.36	13:59:23.70	-60:54:22.36	311.10087	0.88316	–	–	–	–	–	–	17.84	0.11	15.74	0.04	1.34	0.86	y	Fader
VVVv516	VVV J140017.60-611719.20	14:00:17.60	-61:17:19.20	311.10552	0.48563	–	–	–	–	–	–	14.16	0.01	10.80	0.01	1.95	0.81	y	LPV-Mira
VVVv517	VVV J140211.33-610039.77	14:02:11.33	-61:00:39.77	311.40000	0.69215	19.49	0.06	18.71	0.06	17.76	0.05	16.54	0.03	15.48	0.03	1.18	-0.48	y	STV
VVVv518	VVV J140513.13-613222.17	14:05:13.13	-61:32:22.17	311.60408	0.08375	–	–	–	–	–	–	17.29	0.06	12.92	0.01	1.63	0.94	y	LPV-YSO
VVVv519	VVV J140537.97-610446.32	14:05:37.97	-61:04:46.32	311.78161	0.51097	19.63	0.07	17.31	0.02	15.21	0.01	13.58	0.01	12.63	0.01	1.48	–	n	Rare
VVVv520	VVV J140737.39-613408.44	14:07:37.39	-61:34:08.44	311.86998	-0.02642	–	–	–	–	–	–	14.07	0.01	11.15	0.01	1.48	0.16	y	LPV-Mira
VVVv521	VVV J140811.24-611646.87	14:08:11.24	-61:16:46.87	312.01884	0.23068	19.63	0.07	18.79	0.06	17.58	0.05	16.48	0.03	16.05	0.05	1.06	–	y	STV
VVVv522	VVV J141041.45-611941.89	14:10:41.45	-61:19:41.89	312.29134	0.09498	–	–	–	–	18.59	0.09	16.22	0.03	14.75	0.01	1.08	-0.30	y	Dipper
VVVv523	VVV J140956.15-610140.83	14:09:56.15	-61:01:40.83	312.29472	0.40874	–	–	–	–	–	–	17.71	0.10	15.86	0.04	1.40	–	y	STV
VVVv524	VVV J141300.81-610550.91	14:13:00.81	-61:05:50.91	312.62817	0.22920	–	–	–	–	18.05	0.06	15.21	0.01	13.22	0.01	1.57	0.27	y	Dipper
VVVv525	VVV J141245.69-603242.92	14:12:45.69	-60:32:42.92	312.77000	0.76378	19.22	0.06	18.30	0.04	17.33	0.03	16.28	0.03	15.90	0.04	1.18	–	n	STV
VVVv526	VVV J141535.32-605907.91	14:15:35.32	-60:59:07.91	312.95929	0.23732	–	–	–	–	–	–	18.17	0.15	15.79	0.04	1.17	0.73	y	LPV-Mira
VVVv527	VVV J141503.90-604740.38	14:15:03.90	-60:47:40.38	312.95974	0.43864	–	–	–	–	–	–	14.67	0.01	12.12	0.01	1.58	–	n	LPV
VVVv528	VVV J141900.72-610554.36	14:19:00.72	-61:05:54.36	313.31429	-0.00438	–	–	–	–	–	–	16.42	0.03	12.22	0.01	2.41	–	n	LPV
VVVv529	VVV J142040.61-604133.22	14:20:40.61	-60:41:33.22	313.64094	0.31027	–	–	–	–	–	–	–	–	11.77	0.01	3.04	–	n	LPV
VVVv530	VVV J141902.00-600125.01	14:19:02.00	-60:01:25.01	313.67352	1.00864	–	–	–	–	19.10	0.15	14.17	0.01	10.89	0.01	1.72	–	n	LPV
VVVv531	VVV J142212.30-604442.26	14:22:12.30	-60:44:42.26	313.79874	0.19726	–	–	19.65	0.16	18.33	0.08	16.25	0.03	14.74	0.01	1.09	-0.35	y	STV
VVVv532	VVV J142134.09-603135.20	14:21:34.09	-60:31:35.20	313.80021	0.42940	20.73	0.22	19.60	0.15	18.40	0.08	16.96	0.05	16.52	0.07	1.05	–	y	STV
VVVv533	VVV J142226.67-604542.45	14:22:26.67	-60:45:42.45	313.82047	0.17150	–	–	–	–	–	–	–	–	12.96	0.01	1.48	0.06	y	LPV-Mira
VVVv534	VVV J142245.57-605018.07	14:22:45.57	-60:50:18.07	313.83014	0.08639	–	–	–	–	–	–	17.70	0.11	14.79	0.02	1.26	1.39	y	Dipper
VVVv535	VVV J142440.39-603412.20	14:24:40.39	-60:34:12.20	314.14310	0.25620	–	–	–	–	–	–	17.55	0.09	15.28	0.02	1.08	-0.18	y	LPV-YSO
VVVv536	VVV J142524.24-602352.49	14:25:24.24	-60:23:52.49	314.28816	0.38541	–	–	–	–	18.04	0.06	16.28	0.03	15.27	0.02	1.03	0.02	y	Eruptive
VVVv537	VVV J142713.67-595918.35	14:27:13.67	-59:59:18.35	314.64640	0.68661	–	–	19.78	0.18	17.87	0.05	16.61	0.04	15.87	0.04	1.08	–	n	EB
VVVv538	VVV J142815.52-595700.73	14:28:15.52	-59:57:00.73	314.78046	0.67540	19.79	0.10	19.18	0.10	17.30	0.03	16.08	0.02	15.31	0.02	1.02	–	n	EB
VVVv539	VVV J143013.42-602755.92	14:30:13.42	-60:27:55.92	314.81753	0.10640	–	–	–	–	–	–	–	–	16.20	0.05	1.95	1.29	y	Eruptive
VVVv540	VVV J142743.97-593258.83	14:27:43.97	-59:32:58.83	314.86459	1.07255	19.25	0.06	18.92	0.08	18.17	0.07	16.88	0.05	15.88	0.04	1.28	–	y	STV
VVVv541	VVV J142831.88-594338.38	14:28:31.88	-59:43:38.38	314.89380	0.87034	19.43	0.07	18.60	0.06	17.06	0.02	15.36	0.01	13.87	0.01	1.74	0.15	y	Fader
VVVv542	VVV J143142.37-602810.18	14:31:42.37	-60:28:10.18	314.98545	0.03431	–	–	–	–	19.07	0.15	17.35	0.08	16.18	0.05	1.51	0.12	y	STV
VVVv543	VVV J143142.52-602751.76	14:31:42.52	-60:27:51.76	314.98767	0.03893	19.91	0.10	18.75	0.07	17.58	0.04	16.31	0.03	15.66	0.03	1.14	-1.14	y	STV
VVVv544	VVV J143506.67-594150.43	14:35:06.67	-59:41:50.43	315.67339	0.58493	–	–	18.92	0.09	17.47	0.03	16.14	0.02	15.44	0.03	1.11	–	n	STV
VVVv545	VVV J143742.20-595110.66	14:37:42.20	-59:51:10.66	315.91205	0.31350	–	–	–	–	–	–	15.26	0.01	11.74	0.01	2.43	–	n	LPV

Continued on next page

Table C1 – *Continued from previous page*

Object ID	VVV Designation	α (J2000)	δ (J2000)	l (degrees)	b (degrees)	Z (mag)	Z_{err} (mag)	Y (mag)	Y_{err} (mag)	J (mag)	J_{err} (mag)	H (mag)	H_{err} (mag)	K_s (mag)	$K_{s,err}$ (mag)	ΔK_s (mag)	α_{class}	SFR	Class
VVVv546	VVV J143752.06-595303.52	14:37:52.06	-59:53:03.52	315.91849	0.27652	19.05	0.08	17.57	0.03	15.93	0.01	14.25	0.01	13.01	0.01	1.53	–	n	LPV
VVVv547	VVV J143633.66-590426.59	14:36:33.66	-59:04:26.59	316.08736	1.08617	18.72	0.06	17.78	0.03	16.77	0.02	15.90	0.02	15.47	0.03	1.12	–	n	STV
VVVv548	VVV J143915.54-593353.29	14:39:15.54	-59:33:53.29	316.20727	0.49889	–	–	19.08	0.11	17.39	0.03	16.30	0.03	15.64	0.03	1.91	–	n	STV
VVVv549	VVV J144040.89-594625.51	14:40:40.89	-59:46:25.51	316.28658	0.23504	–	–	–	–	–	–	–	–	16.22	0.05	3.05	–	n	LPV
VVVv550	VVV J144054.93-593906.08	14:40:54.93	-59:39:06.08	316.36340	0.33438	18.69	0.06	17.39	0.02	16.06	0.01	14.94	0.01	14.32	0.01	1.09	–	n	EB
VVVv551	VVV J144153.75-595401.48	14:41:53.75	-59:54:01.48	316.37370	0.05693	–	–	–	–	–	–	16.70	0.04	14.34	0.01	1.87	0.67	y	LPV-YSO
VVVv552	VVV J144023.74-590454.89	14:40:23.74	-59:04:54.89	316.53560	0.88153	–	–	–	–	–	–	16.54	0.04	12.46	0.01	1.88	–	n	EB
VVVv553	VVV J144318.26-595246.19	14:43:18.26	-59:52:46.19	316.54309	0.00266	–	–	–	–	–	–	17.65	0.10	15.54	0.03	1.30	0.43	y	Dipper
VVVv554	VVV J144315.42-584340.86	14:43:15.42	-58:43:40.86	317.01816	1.05160	–	–	–	–	–	–	–	–	16.80	0.11	1.63	–	y	Eruptive
VVVv555	VVV J144553.20-592208.58	14:45:53.20	-59:22:08.58	317.05440	0.32777	18.24	0.03	16.79	0.01	15.52	0.01	14.13	0.01	13.26	0.01	1.45	0.95	y	Dipper
VVVv556	VVV J144617.31-592406.72	14:46:17.31	-59:24:06.72	317.08665	0.27626	–	–	–	–	–	–	17.41	0.10	15.84	0.04	1.08	1.36	y	STV
VVVv557	VVV J144648.87-592926.55	14:46:48.87	-59:29:26.55	317.10897	0.16735	–	–	–	–	–	–	17.09	0.07	15.25	0.03	1.25	0.49	y	LPV-YSO
VVVv558	VVV J144656.53-592936.63	14:46:56.53	-59:29:36.63	317.12240	0.15786	–	–	–	–	–	–	18.70	0.32	16.86	0.11	1.14	0.30	y	Eruptive
VVVv559	VVV J144903.47-592411.99	14:49:03.47	-59:24:11.99	317.40378	0.12261	–	–	–	–	–	–	–	–	14.97	0.02	1.73	1.57	y	Dipper
VVVv560	VVV J145047.08-592039.71	14:50:47.08	-59:20:39.71	317.62724	0.07882	–	–	–	–	–	–	17.34	0.09	14.95	0.02	1.46	0.45	y	Dipper
VVVv561	VVV J145322.68-592024.94	14:53:22.68	-59:20:24.94	317.92475	-0.06533	–	–	–	–	–	–	15.33	0.02	11.73	0.01	1.55	0.56	y	LPV-Mira
VVVv562	VVV J145333.59-591021.73	14:53:33.59	-59:10:21.73	318.02120	0.07365	–	–	–	–	16.68	0.02	14.20	0.01	12.46	0.01	2.79	-0.01	y	Fader
VVVv563	VVV J145344.28-590933.73	14:53:44.28	-59:09:33.73	318.04759	0.07521	–	–	–	–	–	–	17.51	0.11	15.40	0.03	1.45	-0.04	y	Fader
VVVv564	VVV J145047.04-581441.58	14:50:47.04	-58:14:41.58	318.11405	1.06467	17.77	0.02	17.28	0.02	16.49	0.02	15.50	0.02	15.01	0.02	1.20	–	n	STV
VVVv565	VVV J145313.19-584603.42	14:53:13.19	-58:46:03.42	318.16502	0.45487	–	–	–	–	18.91	0.14	16.62	0.05	15.34	0.03	2.38	–	n	Rare
VVVv566	VVV J145202.35-580908.23	14:52:02.35	-58:09:08.23	318.30337	1.07401	–	–	–	–	–	–	17.82	0.15	14.81	0.02	1.97	1.81	y	STV
VVVv567	VVV J145513.69-584957.65	14:55:13.69	-58:49:57.65	318.36715	0.27875	–	–	–	–	–	–	18.76	0.35	15.81	0.05	1.01	–	n	STV
VVVv568	VVV J145518.57-582232.03	14:55:18.57	-58:22:32.03	318.58586	0.68029	18.79	0.05	17.77	0.03	16.76	0.02	15.85	0.02	15.28	0.03	1.20	–	y	EB
VVVv569	VVV J145617.26-581944.66	14:56:17.26	-58:19:44.66	318.72119	0.66261	–	–	–	–	–	–	15.44	0.02	13.15	0.01	1.21	0.29	y	STV
VVVv570	VVV J145847.00-575924.03	14:58:47.00	-57:59:24.03	319.17035	0.80954	–	–	–	–	–	–	–	–	16.33	0.07	1.34	1.50	y	STV
VVVv571	VVV J145810.12-574249.73	14:58:10.12	-57:42:49.73	319.22752	1.09185	19.17	0.06	18.54	0.06	17.62	0.05	16.47	0.04	15.87	0.05	1.01	–	n	STV
VVVv572	VVV J145912.95-575224.81	14:59:12.95	-57:52:24.81	319.27580	0.88531	–	–	–	–	–	–	18.52	0.29	13.74	0.01	1.90	0.98	y	STV
VVVv573	VVV J150235.15-580550.76	15:02:35.15	-58:05:50.76	319.56183	0.47568	–	–	19.49	0.16	18.08	0.08	16.92	0.06	16.29	0.07	1.04	–	n	STV
VVVv574	VVV J150443.18-580654.81	15:04:43.18	-58:06:54.81	319.79961	0.32331	15.81	0.01	15.11	0.01	15.02	0.01	14.24	0.01	13.76	0.01	1.11	–	n	EB
VVVv575	VVV J150522.47-574002.48	15:05:22.47	-57:40:02.48	320.09491	0.67110	19.40	0.09	18.30	0.05	16.95	0.03	15.54	0.02	14.72	0.02	1.24	-0.44	y	Eruptive
VVVv576	VVV J150446.21-573111.93	15:04:46.21	-57:31:11.93	320.09657	0.83924	17.57	0.02	16.65	0.01	15.68	0.01	14.83	0.01	14.37	0.01	1.04	-2.14	y	STV
VVVv577	VVV J150523.60-573105.93	15:05:23.60	-57:31:05.93	320.17031	0.79969	–	–	–	–	–	–	17.92	0.16	16.13	0.07	1.96	–	y	STV
VVVv578	VVV J150813.34-575523.33	15:08:13.34	-57:55:23.33	320.29770	0.26088	–	–	–	–	18.39	0.10	16.76	0.05	15.95	0.05	1.03	–	y	EB
VVVv579	VVV J150813.36-573053.59	15:08:13.36	-57:30:53.59	320.50196	0.61437	16.03	0.01	14.44	0.01	12.82	0.01	12.22	0.01	11.60	0.01	1.69	–	n	LPV
VVVv580	VVV J150935.66-573522.61	15:09:35.66	-57:35:22.61	320.62350	0.45732	–	–	–	–	18.51	0.11	15.75	0.02	13.70	0.01	3.81	0.75	y	LPV-YSO
VVVv581	VVV J151047.12-574616.64	15:10:47.12	-57:46:16.64	320.66875	0.22004	–	–	–	–	17.89	0.07	15.91	0.02	14.43	0.01	1.58	-0.31	y	LPV-YSO
VVVv582	VVV J151113.18-574843.98	15:11:13.18	-57:48:43.98	320.69772	0.15535	19.74	0.12	18.45	0.07	17.00	0.03	15.85	0.02	15.24	0.03	1.16	–	y	EB
VVVv583	VVV J151051.98-574337.14	15:10:51.98	-57:43:37.14	320.70057	0.25270	–	–	–	–	–	–	16.96	0.06	15.24	0.03	1.21	0.50	y	Eruptive
VVVv584	VVV J150936.37-571712.15	15:09:36.37	-57:17:12.15	320.77775	0.71802	–	–	19.42	0.16	16.89	0.03	14.56	0.01	12.79	0.01	2.29	0.61	y	Eruptive
VVVv585	VVV J151136.89-565833.71	15:11:36.89	-56:58:33.71	321.17033	0.84723	18.33	0.03	17.52	0.02	16.58	0.02	15.75	0.02	15.26	0.03	1.06	–	n	STV
VVVv586	VVV J151319.74-565132.86	15:13:19.74	-56:51:32.86	321.43110	0.82734	–	–	–	–	–	–	18.01	0.17	14.98	0.02	2.52	1.78	y	LPV-YSO
VVVv587	VVV J151430.53-564509.59	15:14:30.53	-56:45:09.59	321.62440	0.83466	–	–	–	–	18.72	0.12	16.97	0.06	15.77	0.04	1.56	–	n	STV

Continued on next page

Table C1 – *Continued from previous page*

Object ID	VVV Designation	α (J2000)	δ (J2000)	l (degrees)	b (degrees)	Z (mag)	Z_{err} (mag)	Y (mag)	Y_{err} (mag)	J (mag)	J_{err} (mag)	H (mag)	H_{err} (mag)	K_s (mag)	$K_{s,err}$ (mag)	ΔK_s (mag)	α_{class}	SFR	Class
VVVv588	VVV J151728.78-572026.38	15:17:28.78	-57:20:26.38	321.65964	0.12213	–	–	–	–	–	–	–	–	14.03	0.01	2.93	1.71	y	LPV-Mira
VVVv589	VVV J151802.91-571449.28	15:18:02.91	-57:14:49.28	321.77446	0.16075	20.54	0.25	18.63	0.07	16.84	0.02	15.52	0.02	14.84	0.02	1.01	–	n	EB
VVVv590	VVV J151817.23-571140.67	15:18:17.23	-57:11:40.67	321.82968	0.18795	18.94	0.06	18.12	0.04	17.31	0.04	16.12	0.03	15.31	0.03	1.11	–	n	STV
VVVv591	VVV J152050.24-563327.63	15:20:50.24	-56:33:27.63	322.46519	0.53895	18.69	0.05	18.11	0.04	17.40	0.04	16.71	0.05	16.35	0.07	1.14	–	n	STV
VVVv592	VVV J152032.05-562731.91	15:20:32.05	-56:27:31.91	322.48330	0.64470	–	–	–	–	–	–	–	–	16.24	0.07	1.45	1.06	y	STV
VVVv593	VVV J152034.71-562800.83	15:20:34.71	-56:28:00.83	322.48413	0.63463	–	–	–	–	17.44	0.04	16.51	0.04	15.69	0.04	1.31	-0.14	y	STV
VVVv594	VVV J152235.73-565108.49	15:22:35.73	-56:51:08.49	322.50796	0.16049	19.10	0.07	17.23	0.02	15.77	0.01	13.60	0.01	12.14	0.01	1.62	-0.02	y	Fader
VVVv595	VVV J152015.17-560443.04	15:20:15.17	-56:04:43.04	322.65521	0.98611	18.79	0.05	17.91	0.03	16.00	0.01	13.20	0.01	11.64	0.01	1.75	–	n	LPV
VVVv596	VVV J152203.45-560904.17	15:22:03.45	-56:09:04.17	322.82754	0.78903	–	–	–	–	–	–	17.32	0.08	14.85	0.02	1.40	0.49	y	Eruptive
VVVv597	VVV J152535.77-562026.67	15:25:35.77	-56:20:26.67	323.13425	0.36066	–	–	–	–	19.84	0.33	18.03	0.16	17.05	0.14	1.25	–	n	Rare
VVVv598	VVV J152332.89-553918.20	15:23:32.89	-55:39:18.20	323.27351	1.09056	–	–	–	–	18.75	0.13	17.02	0.07	16.31	0.07	1.04	–	n	STV
VVVv599	VVV J152842.74-563040.60	15:28:42.74	-56:30:40.60	323.39604	-0.02164	19.04	0.06	18.18	0.04	17.10	0.03	16.16	0.03	15.74	0.04	1.03	–	y	STV
VVVv600	VVV J152949.95-562243.27	15:29:49.95	-56:22:43.27	323.59868	0.00015	–	–	18.89	0.08	16.92	0.02	14.72	0.01	13.09	0.01	1.00	0.78	y	Dipper
VVVv601	VVV J153113.73-560956.68	15:31:13.73	-56:09:56.68	323.87925	0.06486	17.67	0.02	16.49	0.01	15.47	0.01	14.43	0.01	13.94	0.01	1.33	-2.91	y	EB
VVVv602	VVV J153035.84-555119.45	15:30:35.84	-55:51:19.45	323.98383	0.37009	–	–	–	–	18.86	0.13	16.30	0.04	15.04	0.02	1.14	-0.85	y	EB
VVVv603	VVV J152919.69-552605.15	15:29:19.69	-55:26:05.15	324.07524	0.81801	–	–	–	–	–	–	13.27	0.01	11.54	0.01	2.08	–	n	LPV
VVVv604	VVV J153128.64-554206.72	15:31:28.64	-55:42:06.72	324.17308	0.42551	–	–	–	–	19.83	0.32	17.23	0.09	15.33	0.03	1.61	0.44	y	STV
VVVv605	VVV J153126.10-554107.36	15:31:26.10	-55:41:07.36	324.17761	0.44245	–	–	–	–	–	–	16.71	0.05	14.93	0.02	1.09	-0.04	y	STV
VVVv606	VVV J153331.64-560322.81	15:33:31.64	-56:03:22.81	324.20432	-0.02981	15.66	0.01	14.13	0.01	12.63	0.01	12.22	0.01	11.51	0.01	1.86	–	n	LPV
VVVv607	VVV J153300.09-553308.87	15:33:00.09	-55:33:08.87	324.43498	0.42422	–	–	–	–	19.08	0.16	16.94	0.07	15.56	0.04	1.12	–	n	STV
VVVv608	VVV J153358.87-553908.22	15:33:58.87	-55:39:08.22	324.49017	0.26278	–	–	–	–	–	–	18.48	0.27	16.57	0.09	1.61	–	n	STV
VVVv609	VVV J153341.12-551826.98	15:33:41.12	-55:18:26.98	324.65570	0.56812	17.90	0.02	16.59	0.01	15.28	0.01	14.22	0.01	13.60	0.01	1.49	–	n	EB
VVVv610	VVV J153445.56-552709.77	15:34:45.56	-55:27:09.77	324.69566	0.36133	–	–	20.20	0.27	17.34	0.03	15.12	0.01	13.56	0.01	1.90	-0.54	y	LPV-Mira
VVVv611	VVV J153728.01-552400.62	15:37:28.01	-55:24:00.62	325.03772	0.17888	–	–	–	–	20.03	0.39	17.14	0.08	15.10	0.02	1.53	0.45	y	STV
VVVv612	VVV J153547.48-550202.45	15:35:47.48	-55:02:02.45	325.05941	0.61557	–	–	–	–	18.16	0.07	16.05	0.03	14.87	0.02	1.12	–	n	EB
VVVv613	VVV J153517.84-543929.11	15:35:17.84	-54:39:29.11	325.22134	0.96221	19.95	0.14	18.76	0.08	16.90	0.02	14.88	0.01	13.36	0.01	1.99	–	n	STV
VVVv614	VVV J153510.45-543257.45	15:35:10.45	-54:32:57.45	325.27035	1.06097	17.57	0.02	17.11	0.02	16.36	0.01	15.56	0.02	15.17	0.03	1.05	–	n	STV
VVVv615	VVV J153856.83-550740.23	15:38:56.83	-55:07:40.23	325.36889	0.27354	–	–	–	–	18.87	0.12	16.90	0.05	15.59	0.04	1.15	0.46	y	STV
VVVv616	VVV J154024.96-545754.32	15:40:24.96	-54:57:54.32	325.63482	0.27877	–	–	–	–	–	–	16.62	0.04	12.63	0.01	2.38	–	n	LPV
VVVv617	VVV J154017.25-544511.18	15:40:17.25	-54:45:11.18	325.74680	0.45971	–	–	20.75	0.33	18.65	0.09	16.51	0.04	15.32	0.03	1.21	–	y	Fader
VVVv618	VVV J154254.67-550052.84	15:42:54.67	-55:00:52.84	325.89076	0.02376	20.01	0.10	18.65	0.05	15.74	0.01	13.67	0.01	12.11	0.01	1.14	-0.04	y	LPV-YSO
VVVv619	VVV J154228.33-541935.97	15:42:28.33	-54:19:35.97	326.25638	0.61004	–	–	–	–	–	–	13.96	0.01	12.08	0.01	1.08	-0.68	y	LPV-YSO
VVVv620	VVV J154157.90-541046.98	15:41:57.90	-54:10:46.98	326.28601	0.77191	–	–	–	–	19.17	0.15	17.36	0.08	15.98	0.05	2.76	–	y	Eruptive
VVVv621	VVV J154312.04-542308.80	15:43:12.04	-54:23:08.80	326.30508	0.49874	–	–	–	–	–	–	17.12	0.06	15.49	0.03	1.75	-0.70	y	Eruptive
VVVv622	VVV J154110.25-535422.49	15:41:10.25	-53:54:22.49	326.35747	1.06047	–	–	17.94	0.03	15.88	0.01	13.83	0.01	12.46	0.01	1.25	-0.28	y	EB
VVVv623	VVV J154225.31-540519.18	15:42:25.31	-54:05:19.18	326.39433	0.80412	19.92	0.09	18.94	0.06	17.47	0.03	16.10	0.02	15.29	0.03	1.04	-1.07	y	STV
VVVv624	VVV J154257.11-540416.99	15:42:57.11	-54:04:16.99	326.46668	0.77087	–	–	–	–	19.11	0.15	17.20	0.07	15.77	0.04	1.28	0.32	y	STV
VVVv625	VVV J154317.95-540647.29	15:43:17.95	-54:06:47.29	326.48189	0.70679	–	–	–	–	–	–	18.08	0.15	14.49	0.01	1.46	0.33	y	STV
VVVv626	VVV J154359.60-541135.69	15:43:59.60	-54:11:35.69	326.51393	0.58141	18.54	0.03	18.03	0.03	17.31	0.03	15.40	0.01	11.90	0.01	1.10	-0.10	y	LPV-YSO
VVVv627	VVV J154435.13-540903.57	15:44:35.13	-54:09:03.57	326.60840	0.56210	–	–	20.36	0.23	18.07	0.06	16.24	0.03	15.00	0.02	1.33	–	y	STV
VVVv628	VVV J154449.54-540752.08	15:44:49.54	-54:07:52.08	326.64837	0.55636	–	–	20.46	0.26	17.42	0.03	15.30	0.01	13.76	0.01	1.45	-0.51	y	Dipper
VVVv629	VVV J154505.60-540947.91	15:45:05.60	-54:09:47.91	326.65972	0.50694	–	–	20.21	0.21	18.68	0.10	16.48	0.04	15.11	0.02	1.70	-0.25	y	STV

Continued on next page

Table C1 – *Continued from previous page*

Object ID	VVV Designation	α (J2000)	δ (J2000)	l (degrees)	b (degrees)	Z (mag)	Z_{err} (mag)	Y (mag)	Y_{err} (mag)	J (mag)	J_{err} (mag)	H (mag)	H_{err} (mag)	K_s (mag)	$K_{s,err}$ (mag)	ΔK_s (mag)	α_{class}	SFR	Class
VVVv630	VVV J154456.13-540703.18	15:44:56.13	-54:07:03.18	326.66942	0.55727	–	–	–	–	–	–	18.83	0.31	15.76	0.04	1.90	2.70	y	Eruptive
VVVv631	VVV J154518.36-541036.87	15:45:18.36	-54:10:36.87	326.67601	0.47714	20.94	0.24	19.53	0.11	17.39	0.03	15.13	0.01	13.41	0.01	2.63	-0.14	y	Eruptive
VVVv632	VVV J154409.80-535627.78	15:44:09.80	-53:56:27.78	326.68727	0.76630	16.52	0.01	15.71	0.01	14.35	0.01	12.95	0.01	11.87	0.01	1.51	0.29	y	STV
VVVv633	VVV J154503.52-540248.79	15:45:03.52	-54:02:48.79	326.72692	0.60214	–	–	–	–	–	–	18.02	0.15	15.93	0.05	1.53	–	y	Eruptive
VVVv634	VVV J154616.79-541206.67	15:46:16.79	-54:12:06.67	326.77318	0.37003	–	–	–	–	–	–	–	–	16.88	0.12	1.54	1.70	y	Eruptive
VVVv635	VVV J155022.57-535906.72	15:50:22.57	-53:59:06.72	327.37855	0.16708	–	–	0.00	0.01	–	–	16.93	0.05	12.94	0.01	1.31	-0.36	y	LPV-Mira
VVVv636	VVV J155146.28-532557.31	15:51:46.28	-53:25:57.31	327.88638	0.46727	–	–	0.00	0.01	19.47	0.19	16.15	0.02	13.57	0.01	1.41	0.37	y	LPV-YSO
VVVv637	VVV J155206.86-532019.10	15:52:06.86	-53:20:19.10	327.98532	0.50793	–	–	0.00	0.01	–	–	17.89	0.12	13.68	0.01	1.98	0.64	y	STV
VVVv638	VVV J155319.21-532538.36	15:53:19.21	-53:25:38.36	328.06843	0.32546	–	–	0.00	0.01	19.32	0.17	15.33	0.01	12.81	0.01	1.13	0.02	y	Eruptive
VVVv639	VVV J155352.73-532223.92	15:53:52.73	-53:22:23.92	328.16705	0.31428	–	–	0.00	0.01	–	–	17.03	0.05	11.99	0.01	1.70	0.55	y	LPV-Mira
VVVv640	VVV J155303.38-531108.92	15:53:03.38	-53:11:08.92	328.19111	0.53720	–	–	0.00	0.01	–	–	17.90	0.12	13.79	0.01	2.08	0.84	y	LPV-Mira
VVVv641	VVV J155339.20-530511.82	15:53:39.20	-53:05:11.82	328.32325	0.55705	15.57	0.01	16.00	0.01	16.06	0.01	15.12	0.01	14.85	0.03	1.10	–	y	STV
VVVv642	VVV J155510.51-531104.03	15:55:10.51	-53:11:04.03	328.43675	0.33617	–	–	–	–	–	–	12.91	0.01	10.37	0.01	1.59	–	n	LPV
VVVv643	VVV J155543.20-531025.97	15:55:43.20	-53:10:25.97	328.50623	0.29203	–	–	–	–	–	–	17.47	0.12	16.22	0.11	1.14	0.64	y	STV
VVVv644	VVV J155508.35-530130.78	15:55:08.35	-53:01:30.78	328.53443	0.46204	–	–	–	–	–	–	–	–	14.64	0.03	1.36	-0.16	y	LPV-Mira
VVVv645	VVV J155555.56-525446.51	15:55:55.56	-52:54:46.51	328.69733	0.47242	–	–	–	–	–	–	–	–	16.96	0.22	1.43	3.85	y	LPV-YSO
VVVv646	VVV J155806.68-531630.20	15:58:06.68	-53:16:30.20	328.71482	-0.01592	–	–	–	–	–	–	17.16	0.09	15.47	0.06	1.86	0.26	y	STV
VVVv647	VVV J155412.81-522943.33	15:54:12.81	-52:29:43.33	328.76478	0.95934	–	–	–	–	–	–	14.62	0.01	12.01	0.01	2.12	–	n	LPV
VVVv648	VVV J155542.57-524230.82	15:55:42.57	-52:42:30.82	328.80328	0.65021	–	–	–	–	–	–	–	–	14.76	0.03	1.01	2.97	y	LPV-YSO
VVVv649	VVV J155643.04-524815.52	15:56:43.04	-52:48:15.52	328.85865	0.47888	–	–	–	–	–	–	18.31	0.26	14.99	0.04	2.19	0.65	y	Dipper
VVVv650	VVV J155734.78-525307.67	15:57:34.78	-52:53:07.67	328.90584	0.33289	–	–	–	–	–	–	–	–	13.50	0.01	1.98	0.79	y	LPV-Mira
VVVv651	VVV J155647.56-521908.67	15:56:47.56	-52:19:08.67	329.17983	0.84280	–	–	–	–	17.68	0.05	15.97	0.03	14.76	0.03	1.42	–	n	STV
VVVv652	VVV J155929.70-524223.17	15:59:29.70	-52:42:23.17	329.24234	0.28140	–	–	–	–	–	–	17.88	0.17	14.44	0.02	2.84	–	n	LPV
VVVv653	VVV J155653.63-521254.18	15:56:53.63	-52:12:54.18	329.25868	0.91241	–	–	–	–	–	–	13.85	0.01	10.77	0.01	1.58	–	n	LPV
VVVv654	VVV J155730.34-520227.10	15:57:30.34	-52:02:27.10	329.44281	0.98495	–	–	–	–	–	–	15.26	0.02	11.50	0.01	1.35	–	n	LPV
VVVv655	VVV J155842.66-515029.54	15:58:42.66	-51:50:29.54	329.71348	1.01658	–	–	–	–	–	–	16.72	0.06	15.00	0.04	1.35	-1.23	y	STV
VVVv656	VVV J160352.97-514258.66	16:03:52.97	-51:42:58.66	330.39955	0.58647	–	–	19.03	0.12	17.46	0.04	16.22	0.03	15.56	0.04	1.04	-1.40	y	EB
VVVv657	VVV J160501.51-515346.89	16:05:01.51	-51:53:46.89	330.41201	0.33458	–	–	19.28	0.16	17.93	0.06	16.66	0.05	14.72	0.02	1.08	0.60	y	Eruptive
VVVv658	VVV J160614.37-515406.13	16:06:14.37	-51:54:06.13	330.54800	0.20564	17.17	0.01	16.18	0.01	14.68	0.01	13.21	0.01	12.37	0.01	1.20	-1.67	y	Eruptive
VVVv659	VVV J160436.86-512626.49	16:04:36.86	-51:26:26.49	330.66746	0.71725	–	–	–	–	–	–	14.36	0.01	11.88	0.01	1.85	–	n	LPV
VVVv660	VVV J160558.60-513250.32	16:05:58.60	-51:32:50.32	330.75457	0.49647	–	–	–	–	–	–	16.39	0.04	12.62	0.01	1.89	–	n	LPV
VVVv661	VVV J160553.34-504722.43	16:05:53.34	-50:47:22.43	331.25047	1.06961	–	–	–	–	17.74	0.05	14.74	0.01	12.40	0.01	1.25	1.25	y	STV
VVVv662	VVV J161026.82-512234.13	16:10:26.82	-51:22:34.13	331.38447	0.15390	–	–	–	–	–	–	18.55	0.24	15.30	0.03	1.83	0.81	y	Eruptive
VVVv663	VVV J161031.85-510602.50	16:10:31.85	-51:06:02.50	331.58124	0.34711	–	–	–	–	–	–	15.82	0.02	12.26	0.01	1.46	–	n	LPV
VVVv664	VVV J160930.62-504822.40	16:09:30.62	-50:48:22.40	331.66287	0.67250	–	–	–	–	–	–	17.12	0.06	14.78	0.02	1.44	-0.11	y	Eruptive
VVVv665	VVV J160957.70-504809.42	16:09:57.70	-50:48:09.42	331.71775	0.62685	–	–	–	–	–	–	16.57	0.04	14.09	0.01	1.63	0.95	y	Eruptive
VVVv666	VVV J160917.91-503723.65	16:09:17.91	-50:37:23.65	331.76201	0.82992	–	–	–	–	17.91	0.06	16.28	0.03	15.30	0.03	1.17	–	n	EB
VVVv667	VVV J161200.30-505043.44	16:12:00.30	-50:50:43.44	331.92505	0.37586	–	–	–	–	–	–	17.71	0.11	15.84	0.05	1.24	–	n	LPV
VVVv668	VVV J161146.40-500735.22	16:11:46.40	-50:07:35.22	332.38916	0.92620	18.27	0.03	17.64	0.03	16.52	0.02	15.33	0.01	14.39	0.01	1.17	-1.12	y	Dipper
VVVv669	VVV J161155.45-500827.40	16:11:55.45	-50:08:27.40	332.39693	0.89909	18.91	0.06	18.12	0.05	17.55	0.04	16.58	0.04	15.94	0.05	1.06	–	y	STV
VVVv670	VVV J161543.48-503433.61	16:15:43.48	-50:34:33.61	332.53779	0.16640	20.08	0.17	–	–	17.70	0.05	15.90	0.02	14.73	0.02	1.42	-0.07	y	STV
VVVv671	VVV J161238.40-500318.59	16:12:38.40	-50:03:18.59	332.53936	0.88316	–	–	–	–	–	–	17.39	0.08	15.39	0.03	1.67	0.96	y	Eruptive

Continued on next page

Table C1 – *Continued from previous page*

Object ID	VVV Designation	α (J2000)	δ (J2000)	l (degrees)	b (degrees)	Z (mag)	Z_{err} (mag)	Y (mag)	Y_{err} (mag)	J (mag)	J_{err} (mag)	H (mag)	H_{err} (mag)	K_s (mag)	$K_{s,err}$ (mag)	ΔK_s (mag)	α_{class}	SFR	Class
VVVv672	VVV J161303.16-500721.93	16:13:03.16	-50:07:21.93	332.54124	0.78857	19.52	0.10	18.87	0.10	17.17	0.03	16.12	0.03	15.49	0.04	1.11	-0.95	y	STV
VVVv673	VVV J161644.12-504321.62	16:16:44.12	-50:43:21.62	332.55147	-0.05037	–	–	–	–	–	–	14.62	0.01	11.37	0.01	1.42	0.12	y	LPV-YSO
VVVv674	VVV J161333.07-500522.46	16:13:33.07	-50:05:22.46	332.62215	0.75783	–	–	–	–	–	–	16.30	0.03	15.24	0.03	1.08	–	n	STV
VVVv675	VVV J161646.80-503408.73	16:16:46.80	-50:34:08.73	332.66328	0.05515	15.78	0.01	15.08	0.01	14.32	0.01	13.67	0.01	13.46	0.01	1.09	-0.62	y	EB
VVVv676	VVV J161327.72-494925.09	16:13:27.72	-49:49:25.09	332.79443	0.96095	–	–	–	–	18.80	0.12	16.43	0.04	15.07	0.03	1.48	-0.81	y	STV
VVVv677	VVV J161708.10-502456.26	16:17:08.10	-50:24:56.26	332.81058	0.12617	–	–	–	–	–	–	16.97	0.07	12.55	0.01	1.20	–	n	LPV
VVVv678	VVV J161741.28-502718.42	16:17:41.28	-50:27:18.42	332.84627	0.03651	19.39	0.08	19.00	0.09	18.20	0.07	16.95	0.07	12.61	0.01	1.77	–	n	LPV
VVVv679	VVV J161455.50-495908.92	16:14:55.50	-49:59:08.92	332.85355	0.68113	–	–	–	–	–	–	17.44	0.11	13.14	0.01	1.83	–	n	LPV
VVVv680	VVV J161830.18-501930.00	16:18:30.18	-50:19:30.00	333.03010	0.03900	–	–	–	–	19.06	0.15	17.12	0.08	15.88	0.06	1.55	-0.78	y	Dipper
VVVv681	VVV J161610.85-494746.21	16:16:10.85	-49:47:46.21	333.13083	0.67806	–	–	–	–	–	–	16.97	0.07	14.23	0.01	2.68	0.96	y	Dipper
VVVv682	VVV J161854.71-501158.83	16:18:54.71	-50:11:58.83	333.16448	0.08283	19.55	0.10	18.65	0.06	17.49	0.04	16.33	0.04	15.51	0.04	1.56	–	y	EB
VVVv683	VVV J161533.66-493810.79	16:15:33.66	-49:38:10.79	333.16930	0.86275	–	–	–	–	–	–	16.53	0.05	14.00	0.01	1.31	0.42	y	STV
VVVv684	VVV J161854.96-500838.21	16:18:54.96	-50:08:38.21	333.20395	0.12217	19.35	0.08	18.82	0.07	18.00	0.06	16.41	0.04	13.17	0.01	1.03	0.90	y	LPV-YSO
VVVv685	VVV J161615.48-493458.37	16:16:15.48	-49:34:58.37	333.28778	0.82304	–	–	–	–	–	–	17.16	0.08	15.27	0.03	1.56	-0.37	y	EB
VVVv686	VVV J161916.95-500243.18	16:19:16.95	-50:02:43.18	333.31499	0.15137	–	–	–	–	–	–	–	–	16.11	0.07	1.28	1.42	y	Eruptive
VVVv687	VVV J161650.93-491901.77	16:16:50.93	-49:19:01.77	333.54143	0.94756	19.24	0.07	18.70	0.07	17.52	0.04	16.77	0.06	15.45	0.04	1.00	–	n	STV
VVVv688	VVV J161950.92-493821.50	16:19:50.92	-49:38:21.50	333.66491	0.37663	–	–	–	–	18.92	0.14	–	–	14.57	0.02	1.85	–	n	LPV
VVVv689	VVV J162006.05-493656.76	16:20:06.05	-49:36:56.76	333.71051	0.36468	19.64	0.10	18.61	0.06	17.26	0.03	15.70	0.02	14.76	0.02	2.01	-0.39	y	STV
VVVv690	VVV J161916.31-491409.71	16:19:16.31	-49:14:09.71	333.88107	0.72977	17.18	0.01	16.80	0.01	16.16	0.01	15.39	0.02	15.02	0.03	1.17	–	n	STV
VVVv691	VVV J162051.36-492535.05	16:20:51.36	-49:25:35.05	333.93086	0.41295	17.50	0.02	17.08	0.02	16.20	0.01	15.26	0.01	14.55	0.02	1.12	–	n	STV
VVVv692	VVV J162059.45-491908.03	16:20:59.45	-49:19:08.03	334.02221	0.47373	18.95	0.06	17.98	0.04	16.66	0.02	15.79	0.02	15.13	0.03	1.00	–	n	STV
VVVv693	VVV J162028.12-490800.03	16:20:28.12	-49:08:00.03	334.09242	0.66549	17.35	0.01	16.53	0.01	–	–	14.86	0.01	14.28	0.01	1.01	–	n	STV
VVVv694	VVV J162138.12-491021.21	16:21:38.12	-49:10:21.21	334.20001	0.50317	21.04	0.31	19.13	0.11	17.63	0.06	15.70	0.03	14.34	0.02	1.42	0.09	y	Dipper
VVVv695	VVV J162337.14-491149.89	16:23:37.14	-49:11:49.89	334.41118	0.25600	17.66	0.02	16.54	0.01	15.48	0.01	14.36	0.01	13.39	0.01	1.66	-0.59	y	Dipper
VVVv696	VVV J162050.35-483843.24	16:20:50.35	-48:38:43.24	334.47938	0.96903	18.29	0.03	17.30	0.02	16.10	0.02	15.38	0.02	14.94	0.03	1.08	–	n	EB
VVVv697	VVV J162327.18-490255.08	16:23:27.18	-49:02:55.08	334.49771	0.37978	–	–	–	–	–	–	14.25	0.01	11.59	0.01	2.44	–	n	LPV
VVVv698	VVV J162507.05-491128.22	16:25:07.05	-49:11:28.22	334.58714	0.08569	–	–	–	–	–	–	15.27	0.02	11.85	0.01	1.27	-0.36	y	LPV-Mira
VVVv699	VVV J162344.34-485455.29	16:23:44.34	-48:54:55.29	334.62548	0.44010	–	–	–	–	–	–	–	–	16.19	0.09	2.28	2.78	y	Eruptive
VVVv700	VVV J162708.19-484400.79	16:27:08.19	-48:44:00.79	335.14625	0.16707	–	–	–	–	–	–	–	–	14.75	0.03	3.66	–	n	LPV
VVVv701	VVV J162440.71-475426.69	16:24:40.71	-47:54:26.69	335.45321	1.03612	20.88	0.28	18.99	0.10	17.90	0.08	16.15	0.04	15.41	0.05	1.12	–	n	EB
VVVv702	VVV J162850.16-481432.68	16:28:50.16	-48:14:32.68	335.69555	0.30415	20.22	0.19	18.96	0.10	17.41	0.05	16.13	0.05	15.31	0.05	1.16	–	y	STV
VVVv703	VVV J162726.01-475931.65	16:27:26.01	-47:59:31.65	335.71411	0.64634	–	–	–	–	–	–	15.58	0.03	12.12	0.01	1.87	–	n	LPV
VVVv704	VVV J163001.64-481530.95	16:30:01.64	-48:15:30.95	335.82052	0.14929	–	–	–	–	–	–	16.29	0.06	11.86	0.01	1.03	-0.06	y	LPV-Mira
VVVv705	VVV J162906.01-480536.96	16:29:06.01	-48:05:36.96	335.83362	0.37501	–	–	–	–	17.84	0.08	15.69	0.03	14.19	0.02	1.21	-0.29	y	STV
VVVv706	VVV J163101.05-481842.45	16:31:01.05	-48:18:42.45	335.89495	-0.00698	19.30	0.08	17.03	0.02	14.78	0.01	13.01	0.01	11.90	0.01	1.48	-3.26	y	Fader
VVVv707	VVV J162943.72-475759.56	16:29:43.72	-47:57:59.56	335.99810	0.38646	–	–	–	–	–	–	17.97	0.27	13.80	0.01	2.26	–	n	LPV
VVVv708	VVV J162939.42-475032.13	16:29:39.42	-47:50:32.13	336.07996	0.48075	–	–	–	–	–	–	17.79	0.22	14.37	0.02	1.95	–	n	LPV
VVVv709	VVV J163035.64-474559.55	16:30:35.64	-47:45:59.55	336.24313	0.41855	–	–	–	–	–	–	–	–	16.71	0.17	3.48	3.43	y	LPV-YSO
VVVv710	VVV J163225.37-475338.29	16:32:25.37	-47:53:38.29	336.36024	0.10755	–	–	19.56	0.18	17.85	0.08	16.15	0.05	15.37	0.05	1.56	–	y	Eruptive
VVVv711	VVV J163438.61-472001.77	16:34:38.61	-47:20:01.77	337.02552	0.21358	20.31	0.20	18.49	0.07	16.72	0.03	14.68	0.01	11.37	0.01	1.28	–	n	LPV
VVVv712	VVV J163550.53-472231.49	16:35:50.53	-47:22:31.49	337.13198	0.03578	–	–	–	–	–	–	14.82	0.02	12.56	0.01	2.45	-0.92	y	Fader
VVVv713	VVV J163352.79-465218.51	16:33:52.79	-46:52:18.51	337.27716	0.62227	16.91	0.01	16.04	0.01	13.99	0.01	12.61	0.01	11.47	0.01	2.04	-0.08	y	Fader

Continued on next page

Table C1 – *Continued from previous page*

Object ID	VVV Designation	α (J2000)	δ (J2000)	l (degrees)	b (degrees)	Z (mag)	Z_{err} (mag)	Y (mag)	Y_{err} (mag)	J (mag)	J_{err} (mag)	H (mag)	H_{err} (mag)	K_s (mag)	$K_{s,err}$ (mag)	ΔK_s (mag)	α_{class}	SFR	Class
VVVv714	VVV J163353.64-465134.78	16:33:53.64	-46:51:34.78	337.28772	0.62874	–	–	–	–	–	–	–	–	15.08	0.04	2.18	0.76	y	LPV-YSO
VVVv715	VVV J163702.59-470039.76	16:37:02.59	-47:00:39.76	337.53883	0.12988	–	–	–	–	–	–	–	–	12.34	0.01	1.46	–	n	LPV
VVVv716	VVV J163555.14-464920.63	16:35:55.14	-46:49:20.63	337.54935	0.39883	–	–	–	–	17.14	0.05	15.16	0.02	13.92	0.01	1.02	-1.06	y	LPV-YSO
VVVv717	VVV J163605.56-464040.61	16:36:05.56	-46:40:40.61	337.67616	0.47413	–	–	–	–	–	–	–	–	14.37	0.02	2.47	0.80	y	LPV-YSO
VVVv718	VVV J163854.24-465446.26	16:38:54.24	-46:54:46.26	337.82422	-0.04043	–	–	–	–	–	–	16.35	0.07	14.73	0.03	1.09	-1.37	y	EB
VVVv719	VVV J163907.18-464958.72	16:39:07.18	-46:49:58.72	337.90832	-0.01466	–	–	–	–	–	–	14.63	0.01	11.61	0.01	1.65	0.02	y	LPV-Mira
VVVv720	VVV J163722.54-461329.11	16:37:22.54	-46:13:29.11	338.16032	0.61494	–	–	–	–	–	–	–	–	14.97	0.04	2.08	1.50	y	Eruptive
VVVv721	VVV J163948.77-454847.96	16:39:48.77	-45:48:47.96	338.74912	0.57449	–	–	–	–	18.49	0.16	15.96	0.05	13.98	0.01	1.86	0.87	y	Eruptive
VVVv722	VVV J164042.44-453905.82	16:40:42.44	-45:39:05.82	338.97368	0.56500	–	–	–	–	–	–	17.90	0.27	13.53	0.01	1.04	0.06	y	LPV-Mira
VVVv723	VVV J164231.97-454048.90	16:42:31.97	-45:40:48.90	339.16278	0.30656	–	–	–	–	15.32	0.01	12.99	0.01	11.94	0.01	1.89	-0.21	y	Dipper
VVVv724	VVV J164257.47-444743.95	16:42:57.47	-44:47:43.95	339.87852	0.83198	20.17	0.17	18.37	0.06	16.54	0.03	14.92	0.02	14.19	0.02	1.53	–	n	Rare
VVVv725	VVV J164624.86-451206.07	16:46:24.86	-45:12:06.07	339.96997	0.10400	18.27	0.03	17.77	0.03	17.13	0.04	16.40	0.05	16.07	0.09	1.16	–	n	STV
VVVv726	VVV J164359.99-444504.52	16:43:59.99	-44:45:04.52	340.03324	0.72144	–	–	–	–	–	–	–	–	16.54	0.13	2.07	–	n	LPV
VVVv727	VVV J164622.25-445953.10	16:46:22.25	-44:59:53.10	340.11987	0.24200	–	–	–	–	–	–	14.45	0.01	11.91	0.01	1.46	–	n	LPV
VVVv728	VVV J164734.30-445638.46	16:47:34.30	-44:56:38.46	340.29861	0.11519	–	–	–	–	–	–	15.35	0.02	11.54	0.01	1.51	0.65	y	LPV-Mira
VVVv729	VVV J164803.79-444359.42	16:48:03.79	-44:43:59.42	340.51590	0.18477	–	–	–	–	–	–	16.00	0.04	12.34	0.01	1.50	0.27	y	LPV-Mira
VVVv730	VVV J164639.49-443044.62	16:46:39.49	-44:30:44.62	340.52261	0.51824	20.78	0.28	19.00	0.10	17.41	0.05	15.88	0.03	15.03	0.03	1.30	-1.95	y	EB
VVVv731	VVV J164634.32-442531.34	16:46:34.32	-44:25:31.34	340.57888	0.58638	–	–	–	–	18.30	0.11	15.97	0.04	14.97	0.03	3.70	–	n	Rare
VVVv732	VVV J164622.42-441634.06	16:46:22.42	-44:16:34.06	340.66946	0.71018	–	–	–	–	17.77	0.07	15.99	0.04	15.29	0.04	1.31	–	n	STV
VVVv733	VVV J164620.85-441447.50	16:46:20.85	-44:14:47.50	340.68894	0.73296	18.92	0.05	17.94	0.04	16.84	0.03	15.81	0.03	15.32	0.04	1.55	–	n	EB
VVVv734	VVV J164752.96-442816.11	16:47:52.96	-44:28:16.11	340.69533	0.37842	–	–	–	–	–	–	16.78	0.07	15.26	0.04	1.13	–	y	STV
VVVv735	VVV J165029.33-441952.02	16:50:29.33	-44:19:52.02	341.10170	0.11162	–	–	–	–	–	–	17.10	0.10	15.35	0.04	1.07	-0.47	y	LPV-YSO
VVVv736	VVV J165055.45-440659.40	16:50:55.45	-44:06:59.40	341.31663	0.18874	–	–	–	–	–	–	–	–	15.02	0.03	1.08	1.60	y	Dipper
VVVv737	VVV J165131.99-440044.27	16:51:31.99	-44:00:44.27	341.46665	0.17091	–	–	–	–	–	–	15.57	0.02	11.95	0.01	2.07	0.20	y	LPV-Mira
VVVv738	VVV J165046.51-435041.49	16:50:46.51	-43:50:41.49	341.50858	0.38280	–	–	–	–	–	–	17.58	0.12	16.30	0.09	1.16	–	y	Eruptive
VVVv739	VVV J164822.88-432206.16	16:48:22.88	-43:22:06.16	341.59616	1.02090	18.03	0.02	17.35	0.02	16.60	0.02	15.92	0.03	15.64	0.05	1.02	–	n	STV
VVVv740	VVV J165259.55-440203.79	16:52:59.55	-44:02:03.79	341.61623	-0.04574	–	–	–	–	–	–	16.96	0.07	15.44	0.04	1.36	-0.93	y	STV
VVVv741	VVV J165005.32-432227.21	16:50:05.32	-43:22:27.21	341.79097	0.77929	18.95	0.05	17.98	0.04	17.17	0.03	16.18	0.03	15.84	0.06	1.61	–	n	STV
VVVv742	VVV J165053.55-432707.55	16:50:53.55	-43:27:07.55	341.82441	0.61727	19.01	0.05	18.15	0.04	17.20	0.03	16.33	0.04	15.88	0.06	1.06	–	n	STV
VVVv743	VVV J165251.56-433950.49	16:52:51.56	-43:39:50.49	341.88755	0.20751	–	–	–	–	19.31	0.21	15.04	0.01	12.42	0.01	1.71	0.93	y	LPV-Mira
VVVv744	VVV J165354.84-433809.08	16:53:54.84	-43:38:09.08	342.03005	0.07756	19.36	0.06	18.67	0.06	17.87	0.06	16.56	0.05	13.13	0.01	1.06	-0.05	y	LPV-Mira
VVVv745	VVV J165144.08-431111.91	16:51:44.08	-43:11:11.91	342.12662	0.66842	–	–	–	–	18.90	0.15	16.84	0.06	15.51	0.04	1.26	–	n	STV
VVVv746	VVV J165344.38-432819.36	16:53:44.38	-43:28:19.36	342.13710	0.20551	–	–	–	–	–	–	18.07	0.19	15.74	0.05	1.27	0.91	y	Eruptive
VVVv747	VVV J165205.49-430449.43	16:52:05.49	-43:04:49.43	342.25001	0.68576	–	–	–	–	18.52	0.11	13.76	0.01	11.73	0.01	2.59	–	n	LPV
VVVv748	VVV J165331.07-431512.35	16:53:31.07	-43:15:12.35	342.28104	0.37492	–	–	–	–	–	–	17.05	0.08	15.29	0.03	1.15	0.19	y	STV
VVVv749	VVV J165448.52-432409.89	16:54:48.52	-43:24:09.89	342.31324	0.09858	–	–	–	–	–	–	18.58	0.31	15.33	0.04	1.38	1.69	y	Eruptive
VVVv750	VVV J165244.59-430520.02	16:52:44.59	-43:05:20.02	342.31899	0.58841	–	–	–	–	–	–	–	–	16.28	0.08	2.73	2.55	y	STV
VVVv751	VVV J165249.10-430236.21	16:52:49.10	-43:02:36.21	342.36287	0.60665	18.37	0.03	17.69	0.03	16.19	0.01	14.53	0.01	13.08	0.01	1.22	-0.01	y	Dipper
VVVv752	VVV J165507.68-431244.47	16:55:07.68	-43:12:44.47	342.49782	0.17312	–	–	–	–	–	–	17.55	0.12	15.70	0.05	1.03	0.83	y	STV
VVVv753	VVV J165452.75-430321.11	16:54:52.75	-43:03:21.11	342.59096	0.30682	–	–	–	–	–	–	16.20	0.03	12.68	0.01	1.76	–	n	LPV
VVVv754	VVV J165528.31-430602.58	16:55:28.31	-43:06:02.58	342.62406	0.19447	–	–	–	–	–	–	18.57	0.32	12.70	0.01	1.69	–	n	LPV
VVVv755	VVV J165504.79-425847.58	16:55:04.79	-42:58:47.58	342.67309	0.32610	–	–	–	–	–	–	17.82	0.16	13.62	0.01	1.86	–	n	LPV

Continued on next page

Table C1 – *Continued from previous page*

Object ID	VVV Designation	α (J2000)	δ (J2000)	l (degrees)	b (degrees)	Z (mag)	Z_{err} (mag)	Y (mag)	Y_{err} (mag)	J (mag)	J_{err} (mag)	H (mag)	H_{err} (mag)	K_s (mag)	$K_{s,err}$ (mag)	ΔK_s (mag)	α_{class}	SFR	Class
VVVv756	VVV J165225.39-423432.39	16:52:25.39	-42:34:32.39	342.67855	0.95934	21.01	0.29	19.61	0.16	17.16	0.03	15.27	0.02	13.63	0.01	1.94	0.27	y	Fader
VVVv757	VVV J165231.55-423049.66	16:52:31.55	-42:30:49.66	342.73837	0.98399	–	–	–	–	18.79	0.14	16.63	0.05	15.61	0.05	1.13	–	n	STV
VVVv758	VVV J165625.48-425554.23	16:56:25.48	-42:55:54.23	342.86490	0.16459	19.15	0.15	18.95	0.13	17.80	0.06	14.94	0.01	10.61	0.01	1.34	–	n	LPV
VVVv759	VVV J165330.26-422615.00	16:53:30.26	-42:26:15.00	342.91171	0.89267	–	–	–	–	–	–	17.49	0.11	16.30	0.12	2.38	1.75	y	Eruptive
VVVv760	VVV J165514.44-424026.62	16:55:14.44	-42:40:26.62	342.92954	0.49531	17.09	0.03	16.54	0.02	16.11	0.01	15.16	0.01	14.79	0.03	1.12	-1.77	y	EB
VVVv761	VVV J165639.54-423813.91	16:56:39.54	-42:38:13.91	343.12166	0.31518	–	–	–	–	18.32	0.09	16.46	0.04	15.51	0.06	1.04	–	n	STV
VVVv762	VVV J165704.45-423124.12	16:57:04.45	-42:31:24.12	343.25829	0.32656	17.31	0.03	17.13	0.03	16.58	0.02	15.85	0.02	15.28	0.05	1.01	–	n	LPV
VVVv763	VVV J165657.89-422955.09	16:56:57.89	-42:29:55.09	343.26505	0.35773	–	–	–	–	18.28	0.09	15.27	0.01	13.63	0.01	3.19	–	n	Rare
VVVv764	VVV J165410.03-415356.82	16:54:10.03	-41:53:56.82	343.40683	1.13735	–	–	18.76	0.10	–	–	–	–	11.94	0.01	1.61	0.12	y	LPV-Mira
VVVv765	VVV J165452.35-415132.72	16:54:52.35	-41:51:32.72	343.52064	1.06055	–	–	–	–	18.91	0.16	16.97	0.07	14.58	0.03	1.80	-0.52	y	Dipper
VVVv766	VVV J165959.76-422759.67	16:59:59.76	-42:27:59.67	343.63706	-0.06055	–	–	–	–	–	–	17.87	0.15	15.78	0.08	1.13	-0.27	y	EB
VVVv767	VVV J165646.93-415231.10	16:56:46.93	-41:52:31.10	343.73084	0.77336	14.05	0.01	13.79	0.01	13.46	0.01	–	–	12.25	0.01	1.15	–	n	EB
VVVv768	VVV J170030.35-421248.67	17:00:30.35	-42:12:48.67	343.89438	0.02131	18.53	0.09	18.04	0.05	18.55	0.11	16.73	0.05	14.95	0.04	1.07	-0.39	y	STV
VVVv769	VVV J165846.96-414317.51	16:58:46.96	-41:43:17.51	344.08324	0.57717	–	–	–	–	18.30	0.09	14.37	0.01	12.30	0.01	2.06	–	n	LPV
VVVv770	VVV J170129.39-413942.90	17:01:29.39	-41:39:42.90	344.44189	0.21617	–	–	–	–	–	–	–	–	15.07	0.03	2.39	0.67	y	Eruptive
VVVv771	VVV J165759.50-410834.91	16:57:59.50	-41:08:34.91	344.44477	1.05253	–	–	–	–	16.24	0.01	12.90	0.01	11.63	0.01	1.69	–	n	LPV
VVVv772	VVV J165827.14-405409.28	16:58:27.14	-40:54:09.28	344.68722	1.13379	–	–	–	–	17.26	0.03	13.61	0.01	11.74	0.01	2.02	–	n	LPV
VVVv773	VVV J170129.82-411022.03	17:01:29.82	-41:10:22.03	344.82892	0.51528	–	–	–	–	–	–	15.49	0.02	12.30	0.01	1.22	–	n	LPV
VVVv774	VVV J170028.83-403311.02	17:00:28.83	-40:33:11.02	345.19957	1.04786	18.41	0.03	17.50	0.02	16.48	0.01	15.20	0.01	14.43	0.02	1.17	-0.67	y	STV
VVVv775	VVV J170036.85-403207.80	17:00:36.85	-40:32:07.80	345.22906	1.03865	–	–	20.27	0.26	19.17	0.15	17.42	0.09	15.67	0.05	1.45	1.52	y	STV
VVVv776	VVV J170041.05-403228.55	17:00:41.05	-40:32:28.55	345.23270	1.02463	–	–	–	–	18.95	0.12	16.23	0.03	14.61	0.02	1.11	-0.09	y	STV
VVVv777	VVV J170050.17-403217.91	17:00:50.17	-40:32:17.91	345.25280	1.00368	–	–	–	–	17.52	0.03	15.93	0.02	14.91	0.02	1.38	-0.78	y	STV
VVVv778	VVV J170038.73-402958.86	17:00:38.73	-40:29:58.86	345.26095	1.05602	–	–	–	–	18.78	0.11	14.92	0.01	12.17	0.01	1.55	1.09	y	STV
VVVv779	VVV J170202.20-404118.61	17:02:02.20	-40:41:18.61	345.27405	0.73163	–	–	–	–	–	–	15.53	0.02	12.25	0.01	2.17	0.91	y	LPV-Mira
VVVv780	VVV J170104.38-402659.86	17:01:04.38	-40:26:59.86	345.35017	1.02249	19.90	0.11	18.63	0.06	16.85	0.02	15.20	0.01	14.15	0.01	1.07	-0.52	y	STV
VVVv781	VVV J170103.96-402640.28	17:01:03.96	-40:26:40.28	345.35366	1.02686	–	–	–	–	18.61	0.09	15.73	0.02	13.90	0.01	1.85	1.51	y	Fader
VVVv782	VVV J170558.41-405720.74	17:05:58.41	-40:57:20.74	345.51464	-0.02221	–	–	–	–	–	–	16.64	0.05	14.82	0.02	1.04	-1.07	y	EB
VVVv783	VVV J170215.24-395854.81	17:02:15.24	-39:58:54.81	345.85827	1.13137	18.74	0.04	18.00	0.04	16.38	0.02	15.12	0.02	14.26	0.02	1.31	-1.01	y	STV
VVVv784	VVV J170450.47-401830.72	17:04:50.47	-40:18:30.72	345.90020	0.54029	–	–	–	–	–	–	15.58	0.02	13.34	0.01	1.56	0.16	y	STV
VVVv785	VVV J170601.51-402746.57	17:06:01.51	-40:27:46.57	345.91354	0.26736	–	–	–	–	–	–	16.55	0.06	12.51	0.01	1.98	0.77	y	LPV-Mira
VVVv786	VVV J170448.34-401326.37	17:04:48.34	-40:13:26.37	345.96334	0.59691	–	–	–	–	18.23	0.09	15.30	0.02	13.69	0.01	1.63	0.27	y	Dipper
VVVv787	VVV J170648.69-402635.41	17:06:48.69	-40:26:35.41	346.01944	0.15986	–	–	–	–	–	–	–	–	13.75	0.01	1.88	–	n	LPV
VVVv788	VVV J170711.21-400902.64	17:07:11.21	-40:09:02.64	346.29617	0.27844	18.59	0.03	17.82	0.03	16.92	0.03	16.04	0.04	15.70	0.06	1.04	–	n	STV
VVVv789	VVV J170811.64-392444.91	17:08:11.64	-39:24:44.91	347.00307	0.56616	20.30	0.15	18.79	0.07	17.37	0.04	16.29	0.04	15.52	0.05	1.33	–	n	EB
VVVv790	VVV J170810.22-391409.92	17:08:10.22	-39:14:09.92	347.14166	0.67538	–	–	–	–	–	–	17.81	0.19	16.60	0.13	1.65	–	n	STV
VVVv791	VVV J170806.33-385911.97	17:08:06.33	-38:59:11.97	347.33399	0.83472	–	–	–	–	–	–	–	–	13.13	0.01	2.85	–	n	LPV
VVVv792	VVV J170919.43-390259.83	17:09:19.43	-39:02:59.83	347.42453	0.60711	–	–	–	–	–	–	–	–	12.76	0.01	2.01	–	n	LPV
VVVv793	VVV J170856.29-385848.19	17:08:56.29	-38:58:48.19	347.43599	0.70892	–	–	–	–	–	–	16.24	0.05	12.72	0.01	2.85	–	n	LPV
VVVv794	VVV J171250.14-391027.51	17:12:50.14	-39:10:27.51	347.72752	-0.01558	20.24	0.19	18.85	0.11	17.07	0.04	15.98	0.04	15.40	0.05	1.04	–	y	EB
VVVv795	VVV J171312.64-385041.41	17:13:12.64	-38:50:41.41	348.03690	0.11908	–	–	–	–	19.32	0.29	17.47	0.16	16.61	0.15	1.53	–	y	Eruptive
VVVv796	VVV J171207.43-384126.86	17:12:07.43	-38:41:26.86	348.03683	0.38101	–	–	–	–	–	–	16.87	0.09	12.45	0.01	2.94	1.10	y	LPV-Mira
VVVv797	VVV J171219.10-382941.67	17:12:19.10	-38:29:41.67	348.21749	0.46574	–	–	18.89	0.11	17.89	0.08	16.78	0.09	15.90	0.08	1.37	–	y	STV

Continued on next page

Table C1 – *Continued from previous page*

Object ID	VVV Designation	α (J2000)	δ (J2000)	l (degrees)	b (degrees)	Z (mag)	Z_{err} (mag)	Y (mag)	Y_{err} (mag)	J (mag)	J_{err} (mag)	H (mag)	H_{err} (mag)	K_s (mag)	$K_{s,err}$ (mag)	ΔK_s (mag)	α_{class}	SFR	Class
VVVv798	VVV J171244.16-382639.53	17:12:44.16	-38:26:39.53	348.30653	0.42941	–	–	–	–	–	–	–	–	14.05	0.01	1.03	1.60	y	LPV-Mira
VVVv799	VVV J171316.81-383051.00	17:13:16.81	-38:30:51.00	348.31258	0.30220	–	–	–	–	16.25	0.02	13.10	0.01	11.73	0.01	1.38	-1.33	y	Dipper
VVVv800	VVV J171246.04-382524.63	17:12:46.04	-38:25:24.63	348.32696	0.43669	–	–	–	–	18.89	0.20	15.80	0.04	12.89	0.01	1.65	1.44	y	Eruptive
VVVv801	VVV J171222.63-381837.43	17:12:22.63	-38:18:37.43	348.37339	0.56511	–	–	–	–	–	–	14.13	0.01	11.43	0.01	1.68	0.07	y	LPV-YSO
VVVv802	VVV J171410.63-383011.83	17:14:10.63	-38:30:11.83	348.42421	0.16640	19.70	0.12	–	–	18.13	0.10	16.31	0.06	13.30	0.01	1.42	1.38	y	LPV-Mira
VVVv803	VVV J171343.94-381016.01	17:13:43.94	-38:10:16.01	348.64244	0.43158	–	–	–	–	–	–	–	–	13.58	0.01	2.41	–	n	LPV
VVVv804	VVV J171504.10-380938.79	17:15:04.10	-38:09:38.79	348.80431	0.22455	–	–	–	–	18.45	0.13	14.38	0.01	11.87	0.01	1.51	0.08	y	LPV-Mira
VVVv805	VVV J171524.97-380818.55	17:15:24.97	-38:08:18.55	348.86227	0.18196	–	–	–	–	–	–	16.75	0.10	13.00	0.01	1.22	0.17	y	LPV-Mira
VVVv806	VVV J171406.87-374640.84	17:14:06.87	-37:46:40.84	349.00522	0.60069	–	–	–	–	–	–	–	–	14.46	0.02	3.37	–	n	LPV
VVVv807	VVV J171643.72-374852.74	17:16:43.72	-37:48:52.74	349.27611	0.15949	–	–	–	–	–	–	–	–	15.52	0.06	2.70	1.29	y	LPV-YSO
VVVv808	VVV J171632.78-374609.27	17:16:32.78	-37:46:09.27	349.29224	0.21515	–	–	–	–	–	–	–	–	16.45	0.14	2.26	–	y	Eruptive
VVVv809	VVV J171713.14-373941.72	17:17:13.14	-37:39:41.72	349.45704	0.16903	–	–	–	–	–	–	–	–	16.66	0.17	2.01	2.72	y	Eruptive
VVVv810	VVV J171707.96-373320.37	17:17:07.96	-37:33:20.37	349.53356	0.24425	–	–	–	–	–	–	–	–	14.70	0.03	2.34	–	n	LPV
VVVv811	VVV J171714.07-372347.84	17:17:14.07	-37:23:47.84	349.67499	0.31974	–	–	–	–	–	17.32	0.16	12.53	0.01	1.62	–	n	LPV	
VVVv812	VVV J171726.31-372352.20	17:17:26.31	-37:23:52.20	349.69743	0.28597	–	–	–	–	–	–	–	–	14.55	0.02	3.47	–	n	LPV
VVVv813	VVV J171525.93-364642.02	17:15:25.93	-36:46:42.02	349.97008	0.97119	–	–	–	–	18.06	0.09	14.50	0.01	11.61	0.01	1.42	–	n	LPV
VVVv814	VVV J171810.35-370848.64	17:18:10.35	-37:08:48.64	349.98669	0.31152	–	–	–	–	–	17.59	0.21	15.82	0.08	1.41	–	n	LPV	
VVVv815	VVV J142604.95-604116.81	14:26:04.95	-60:41:16.81	314.26286	0.08460	–	–	–	–	19.17	0.16	17.90	0.13	14.94	0.02	1.71	1.58	y	Eruptive
VVVv816	VVV J130950.13-624631.76	13:09:50.13	-62:46:31.76	305.03425	0.02114	–	–	–	–	–	–	–	–	15.0	0.03	1.37	2.29	y	LPV-Mira